THESIS

JOINT ELIMINATION RETROFITS AND THERMAL LOADING ANALYSIS IN PLATE GIRDER BRIDGE USING HEALTH MONITORING AND FINITE ELEMENT SIMULATIONS

Submitted by

Karly Rager

Department of Civil and Environmental Engineering

In partial fulfillment of the requirements

For the Degree of Master of Science

Colorado State University

Fort Collins, Colorado

Summer 2016

Master's Committee:

Advisor: Hussam Mahmoud
Co-Advisor: Rebecca Atadero

Kelly Strong

ABSTRACT

JOINT ELIMINATION RETROFITS AND THERMAL LOADING ANALYSIS IN PLATE GIRDER BRIDGE USING HEALTH MONITORING AND FINITE ELEMENT SIMULATIONS

Degradation of United States' public infrastructure has attracted attention from the public and governing agencies alike. A challenge facing transportation departments is management of leaking and clogged expansion joints in bridge structures, which result in significant deterioration to bridge substructures and superstructures. Some agencies have started eliminating these joints. However, technical understanding of which retrofit methodology to employ based on thermal loading and specific characteristics of the structure is lacking. In this study, this problem is investigated with both numerical modeling and analysis of field measurements. Various sensors were installed on the bridge including thermocouples, strain gauges, and linear differential displacement transducers. Following sensor installation, controlled load testing was conducted and the collected data evaluated against numerical and analytical predictions. The installed sensors will allow for long-term monitoring of the bridge to evaluate the effect of seasonal temperature profiles that are characteristic of Colorado on bridge behavior.

In addition to gaining technical understanding of site-specific bridge characteristics that influence joint movement using field-testing, numerical finite element analysis was conducted. Specifically, a 3D finite element model was developed and used in a parametric study to assess the effect of various parameters on the stresses occurring in the bridge. The stresses occur due to 1) variation in thermal loading and thermal gradient, 2) clogging of the joint with different

materials including gravel and sand, and 3) employment of various repair techniques in eliminating the expansion joints.

The results of the numerical models show that clogged joints induce some localized stress but do not significantly affect the global performance of the superstructure. The results also show that a reduction in moment demand on the superstructure is not apparent until a Full-Moment Splice connection is utilized. This study will help engineers to choose the most appropriate method of designing a retrofit for expansion joint removal.

TABLE OF CONTENTS

LIST OF TABLES

LIST OF FIGURES

CHAPTER 1

INTRODUCTION

1.1 Statement of the Problem

Current conditions of highway bridges have shifted the attention of state agencies, researchers, and practitioners alike towards bridge maintenance and led them to question necessity of deck joints in bridges. Deck joints, a structural discontinuity between two elements in which at least one is a deck element, are designed to accommodate thermal movements, both translational and rotational, between the two elements. Bearings are devices used in bridges to transfer vertical, translational and rotational loads from the superstructure to the abutments or piers (*AASHTO LRFD Bridge Design Specifications* 2012). It is commonly recognized that deck joints and bearings are costly and complicated to install (Tsiatas and Boardman 2002; Wasserman 1987).

In addition to greater complexity of construction, deck joints and bearings require maintenance throughout their life cycles to remain functional and to prevent damage to the superstructure (Hawk 2003). Water seepage through deck joints can cause significant corrosion of the superstructure below (Lam et al. 2008; Loveall 1985). The American Association of State Highway and Transportation Officials (AASHTO) also recognizes this problem in the commentary section of Chapter 2.5 of the current *AASHTO LRFD Bridge Design Specifications*, which states:

> *"Other than the deterioration of the concrete deck itself, the single most prevalent bridge maintenance problem is the disintegration of beam ends, bearings, pedestals, piers, and abutments due to percolation of waterborne road salts through the deck joints. Experience appears to indicate that a structurally continuous deck provides the best protection for components below the deck."*

Furthermore, bridges supporting roadways in colder climates often exhibit significantly greater corrosion than bridges in warmer climates due to contact with chemicals that are found in deicing salts (Shi et al. 2009; Tsiatas and Boardman 2002). Generally, deicing chemicals contain chlorides that cause the corrosion of the superstructure to occur if leaked onto the superstructure (Lam et al. 2008; Shi et al. 2009). Deck joints increase the likelihood of such leakage to occur; thereby increasing the potential for corrosion problems.

The current abundance of deck joints originated from the straightforwardness of simply supported bridge span design. When simple span bridge construction was prevalent, the infrastructure system in the US rapidly grew into its current state and a large quantity of bridges and roadways were constructed. A noticeable expansion of the US Interstate System occurred after *The Federal-Aid Highway Act of 1956* was signed by President Eisenhower (Federal Highway Administration n.d.). Many of these bridges were designed prior to common usage of structural analysis software programs capable of analyzing continuous span superstructures. Even after Hardy Cross introduced a method to analyze continuous frames by distributing fixed-end moments (Cross 1930), the necessary structural analysis for continuous span bridges was often too cumbersome to complete by hand while maintaining profitable consulting practices. Simple span, non-continuous bridges, however, could be designed and analyzed more quickly and economically by bridge designers and consulting firms. Without information available regarding the necessary maintenance and repair costs of deck joints, a multitude of bridges were constructed as multiple simple spans and separated at each pier with deck joints (Tsiatas and Boardman 2002). Recently, the use of structural analysis software programs by practicing engineers has become commonplace and, therefore, continuous span bridges can now be designed with less effort than in the past. These software programs have enabled practitioners to

economically design and construct continuous span and integral bridges. However, a substantial amount of older bridges with numerous deck joints still exist and pose maintenance and performance challenges to state transportation agencies. Bridge retrofits to eliminate deck joints and bearings have been proposed and implemented in many cases to alleviate the substandard performance of the deck joints (Burke Jr. 1990; Tsiatas and Boardman 2002; Wasserman 1987).

One of the main considerations of deck joint elimination is longitudinal movement and it is calculated with a linear thermal expansion equation as defined in the AASHTO LRFD Bridge Design Specifications. Thermal gradients in the longitudinal, transverse and vertical directions have also been the subject of recent research and have been shown to influence bridge movements. A further understanding of deck joint performance in Colorado, thermal bridge loading, and a more robust design procedure to retrofit bridges could potentially reduce the life cycle cost of bridges, reduce maintenance costs, and in some cases increase the moment capacity of the bridge itself.

1.2 Objectives and Scope of Research

The overall goal of this study is to increase understanding of thermal loading and movement that is exhibited in bridges in Colorado and to provide recommendations for the elimination of deck joints in existing bridges. Specific objectives of this goal were developed through discussion and coordination between researchers at Colorado State University (CSU) and the Colorado Department of Transportation (CDOT). Four main tasks were identified. The tasks include: 1) collection long-term thermal loading data (minimum of 24 months) to assess joint movement of two bridges; 2) development and validation of finite element models of one steel bridge and one concrete bridge; 3) assessment of joint elimination options; and 4)

assessment of the life-cycle cost and the implications associated with joint removal. The long-term data collected in Task 1 will provide information to CDOT about the actual movement of the selected bridges and joints. This can then be compared to the deck joint movement and thermal loading requirements outlined in the AASHTO LRFD Bridge Design Specifications. Development of the finite element models in Task 2 will help assess the stresses induced in the bridge from different connection types and thermal loading scenarios. Development of retrofit connection types in Task 3 will provide CDOT with options to eliminate deck joints in bridges with confidence. Assessment of the life cycle cost implications in Task 4 will help CDOT make decisions about which bridges to retrofit to eliminate deck joints and when a joint eliminating retrofit is the most appropriate option.

This thesis focuses on background and literature review, selection and instrumentation of a steel bridge, development of a finite element model of the steel bridge selected, control load testing on the steel bridge to validate the finite element models, instrument and model a concrete bridge, and a parametric study to analyze the effects of various thermal loads, connection types, and clogged deck joints. Future CSU researchers will conduct further studies to calibrate the finite element models, process and analyze the data collected, and conduct robust and comprehensive life-cycle cost analysis to determine the implications of removing deck joints.

The steel bridge selected for instrumentation and finite element analysis carries County Road 58 over Interstate 25 approximately 10 miles northeast of Fort Collins, CO. Basic characteristics that were desired were minimal skew, curvature, and at least one simply supported span with deck joints on both ends. These characteristics were selected to isolate the bridge movement caused by thermal loading. The bridge was instrumented with strain, displacement, and temperature sensors to collect data on the thermal loading. These sensors will

be in field for at least 24 months to gather information about seasonal changes. Control load testing was conducted to validate the accuracy of the finite element model. Then, using the validated finite element models, a parametric study was conducted to analyze the combined effects of temperature gradients, retrofit connection types, and clogged joints.

CHAPTER 2

BACKGROUND AND LITERATURE REVIEW

2.1 Introduction

To achieve a thorough understanding of the problem and the state of the current research relating to the elimination of deck joints, an extensive literature review was performed. Topics such as origins of code provisions, local behavior at joints, global bridge performance, leading agencies in the field, and thermal loads are included in the discussion. The literature review and this thesis focus on steel superstructures.

2.2 Girder to Abutment Consideration

Various structural systems have been developed to allow for thermal movements while reducing or eliminating deck joints. Placing the joints at the ends of approach slabs or only at the abutments is one method used. Allowing rotation of the abutments is another method that has been utilized. This section aims to discuss these differences and the nomenclature that has been put into place by the transportation agencies.

Integral bridges are bridges without deck joints (*AASHTO LRFD Bridge Design Specifications* 2012) and have been increasingly used in recent years by government agencies (Burke Jr. 1990; Tsiatas and Boardman 2002; Wasserman 1987). Though the current AASHTO code provides an umbrella definition for integral bridges, some state or local transportation agencies have developed definitions for fully integral bridges and semi-integral bridges. In an integral bridge, the total longitudinal movement is accommodated either through thermal stresses

in the superstructure, rotation of abutments, piers, or foundations, or a combination of those. Therefore, understanding of integral bridge behavior is a vital part of designing the other elements of the structure that will need to accommodate the longitudinal thermal movement.

Fully integral bridges are characterized by the absence of deck joints and a girder system that is monolithic with the abutment. Often, the foundation piles supporting the abutment are constructed to accommodate longitudinal movement from the bridge superstructure through rotation. Constructing the abutment foundation from steel H-piles that are weak-axis oriented (to be rotationally flexible) is one method used. Alternatively, a structural hinge can be used at the base of the abutment to prevent moment build up (Albhaisi and Nassif 2014; Wasserman 1987). For fully integral bridges, a joint is often placed at the end of the approach slab, where a leak would not as adversely affect the structural integrity of the bridge (Husain and Bagnariol 2000).

Semi-integral bridges, however, are characterized by the absence of deck joints throughout the spans and by girders that are not monolithic with the abutment. Instead, of a monolithic girder-abutment connection, a bearing is used at the seat of the abutment to allow global bridge movements. The foundation system for a semi-integral bridge is rigid and the approach slab is continuous with the bridge deck. Semi-integral bridges require less maintenance than bridges with multiple deck joints. However, the bearings must be inspected and maintained – a concern not relevant to fully integral bridges. An advantage to using semi-integral bridges is that they can be used for longer bridges than fully integral bridges because they have expansion joints at the abutments. The expansion joints at the abutments allow for some thermal movement, whereas fully integral bridges allow for no thermal movements without inducing stresses in the structure (Husain and Bagnariol 2000). Though a fully integral bridge and a semi-integral bridge are both considered integral bridges by the current AASHTO definition, the physical difference

between the structural systems is noteworthy when further understanding of bridge movements and stresses are of interest.

2.3 Leading Agencies

Samples of past experiences published by transportation agencies are presented. The agencies discussed are not necessarily an exhaustive list, but are agencies with a significant published history of their work relating to elimination of deck joints or the analysis of thermal loading.

2.3.1 Tennessee Department of Transportation (TDOT)

The Tennessee Department of Transportation (TDOT) has published many articles and reports describing their experience with integral bridges. During the past several decades, almost all of the bridges in Tennessee have been constructed without deck joints up to several hundred feet. In extreme cases, bridges that could not be constructed entirely continuous were constructed with a bearing at the abutment to allow for global bridge movements – a semi-integral bridge. Steel bridges in Tennessee have been constructed with entirely continuous superstructures up to a length of 127 m (416 ft). When bridges without deck joints or joints at the abutments were studied, the stresses in the bridges were lower than expected. However, TDOT admits to not fully understanding why these integral bridges perform so well (Wasserman 1987). Through experience, they have become more confident in increasing the length of their integral bridges. However, to develop a generalized procedure that can be followed with confidence by all bridge designers, it is necessary to improve understanding about how these structures behave spatially,

thermally, and throughout seasonal cycles rather than relying on past experience which lacks analytical explanations.

2.3.2 Transportation Ministry of Ontario (MTO)

The Transportation Ministry of Ontario (MTO) has also found success with integral bridges since implementation of deck elimination retrofit program in 1995. MTO focuses on connecting the slabs over the joint and leaving the girders discontinuous (Ontario Ministry of Transportation 2014). Due to the variability of superstructure types, material, and loading scenarios, three retrofit designs were developed and used: 1) casting a deck and concrete diaphragm monolithically with the girders, 2) casting a thin flexible deck, and 3) casting a flexible deck de-bonded from girders. Generally, limits on skew, girder end rotations, and girder heights help guide designers to a retrofit choice. All three options were found feasible for steel girder systems. To avoid cracking caused in the negative moment regions, fiber reinforced concrete was suggested (Lam et al. 2008). MTO limited eligibility for the retrofit program to bridges with less than a 20 degree skew, a total bridge length of less than 150 m (492 ft) and an angle subtended by a 30 meter arc along the length of the structure that is less than 5 degrees (Husain and Bagnariol 2000). Details of their program provide a suitable starting point for retrofitting bridges in Colorado to eliminate deck joints.

2.3.3 Colorado Department of Transportation (CDOT)

Many state departments of transportation, including the Colorado Department of Transportation (CDOT) also limit the length or skew of integral bridges (CDOT 2012). Provisions in the CDOT Bridge Design Manual for integral bridges provide limits on the bridge length. Bridge lengths are limited to 195 m (640 ft) for steel bridges (CDOT 2012). Further

analysis of the thermal effects and connection types could help validate, tighten or loosen these restrictions in some scenarios.

2.4 Types of Retrofit Connections

In addition to reducing maintenance and repair costs, integral bridge construction and retrofit programs can potentially increase the load rating and design life of the bridge. However, further understanding of the thermal effects induced in a jointless bridge needs to be developed to allow bridge designers to implement integral bridges with confidence. It has been shown that substantial differentials of stresses and movement occur in bridge girder systems due to thermal effects (Chen 2008; Koo et al. 2013). Additionally, state departments have used numerous methods of connecting two simple spans. These different connections and bridge conditions may have varying benefits, load-rating implications, and life cycle costs implications.

A study completed with the Rhode Island Department of Transportation at the University of Rhone Island investigated the effect that converting a simple span bridge to a continuous span bridge would have on load ratings (Tsiatas and Boardman 2002). Linear, two-dimensional models were developed to examine the potentially increased moment capacity of bridges that were converted from simple spans with deck joints to continuous structures without deck joints. Multiple retrofit connection types that had been used by state transportation agencies were included in the study including Deck Only, Deck and Top Flange, Deck and Bottom Flange, Deck, Top and Bottom Flange, and Full Moment Splice. The results of the study indicated that moment capacity was only increased when the Deck and Bottom Flange, Deck, Top and Bottom Flange, and Full Moment Splice retrofits were implemented. However, the Deck Only connection type was found to be the least expensive and most popular with government agencies.

Based on the two-dimensional model, these connection types had the highest potential for cracking and did not increase the load carrying capacity of the bridge (Tsiatas and Boardman 2002).

2.5 Thermal Effects on Bridges

One of the main considerations of deck joint elimination is longitudinal movement. Longitudinal thermal movement is currently accounted for in Section 3 of the AASHTO Bridge Design Specifications. The global thermal longitudinal movement has been shown to be accurately predicted by the average temperature of the bridge (Moorty and Roeder 1992). Some methods used to accommodate longitudinal movements in integral bridges include flexible pile foundations (Albhaisi and Nassif 2014) or an appropriately selected bearing or a hinge at the bottom of an abutment (Wasserman 1987). However, the total bridge performance and local behavior cannot be entirely described by the average temperature of the structure. The uneven heating and resulting thermal stresses may also require consideration in order to eliminate deck joints without adversely affecting a structural performance.

Thermal gradients are the most uneven at times of heating or cooling of the bridge. Heat transfer due to direct radiation from the sun, conduction, or convection occurs every time that the ambient air temperature changes – usually every morning and evening. Bridge orientation, length of concrete overhang, depth of girders, height of concrete slab, and girder spacing are all parameters that affect how evenly the bridge gains and loses heat (Chen 2008). Commonly, uneven bridge movements are accommodated through pier, bearing, joint, and girder movement or rotation. Notably, however, an integral bridge would not possess a joint to allow for uneven movements of a superstructure. A more detailed study on thermal stress distribution for bridges

in Colorado could allow integral bridges to be designed confidently with longer lengths, greater skew angles, and greater curvature.

The coefficient of thermal expansion, commonly expressed as μ or α, describes the increase in length of a material for a given increase in temperature. Change in length of a homogeneous material due to uniform change in temperature can be expressed in the Equation 1:

$$\Delta L = \Delta T * \alpha * L_0 \qquad (Eq. 1)$$

where ΔL is the change in length, ΔT is the change in temperature or the final temperature minus the initial temperature, α is the thermal expansion coefficient, L_0 is the original length of the material considered. A negative result for the change in length corresponds to a shortening of the material and a positive value for the change in length corresponds to an increase in length of the material. Concrete has a coefficient of thermal expansion that is about eight percent less than that of steel (Chen 2008) and this results in an change in length of a steel girder that is about eight percent greater than what a concrete girder would experience. When these two materials are rigidly connected, such as in a steel composite bridge, the change of length is restricted and corresponding stresses develop.

A concept worthy of recognition is the difference in timing between critical thermal movements and critical thermal stresses. The maximum expansion and contraction from setting length for global bridge movement occurs during the warmest days in summer and the coolest nights in winter, respectively. However, the maximum thermal stresses due to uneven heat transfer in the superstructure occur during the warming of the bridge in the early afternoon or the cooling of the bridge in the evening (Moorty and Roeder 1992). Verification of this concept and further understanding of the heating and cooling cycles on Colorado bridges can be further understood with temperature data from instrumentation of in-service bridges.

Thermal stresses are localized stresses due to overall temperature change and due to temperature gradients along any axis (transverse, longitudinal, or vertical) of bridge. Currently, thermal gradient in the transverse direction is not accounted for in AASHTO LRFD Bridge Design Specifications. The thermal gradient in the vertical direction is mentioned in the current AASHTO provisions, but does not need to be considered if "experience has shown that neglecting temperature gradient in the design of a given type of structure has not lead to structural distress" (*AASHTO LRFD Bridge Design Specifications* 2012). The ambiguity of this statement leads many practitioners to neglect the thermal stresses that result from thermal gradients in the vertical direction. However, these stresses have been shown to exist on the order of +/- 5 ksi in a daily heat cycle of a steel box girder superstructure in Texas (Chen 2008). This could be significant depending on how economically the bridge was designed initially.

2.6 Increasing Popularity

Overall, the use of integral bridge retrofits and construction has increased in popularity in the US and Canada in recent years. As of 2002, over 500 existing bridges have been made continuous in the US and Canada (Tsiatas and Boardman 2002). The bridge types that have been retrofitted are up to 6 span structures with spans up to 300 ft (Wasserman 1987). Though the popularity of bridges without deck joints is increasing, one of the current barriers of more universal use of integral bridges is the lack of understanding of thermal gradients in bridges. To improve the success of joint elimination retrofit programs and new construction for bridges without deck joints, increased understanding of the thermal effects in bridges is requisite. Knowledge of thermal effects, especially in regards to local behavior at connections, will allow

researchers and designers develop a more diverse palate of retrofit options and improve estimates of life cycle cost savings, load rating improvements, and values of expected stresses.

2.7 Global Bridge Performance

The global performance of an integral bridge under thermal loading is a function of multiple parameters. Total longitudinal movement of the superstructure, the rotation of piers, abutments, and foundations that accommodate the longitudinal movement, effect of curvature, length and skew, and a potentially improved moment capacity and seismic performance are all of interest to a practitioner designing an integral abutment bridge. Multiple studies have been completed on these parameters of interest for integral bridges, however, most have focused on concrete girder systems (Tsiatas and Boardman 2002). Less work has been completed on steel girder performance and connection retrofit types in steel bridges than for concrete superstructures.

2.7.1 Longitudinal Movement

A case study has shown that the total longitudinal movement of a bridge can be predicted by the bridge's average temperature (Roeder 2003) and this is the method currently described by the AASHTO Bridge Design Specifications, specifically in sections 3, 5, and 15 (*AASHTO LRFD Bridge Design Specifications* 2012). This global expansion and contraction of the superstructure is the primary focus of design codes (Zhu et al. 2010). The coolest and warmest temperatures expected for steel bridges with concrete decks are described by a temperature contour map of the United States and are experienced in the coldest nights of winter and warmest days of summer, respectively. The contour map showing the maximum design temperature,

developed by Roeder, in 2002, is shown as an example in Figure 2-1. The minimum design temperatures are also provided by AASHTO LRFD Bridge Design Specifications in Chapter 3.12 but only the maximum temperature is shown in this paper to illustrate the method. The expected extreme temperatures for steel bridges have a greater range than for concrete bridges.

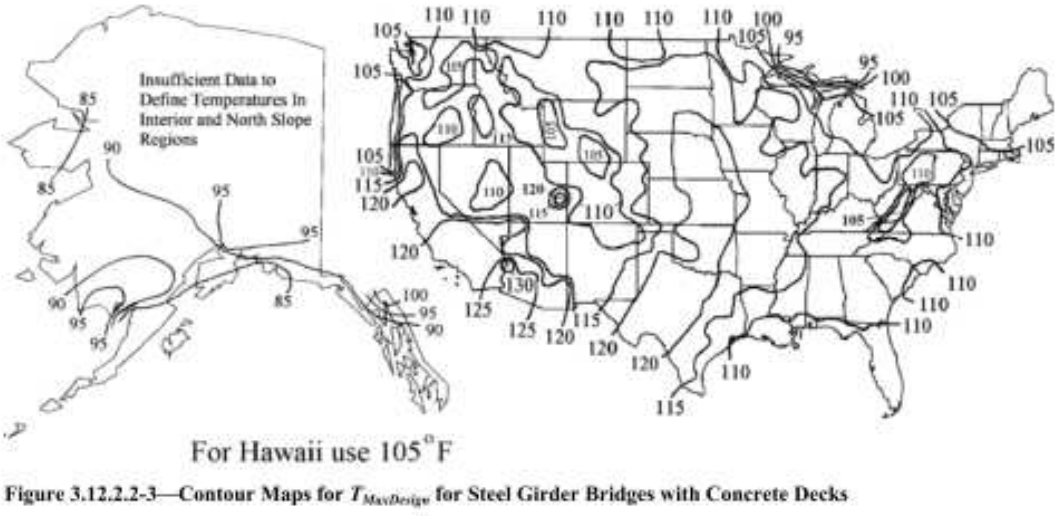

Figure 2-1. Maximum Expected Temperature for Steel Bridges with Concrete Decks

In addition to the difference in longitudinal bridge movement due to differences of the coefficient of thermal expansion, concrete girders generally contain a larger volume and mass than steel girders. Therefore, concrete superstructures act more as a heat sink and do not reach the air temperature as quickly as steel superstructures (Wasserman 1987). For these reasons, concrete girder bridges are often designed for less extreme longitudinal movement than bridges with steel girders. In integral bridge construction or deck joint elimination candidates, this difference in longitudinal thermal movement is manifested in codes through more restrictive maximum length limits on steel integral bridges than for concrete integral bridges; 120 m (~400 ft) to 150 m (~500 ft) is considered the longer end of the spectrum for integral bridge construction in steel bridges (Burke Jr. 1990).

One method used to allow the longitudinal thermal movement of integral bridges is placing a hinge at the bottom of the abutment or pier to prevent moment build up (Loveall 1985; Wasserman 1987). The top of the abutment will rotate away from the bridge during warmer days during to thermal expansion and will rotate toward the bridge superstructure during cooler days during to thermal contraction. This method has been used with success by the Tennessee Department of Transportation (TDOT).

Another method used to accommodate longitudinal thermal movement of integral bridges is flexible foundations beneath the abutments. Typically, a single row of weak-axis oriented H piles is used that can rotate when the bridge expands and contracts (Pugasap et al. 2009; Zhu et al. 2010). Zhu et al. completed a calibrated finite element model of pier footings to examine the robustness of the AASHTO provisions for the movements and soil stresses encountered under the footings due to thermal loads. The pressures encountered were well within the allowable bearing pressure. However, the focus of the study was on the pier footings, rather than the single row piles. Lastly, the girders were constructed of concrete, rather than steel and the soil considered was not clay, which is commonly experienced as a problematic soil in Colorado.

Kim and Laman completed another parametric study in 2010 to examine the thermal effects on flexible rotations. A finite element model was developed and the influence of the thermal expansion coefficient, the span length, the backfill height, the backfill stiffness, and the pile soil stiffness was considered. It was concluded that the backfill height and the backfill soil stiffness have relatively insignificant effects on the global bridge responses. However, as the pile soil stiffness increases, the maximum pile lateral force and pile moment also increases. Of the parameters of interest, the thermal expansion coefficient and span length influence the girder axial force, pile lateral force, pile moment and pile head displacement significantly (Kim and

Laman 2010). Finally, the authors conclude by recommending that the effects of thermal stresses are included in all integral abutment bridges.

2.7.2 Effects of Bridge Geometry (Skew and Curvature)

Effects of curvature and skew have been examined to determine if global longitudinal bridge movements can or cannot be totally described by the one-dimensional AASHTO provisions in cases where the curvature and skew of the bridge are significant. Several transportation agencies have set limits on the skew and curvature of bridges eligible for integral construction and retrofits (Burke Jr. 1990; CDOT 2012; Husain and Bagnariol 2000). Further understanding of connection retrofits could help loosen the restraints on skew and curvature limitations.

A three-dimensional finite element model was developed and verified by Moorty and Roeder in 1992 to examine effects of skew, length, width, girder depth, cloud cover, wind speed, air temperature, bridge temperature differentials, and horizontal curvature in bridges under thermal loading. Their studies were performed on bridges with bearings between the girder system and the piers and abutments. Bridges with horizontal curvature were found to exhibit significant radial displacements near center of curvature and significant tangential displacements at point furthest away from rigid supports. Also, radial displacements were found to increase as the curvature of the bridge increased. Lastly, the radial displacements were shown to increase when the stiffness of bearings were greater (Moorty and Roeder 1992). This is of importance to integral bridges where the superstructure connects monolithically with the piers and abutments. The stiffness in these connections is many orders of magnitude greater than the stiffness of a bearing. Therefore, it is not unreasonable to expect significant stress build up in connections or

significant radial movements in curved bridges without bearing pads that are subjected to thermal expansion and contraction along their longitudinal axis.

The finite element model developed by Moorty and Roeder also considered the effects of skew. The longitudinal and transverse deflections due to thermal loads were found to vary in the transverse direction in skewed bridges. Displacements were greatest at points furthest away from rigid supports. Lastly, it was recommended that bearings used on skewed bridges be unguided (not restricted to a single line of movement) to allow for transverse movements (Moorty and Roeder 1992). In an integral bridge without bearings, however, these movements would be restrained and the bridge would need to be able to accommodate these stresses through movement in a different location or with the strength of structural elements.

Questions remain about the effects of curvature and skew in integral bridges. However, understanding the movement of non-integral bridges provides a link to how the stresses would accumulate in curved and skewed integral bridges. Current AASHTO commentary (Section C3.12.2.1) states that bridges with large skew or curvature should not be built upon bearings that only allow movement in the longitudinal direction due to radial or tangential movement that is expected. Understanding of restraints and connections used combined with structural solid mechanics could yield estimate for the accumulated stresses. Or, the vertical supports could be decreased in stiffness to allow for the thermal movements to occur without the accumulation of stress.

2.7.3 Potential Increase in Moment Capacity

Eliminating deck joints and making the girders and deck continuous has the potential to increase moment capacity. However, due to the multiple ways a bridge can be connected and made continuous, the extent of the increased load rating is largely dependent on which detail is

used and what elements of the superstructure become connected (Tsiatas and Boardman 2002). A study conducted in 2002 by Tsiatas and Boardman examined Deck Only, Deck and Top Flange, Deck and Bottom Flange, Deck, Top and Bottom Flange, and Full Moment Splice connections. The study concluded that no increase in moment capacity was exhibited when Deck Only and Deck and Top Flange connections were used. The Deck Only and Deck and Top Flange connections also were found to possess the highest potential for cracking due to the negative moment experienced in the bridge over the piers or supports.

Connections that did improve the moment capacity of the bridge included the Deck, Top and Bottom Flange connection and the Full Moment Splice connection (Tsiatas and Boardman 2002). Unsurprisingly, these connections are more expensive and laborious to construct. However, for bridges that are expected to carry more traffic in the near future, this option may be worth considering. Worth noting is that the model used to draw these conclusions was two-dimensional. It is uncertain whether this model included some of the benefits or disadvantages of the local behavior of the connection types considered. A three-dimensional model and more field verification of this model would strengthen the claims asserted.

2.7.4 Conclusion

Overall, the impact of constructing a bridge without deck joints or bearings or eliminating all deck joints and bearings by retrofitting an existing bridge is significant. The behaviors of interest and parameters influencing them are numerous. However, more scientifically verified information of the response of steel bridges and development of well-understood replacement connections would assist in furthering the concept of deck joint replacement and, therefore, decrease maintenance management costs and increase the durability of bridges' superstructure.

2.8 Local Superstructure Behavior

The parameters and areas of interest of local behavior for bridges with deck joints differ from those without. Local superstructure behavior of interest for bridges with deck joints includes corrosion of girders under leaking joints, joints unable to perform due to debris build up and performance of joints and bearing pads under extreme temperatures. Local superstructure behavior of interest for integral bridge construction and retrofits (bridges without deck joints) includes lateral-torsional buckling (LTB) risk, thermal stress differentials in the superstructure cross-section, stresses in connections, rotation at girder ends, shear lag at girder ends, and understanding the advantages and disadvantages of numerous connection types. Local behavior of these forms could be non-linear and not fully described by two-dimensional models. Instead, verified, detailed three-dimensional finite element analysis would increase the understanding of the complex behaviors exhibited. An examination of previous research completed in these areas of interest follows.

2.8.1 Corrosion

Corrosion, one of the central issues with deck joints, is caused in the superstructure when deck joints leak (Hawk 2003; Lam et al. 2008). This corrosion at the deck joints, which are commonly located at the piers, abutments, or other vertical supports, causes the structural integrity of the superstructure and bearings to deteriorate. Often, local behavior of the bearings, connections, girders, pier caps, and piers under these decks will be adversely affected. The use of deicing chemicals, and their subsequent runoff from roadways, increases the rate of corrosion to girder systems under deck joints (Tsiatas and Boardman 2002). When deck joints leak, maintenance and eventually replacement are necessary to maintain a safe structure.

2.8.2 Blocked Expansion

In order to function properly, expansion joints must be able to freely expand and contract without significantly affecting the driving surface of the road. As illustrated in Figure 2-2, debris build up in an expansion joint less than six months old can prevent it from closing in warmer weather to accommodate thermal loads (Chen 2008). Routine maintenance is required to keep expansion joints in working order.

Figure 2-2. Debris in expansion joint in service for less than six months (Chen 2008)

If excessive debris is allowed to build up in an expansion joint, pavement growth can occur. Pavement growth, as defined by the Michigan Department of Transportation (MDOT), is the widening of joints from debris build up. If traffic removes a compression seal or debris builds up from other causes, the effect on the structure can be severe. When a joint with debris build-up opens further due to reduction of average bridge temperature, the debris settles further into the joint and now takes up the entire new width of the joint opening. This is very damaging because

at this point, the joint will not be able to close any further than the current cool weather, wider debris opening. As a result of this increased opening, more debris is allowed to build up and the distance from one end of the pavement to the other "grows". If the average bridge temperature were to increase, the joint would not be able to close to alleviate thermal stresses. However, if the temperature only decreases to a greater extent, the joint will open further and the newly added debris will settle into the joint and prevent even more movement, as shown in Figure 2-3. This cycle continues if the bridge deck joint is not maintained and significant stresses can be induced into the bridge local connections, bearing pads, and superstructure elements (Rogers et al. 2012). Eliminating deck joints would allow for reduction of damage or reduction of cost of maintenance to prevent damage.

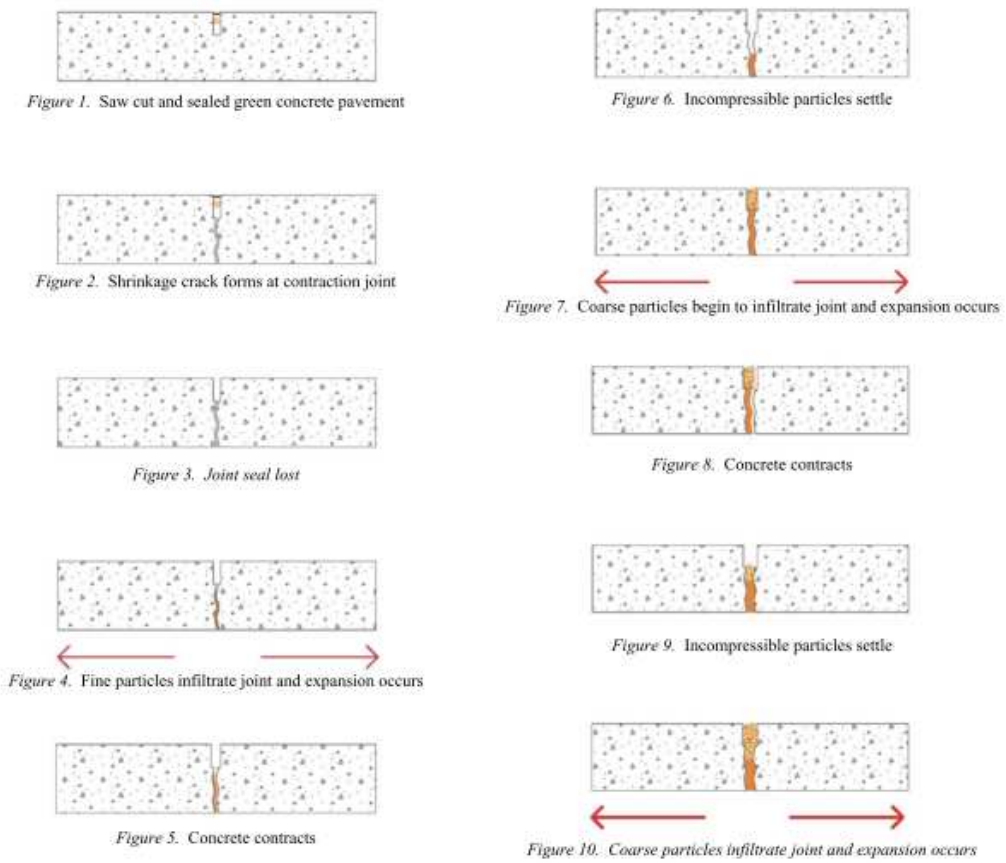

Figure 2-3. Cycles of Pavement Growth (Rogers and Schiefer 2012)

2.8.3 Lateral Torsional Buckling Risk

In bridges that are constructed without deck joints originally or retrofitted such that deck joints are eliminated, a potential lateral-torsional buckling risk occurs in composite steel girder systems. Positive moment regions of the bridge (near mid-span) exhibit compressive stresses on the top of the superstructure cross-section. Since most steel girder systems are composite with a concrete deck, the neutral axis of the cross-section is raised and the majority of the compressive stresses are carried in the concrete deck in the positive moment regions of the bridge. The compression that occurs in the top flange is relatively small and the flange is held in place by a composite concrete deck. However, in the negative moment regions of the bridge, which are commonly where a deck joint is eliminated and the bridge can be made continuous, the new cross-section under negative moment will exhibit compressive stresses on the bottom flange of steel girders that is not supported or carried by a composite concrete deck (Vasseghi 2013). These high compressive stresses in the bottom of the section below the neutral axis and the tensile forces experienced above the neutral axis cause a potential for lateral-torsional buckling, or kicking-out-of-plane. Analysis of this type of behavior is requisite to making a superstructure continuous and stable.

Compact sections are cross-sections that are not at risk of lateral-torsional buckling. Whether or not standardly compact sections, as specified by AISC Code are clear of this risk in all integral bridges could be verified by numerical modeling or laboratory tests. Sections that are not classified by the American Institute of Steel Construction as compact should definitely be analyzed for this behavior before a retrofit or new construction of an integral steel bridge is completed. The stresses occurring in the connections and girder system are a function of what kind of connection and girders are in place. Therefore, an analysis of buckling behavior for

current and possible retrofit connections and girder systems would be a helpful step in quelling the potential for lateral-torsional buckling. Lateral bracing in the form of stiffeners or torsional bracing in the form of diaphragms or cross frames can be implemented near the part of the girder in compression to prevent lateral torsional buckling (Vasseghi 2013, Segui 2012).

2.8.4 Temperature Gradient

Another significant factor to consider when eliminating deck joints is uneven temperature in the transverse and vertical direction across a bridge and girder cross-section. During times of the day in which the ambient air temperature is changing, the entire bridge is also changing in temperature through radiation, convection, and conduction. Radiation is the energy emitted by the sun in the form of electromagnetic waves through the medium of the atmosphere. Usually, only the deck receives direct solar radiation, while the girder system does not. Convection is the mode of heat transfer between the bridge's solid surface and the adjacent air that is in motion (e.g. wind) and involves the combined effects of fluid motion and conduction. The outer girders and deck may experience the effects of convection to a greater extent than the interior girders. Conduction is the transfer of energy of more energetic particles in one solid to less energetic particles in another solid through direct contact (Cengel 2012). The constant and inconsistent temperature changes across the cross-section manifest themselves in uneven expansion, or, if restrained, uneven thermal stresses in the bridge structure.

In 2008, Li et al. completed a study on the thermal loading and expansion joint movement of Confederation Bridge, an existing, long-span concrete girder bridge. Though this is not a steel bridge, the methodology to analyze and monitor a concrete bridge would be similar for a steel bridge. Temperature differentials in the vertical and transverse direction in the girder cross-section were examined with three years of data gathered from thermocouples installed on

the bridge. The rate of temperature change and temperature gradient was discovered to develop in different rates and patterns in the transverse direction than in the vertical directions (Li et al. 2008). It was also found that shallow sections did not need to consider temperature variation in the transverse direction (the direction perpendicular to traffic flow). Though this seems like a promising way to simplify a design method, what constitutes a shallow section was not explicitly stated by the authors. Rather, the shallowest section of the bridge, a concrete box girder with a height of 177 in (4.5 m) was the shallowest section considered and it did not appear to have significant temperature variation in the transverse direction (Li et al. 2008). A boundary between shallow sections and deep sections is never explained, but a qualitative conclusion that shallow sections have negligible temperature variation in the transverse directions helps further understanding about thermal effects in a cross-section. However, a quantitative definition of shallow in relation to other parameters would be more useful to a practitioner designing an integral bridge.

Another notable study was performed by French et al. in 2013 to assess the thermal gradient effects in the Interstate 35 St. Anthony Falls Bridge in Minneapolis, MN. This posttensioned concrete box girder bridge was monitored over a duration of three years. Finite element modeling in ABAQUS was developed and gradients from two code provisions were considered. Vertical thermal gradients from AASHTO LRFD Bridge Design Specifications (developed by Imbsen et al. in 1985) and the New Zealand Bridge design code (developed by Priestley in 1978) were considered. A fifth-order design thermal gradient, as specified by the New Zealand Bridge Design Code, was determined to be the most appropriate for this bridge with the top surface temperature matching the temperature assigned in the AASHTO provisions for Minneapolis, MN (French et al. 2013). Additionally, the global structural demand modeled

with the AASHTO provisions of vertical thermal gradient were found to be much lower than the measured stresses (French et al. 2013). This study further encourages the examination of the vertical gradient developed by Imbsen et al. in AASHTO for other bridge girder types and in other geographical locations.

Further studies performed by Chen in 2008 analyzed temperature differentials and the corresponding thermal stresses in steel bridges in Texas. This study is particularly relevant because the bulk of research involving elimination of deck joints and thermal gradients has been conducted on concrete girder bridges. Analysis in this study involved finite element models verified by field monitoring and experimental testing performed in the Ferguson Structural Engineering Laboratory in Austin, Texas. The dissertation addresses the robustness of thermal stresses that occur in bridges that are accounted for in the current AASHTO Bridge Design Specifications. Also, stresses that are not currently accounted for in the AASHTO Bridge Design Specifications are examined (Chen 2008). According the temperature contour map provided by AASHTO the temperatures range is cooler in Colorado than in Texas. The maximum expected temperature for Colorado and Texas is 100^{o}F-110^{o}F and 105^{o}F-115^{o}F, respectively. The minimum expected temperature in Colorado and Texas is approximately -30^{o}F-0^{o}F and 10^{o}F-40^{o}F, respectively (AASHTO 2012, Figure 3.12.2.2-1 and Figure 3.12.2.2-2). The range of expected temperatures for Colorado is larger than in Texas and therefore the stresses found in steel bridges in Texas may actually be less than what a similar steel bridge in Colorado would experience.

Though current AASHTO provisions only require consideration of the total longitudinal thermal movement based on the average bridge temperature, stresses due to temperature differentials in the cross section were shown to commonly be above +/- 5 ksi in steel box girder

bridges in Texas. Though different girder widths, depth and bridge location would change the value of these stresses, it is clear that the significance of these stresses is worth analyzing in Colorado's steel bridges if an order of magnitude of 5 ksi is reached on a regular basis in Texas steel bridges.

The heating and cooling of steel girder systems with composite bridge decks was analyzed in Chen's research. Due to the differences in thermal expansion coefficient and different exposure to radiation, convection and conduction, the heating and cooling of a composite girder cross-section is non-uniform as shown in Figure 2-4 and 2-5. If these two components of the superstructure, the deck and the girder, are restrained in the same place, thermal stresses will develop due to the uneven heating or cooling of the structure. Accounting for these additional stresses through increases in material strength, flexible piles, hinged abutments, and/or bearings could help alleviate stresses in this local behavior.

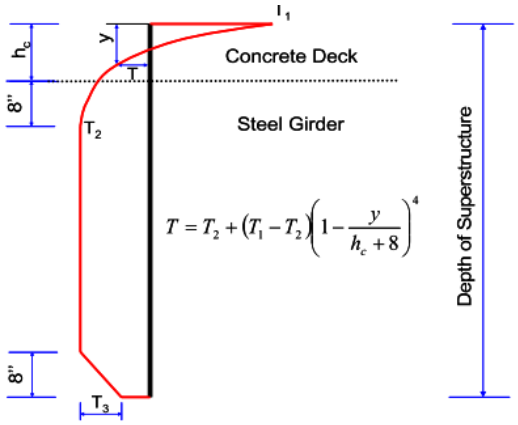

Figure 2-4. Vertical Temperature Distributions of Heating of Steel Composite Girders (Chen 2008)

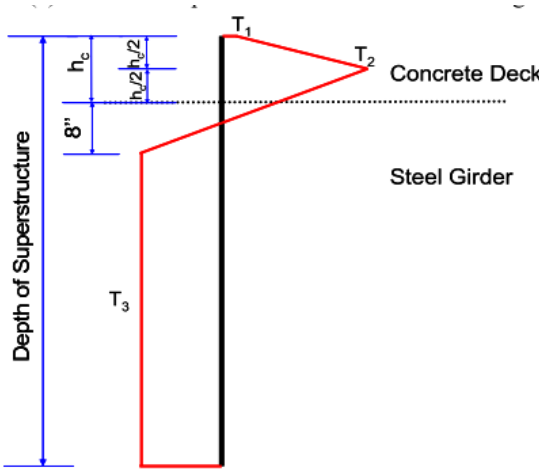

Figure 2-5. Vertical Temperature Distributions of Cooling of Steel Composite Girders (Chen 2008)

Regarding integral bridges, material strength must be increased or movement must be allowed to accommodate these uneven movements to occur. Non-integral bridges with expansion joints can expand or contract at slightly different rates without inducing stresses because of the gap that is present. For example, if the concrete deck heats and expands sooner and then the steel girder below it due to solar radiation on the deck, the gap in the expansion joint would close more near its top and less near its bottom. However, this uneven expansion joint opening would induce no stresses. For integral bridges, on the other hand, any uneven thermal expansion or contraction would induce a stress in the element because it is not allowed to move independently from the adjacent span at the vertical supports. Movements would need to be absorbed through pier deflection, foundation deflection, strength of material, bearing movements, girder deformation, or a combination of all of these (Chen 2008). It should be noted that for both integral and non-integral bridges, stresses at the interface of the steel girders and concrete deck would be expected due to the uneven heating shown in Figure 2-4 and 2-5. The magnitude of these stresses is relatively unexamined, but worth analyzing for design of shear studs and connections between the deck and the girder system.

Effort also was made in this study to identify the conditions with the greatest thermal effects. It was found that bridges with north-south orientation, shorter lengths of the concrete deck overhang, deeper steel girder webs, thinner concrete decks, and wider girder spacing resulted in the most extreme cases of thermal stresses (Chen 2008). Though this is a qualitative result, it may be beneficial to know these most extreme conditions to strategize a way to reduce thermal effects in the design of a new bridge.

2.8.5 Temperature Data

Lastly, a statistical analysis was performed to compare the temperature data found with the expected values provided in the AASHTO Bridge Design Specifications. The temperatures provided in AASHTO are meant to show the minimum and maximum temperatures expected in a region with a 100 year return period. This study found that, for the Houston Area, the AASHTO code provided a lower bound temperature with a return period of only 16 years. The authors recommended that the expected minimum temperatures be adjusted to a true 100-year return period (Chen 2008). This discrepancy in temperature data is concerning for the bridge designs in Colorado as well. Statistical analysis for minimum and maximum bridge temperatures in Colorado may help designers construct bridges in a more accurate temperature range than provided in the current AASHTO provisions or help AASHTO modify their provisions.

2.8.6 Influence of Temperature compared to other variables

Another case study performed on the Tamar Bridge, a 335 m span suspension bridge in Plymouth, United Kingdom, aimed to examine the effects of environmental loading on the bridge from temperature, wind, and traffic. Out of levelness, tension response in cables, bridge temperature, and wind loading were all monitored during the study. It was determined that out of

levelness, tension response of cables, and stresses across the girder system were most driven by the effects of temperature (Koo et al. 2013). Wind and traffic loading were found to have an insignificant effect in comparison. It was also found in this study, like in others, that the temperature of the bridge deck is routinely warmer than the supporting superstructure below (Koo et al. 2013) which reaffirms that shear stresses will exist at the connections between the two elements if rigidly connected. Overall, this study showed that the effects of temperature differentials in the cross section are significant in local behavior such as stresses, out of levelness, and deformation.

2.8.7 Conclusion and Research Approach

Other connection behavior to consider includes stresses induced in different connection options, shear lag in connections with small contact area to adjacent girders, and how to evaluate the numerous connection types that are being developed. Due to the complexity of the connection behavior and the large amount of parameters to consider, three-dimensional models may be best suited for understanding the local behavior of integral bridge retrofit options. Of particular interest to steel composite bridges is the stresses that build up at the interface between the steel girders and the concrete deck due to uneven thermal movement. In addition to collection of field data from bridges in Colorado, comparisons to the vertical thermal gradient in multiple code provisions will be a vital step to determining the best method for deck joint elimination in Colorado.

2.9 Current AASHTO Provisions for Integral Bridges

In the current AASHTO LFRD Bridge Design Specifications discussion of thermal effects and discussion of joints and bearings are found in Sections 3 and 14, respectively. The code describes multiple requirements for the performance of deck joints and bearings are listed. However, in the discussion the code states that the amount of both deck joints and bearings should be minimized. Also, the code specifies that no material should have less than a 75-year design life. Recognition of thermal differentials is stated in commentary C3.12.1, which states:

"Although temperature changes in a bridge do not occur uniformly, bridges generally are designed for an assumed uniform temperature change."

No mention of gradient in temperature is specifically mentioned along longitudinal axes. The consideration of a vertical thermal gradient is included in Section 3, but consideration of this gradient is not required.

2.9.1 Setting Temperature

Setting temperature is defined as "a structure's average temperature, which is used to determine the dimensions of a structure when a component is added or set in place." (AASHTO Bridge Design Specifications, Section 3-3). Clearly, the setting temperature will have an effect on the total expansion or contraction a bridge will experience over its service life. For example, if a structure's girder system is set on a summer day, the movement due to expansion that the bridge will experience will be less than the movement due to contraction. Therefore, for bridges with deck joints, the setting temperature will influence the initial joint opening that should be used for construction. Often in practice, a table is provided with the construction document that specifies initial joint openings depending on the air temperature in which the construction is taking place. However, the actual structures temperature still may be different than the current air

temperature if the weather is changing (e.g., mid-morning or late-afternoon). Code provisions to account for this behavior could help ensure that a table is provided on the construction documents for initial joint opening and its corresponding dependence on setting temperature.

In addition to variability of joint openings due to setting temperature, further concern exists due to the different temperatures at which parts of a bridge are constructed. For example, if a foundation is laid in the winter, the piers are connected in the spring, and the superstructure is added in the summer, a residual thermal stress would most likely exist at the moment the different elements are connected to one another. The magnitude of such stresses is unknown and not mentioned in the current AASHTO provisions.

2.9.2 Uniform Temperature Change

Two procedures, Procedure A and Procedure B, are presented as methods to find the temperature range expected for a particular bridge material and region of the United States for uniform temperature change. Procedure A or Procedure B can be used for concrete deck bridges with either steel or concrete girders (AASHTO 2012, Section 3.12.2). Procedure A is used for all other bridge types. Procedure A consists of a table that provides expected maximum and minimum temperatures for moderate climates or cold climates and for a certain bridge material. A moderate climate exists in a location where the number of freezing days (a day with an average temperature of less than 32^{o}F) is less than 14 per year. Procedure B, provides temperature contour maps of the United States for both maximum and minimum bridge temperatures to be expected and was developed by Roeder in 2002 by examining extreme temperatures over 70 years. Though the commentary of the section recognizes that bridges do not change temperatures uniformly, it states that bridges are usually designed for an assumed uniform temperature change (AASHTO C3.12.2.1).

Once the maximum ($T_{MaxDesign}$) and minimum ($T_{MinDesign}$) temperatures are determined, either from Procedure A or B, the uniform thermal movement expected is calculated using Equation 2 below.

$$\Delta_T = \alpha L(T_{\max design} - T_{\min design}) \qquad (Eq.2)$$

Where Δ_T represents the expected movement due to uniform temperature change (in.), α represents the coefficient of thermal expansion (in./in./^{o}F), and L represents the length considered (in.). This equation corresponds to Equation (3.12.2.3-1) in the current AASHTO provisions.

2.9.3 Vertical Thermal Gradient

The 2012 version of the AASHTO guidelines recognize the existence of thermal gradients. Thermal gradients are first mentioned in the general provisions in Section 3.12: Force Effects Due To Superimposed Deformation, which states:

"The effect of a temperature gradient should be included where appropriate."

The provisions due not, however, expand on when the conditions are appropriate to consider thermal gradient. Additionally, the provisions do not require the thermal gradient be considered in design if past experience indicates that it is not necessary to maintain the functionality of the bridge. Specifically, commentary to Section 3.12.3 states:

> *"Temperature gradient is included in various load combinations in Table 3.4.1-1. This does not mean that it need be investigated for all types of structures. If experience has shown that neglecting temperature gradient in the design of a given type of structure has not lead to structural distress, the Owner may choose to exclude temperature gradient."*

The possessor of this past experience, who can determine if thermal gradient needs to be considered on the current structure under consideration, is not specified. A more clear indication of this guideline would be helpful when designing a new bridge or retrofitting an existing bridge. Rather than allow an undefined person's past experience dictate the neglect or inclusion of thermal gradient in a design, a limit on bridge length, depth, or materials could be provided that would determine when thermal gradients can be neglected. The particular length, skew, or curvature is not currently mentioned in the commentary permitting neglect of the vertical temperature differential. Refinement of the verbiage used in the commentary and the provisions could significantly assist design engineers in determining when a thermal gradient should be considered.

The current design standards for vertical temperature gradients are based on research completed in 1985 by Imbsen and Vancershaf for the Transportation Research Board for concrete bridges. The design considerations for steel bridges are adopted from the Australian provisions found in AUSTROADS. Figure 2-6 shows the suggested vertical thermal gradient to use if the designer determines that a thermal gradient should be considered.

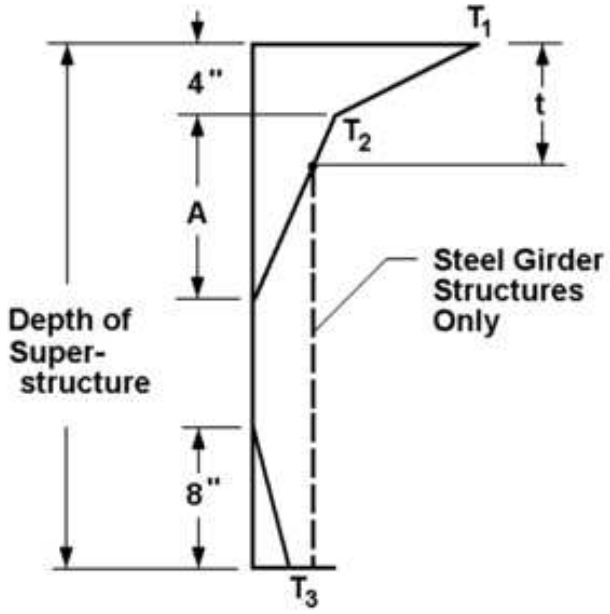

Figure 2-6. Positive Vertical Temperature Gradient in Concrete and Steel Bridges (AASHTO 2012, Section 3.12.3)

Different values are assigned to the variables displayed, but only one value is assigned to encompass the behavior of any steel bridge. The dimension *A* is taken as 12 inches and the dimension *t* is taken as the depth of the concrete deck. For steel structures, the dimension t is taken as the depth of the concrete deck. A complete definition of dimension *A* is shown in the table below.

Table 2-1. Dimension A (AASHTO 3.12.3)

Concrete superstructures that are 16.0 in. or more in depth	12 in.
Concrete sections shallower than 16.0 in.	4 in. less than the actual depth
Steel superstructures	12 in.

This way of defining the dimension, the extent to which the positive thermal gradient extends downwards below the deck surface, appears over-simplified. The depth, width,

orientation or length of a steel superstructure has no bearing the value of A. Perhaps a further subdivision in this dimension for steel superstructures, as seen for the concrete superstructures, would be appropriate. A more general, all-encompassing equation for the value of *A* would seem most sophisticated and accurate. This could allow the variation to occur linearly, quadratically, or whatever is determined appropriate rather than in a piecewise manner. There is always a tradeoff between accuracy and simplicity in design. A complicated model that captures thermal behavior very accurately might cause problems if it is so hard to use that computation errors are introduced.

The values for T_1 and T_2 are determined using a contour map that subdivides the United States into radiation zones to which different values of T_1 and T_2 are assigned. The contour map used is shown in Figure 2-8. Table 2-2 shows the corresponding values of T_1 and T_2.

Figure 2-7. Solar Radiation Zones of the United States
(AASHTO 2012, Figure 3.12.3-1)

Table 2-2. Temperature Gradient Benchmarks (AASHTO 3.12.3-1)

1	54	14
4	46	12
3	41	11
4	38	9

The value of T_3 is taken as 0^oF unless a site specific study is conducted and yields a different value. In no circumstance is T_3 to be taken as greater than 5^oF (AASHTO Bridge Design Specifications, Section 3.12.3).

This representation does not include equations or methods of taking into consideration other parameters such as girder depth, bridge length, connection type, deck joint presence, bearing presence, bridge skew, or bridge curvature. A more representative, multiple parameter equation to represent this behavior would allow practitioners to better evaluate and design for the vertical temperature gradient in steel bridges.

2.9.4 Transverse Thermal Gradient

The topic of transverse (perpendicular to the longitudinal axis) thermal gradient is mentioned in current AASHTO provisions in the commentary of Section 3.12, which states:

1) *"Wide bridges are particularly prone to large lateral thermal forces because the bridge expands radially as well as longitudinally."*
2) *"Redistribution of reactive loads, both longitudinally and transversely, should also be calculated and considered in the design of the bearings and substructures."*

However, no specific procedure or gradient is suggested or required to account for the transverse thermal gradient.

It is not difficult to find a circumstance in which a transverse gradient demands consideration. For example, on integral bridges with a north-south orientation, the warming of

the east side of the bridge will occur earlier in the day than warming of the west side of the bridge. The longitudinal deformation of the bridge would be greater on the east side than on the west side in the morning. This could cause a slight bend of the bridge's longitudinal axis if the bridge was allowed to freely rotate and move and was constructed without deck joints to accommodate the uneven movements. If the bridge is retrained rigidly at either abutment throughout the cross section without bearings, axial compression would develop in the warmer side of the bridge and tension would develop in the cooler side of the bridge. The significance of this differential warming would depend on the bridge length, skew, curvature at uniform temperature, and connection types at the piers and abutments. Further research on the transverse temperature gradient could determine how consideration of this phenomenon can be incorporated into the design.

2.10 Conclusion

Multiple studies have been conducted on the subject of deck joint elimination and thermal loading on bridges. Often there is enough lacking from the studies to develop a specific design and modeling procedure to apply steel bridges in Colorado. Much of the numerical and finite element analysis that has been conducted involving eliminating existing deck joints has been conducted using two-dimensional modeling. However, three-dimensional modeling would be more accurate because thermal gradients can be added to the analysis and local behavior can be analyzed. Additionally, connecting the analysis of thermal loading of geographically specific bridges and of deck joint elimination in one study will enable Colorado to develop a design procedure specific to the region. Finally, a clear need for life-cycle cost analysis for eliminating deck joints exists in this field. By combining field-measured thermal loading analysis, finite

element modeling of deck joint elimination, and life-cycle cost analysis, a method can be establish that is specific to Colorado that will assist in the decision making process of deck join elimination and the resulting design procedure.

CHAPTER 3

BRIDGE SELECTION AND FIELD INSTRUMENTATION

3.1 Introduction

In collaboration with the Colorado Department of Transportation, multiple bridges were considered for instrumentation to investigate thermal loading and the implications of deck joint elimination. To correlate the movements detected by the instrumentation as much as possible to those due thermal effects, specific geometries and characteristics of candidate bridges were desired. The bridges selected for modeling needed to possess at least one deck joint and simply supported structural elements that frame into the deck joint. Safe access to bridges for instrumentation purposes was also an important factor considered when assessing bridge candidates. Bridges with minimal skew, minimal horizontal curvature, and minimal vertical curvature were sought.

As discussed in Chapter 2, skew and curvature have an effect on the movements of bridges under thermal loading. However, this study focuses primarily on the vertical thermal gradient. In order to truly assess how a vertical thermal gradient manifests itself in bridge movement and performance, it was necessary to minimize the effects that other bridge characteristics would have on the sensors' measurements. Therefore, bridges possessing minimal-to-no skew and curvature were considered for model calibration and deck joint performance assessment.

One concrete and one steel bridge were chosen for field testing and for numerical modeling in CSi Bridge, a finite element software produced by the maker of SAP2000. An instrumentation plan was developed to capture the thermal loading throughout the superstructure

depth at the expansion joint and the structural response. Therefore, temperature sensors, strain sensors and displacement sensors were used on the bridges selected for fine instrumentation. Details of the instrumentation plans for the two bridges chosen to be finely instrumented are discussed further in Section 3.4.

An additional 16 bridges were chosen to be instrumented across the state of Colorado with scratch gauges. A scratch gauge is a displacement sensor that was developed by the Colorado Department of Transportation and manufactured at the Structural Engineering Laboratory at Colorado State University. It is a non-electronic displacement sensor developed to assess the influence of regional variations on expansion joint movement. Further details on the scratch gauge configuration are discussed in Section 3.4.

3.2 B-16-FM

The steel bridge selected for the study, B-16-FM, is located approximately 10 miles north of Fort Collins, CO and allows County Road 58 to pass over Interstate 25. The proximity to Colorado State University will give future researchers access to the bridge to troubleshoot any difficulties with the Data Acquisition System (DAQ) and/or instrumentation sensors. The figure below shows an aerial view of B-16-FM.

Figure 3-1. Plate Girders for Bridge B-16-FM (Google Maps Image)

The bridge possesses three steel plate girders with varying flange thicknesses, bearing and intermediate stiffeners, and steel diaphragms. Traffic crosses the bridge through one east bound and one westbound lane. Figure 3-2 the superstructure from under the west abutment of the bridge.

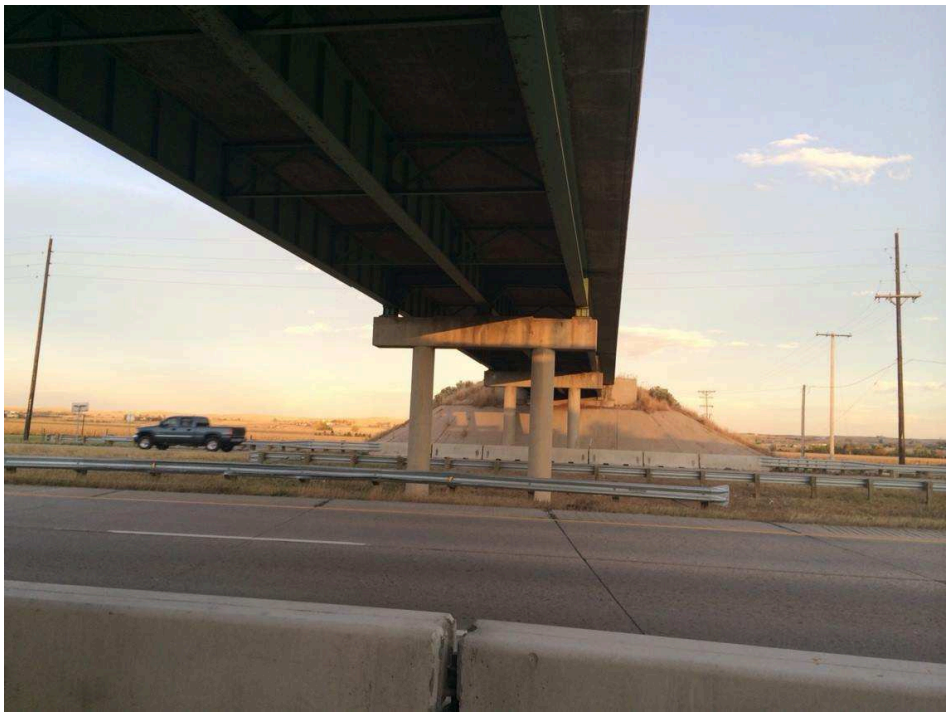

Figure 3-2. B-16-FM Superstructure from the West Abutment (photo by Author)

The bridge consists of 4 spans (3 steel spans and 1 short, concrete approach span). The three steel spans are 74’6” feet in length, simply supported, and separated by expansion joints. Figure 3-3 shows another view of the superstructure and piers. Finger joints, a common type of expansion joint, shown in Figure 3-4, are in place over the expansion joints to allow thermal movement. The spans are supported on rocker bearings that transfer the loads to the piers.

Figure 3-3. View of B-16-FM from East Abutment (Photo courtesy of CDOT)

Figure 3-4. Finger Joint Clogged by Debris on B-16-FM (Photo courtesy of CDOT)

The bridge superstructure was instrumented at the centermost pier, labeled pier 3 by CDOT nomenclature. Thermocouples, strain gauges, and linear potentiometers were used to collect information about temperature, strain, and displacement, respectively. In addition to instrumenting the joint with sensors, an additional strain gauge was placed at the bottom of the web of the plate girder at mid-span of an adjacent span to validate the finite element model. Data used in calibration were obtained using control load testing. The test was conducted using a truck with known dimensions and axle weights, which was provided by CDOT. More information about the control load testing can be found in Chapter 5.

3.3 C-17-AT

A three-span, five-girder traditionally reinforced concrete bridge was chosen as the concrete bridge for the study. C-17-AT carries northbound Interstate 25 over a gravel service road and is shown in Figure 3-5 and Figure 3-6 below. The bridge is located approximately 30 miles south of Colorado State University. The proximity to Colorado State University will give future researchers access to the bridge to troubleshoot any difficulties with the Data Acquisition System (DAQ) and/or instrumentation sensors.

Figure 3-5. Aerial View of C-17-AT (Photo courtesy CDOT)

Figure 3-6. C-17-AT (Photo courtesy CDOT)

The concrete girders are traditionally reinforced, the spans are simply supported, and two expansion joints separate the three spans. Extensive corrosion and damage is observable below the deck joints. Figure 3-7 shows the discoloration of the pier caps that are directly below the expansion joints.

Figure 3-7. Discoloration under expansion joint on C-17-AT (Photo courtesy CDOT)

3.4 Scratch Gauge Bridge Selection

The Colorado Department of Transportation is divided into five regions as shown in Figure 3-8. Bridges selected for instrumentation with scratch gauges at expansion joints were chosen largely through coordination with CDOT maintenance and engineering staff that work in the regions of interest. The staff for each region was very knowledgeable about the issues their bridges were facing and helped ensure that the bridges chosen were the most logical choices. A list of the bridges selected is provided in Table 3-1.

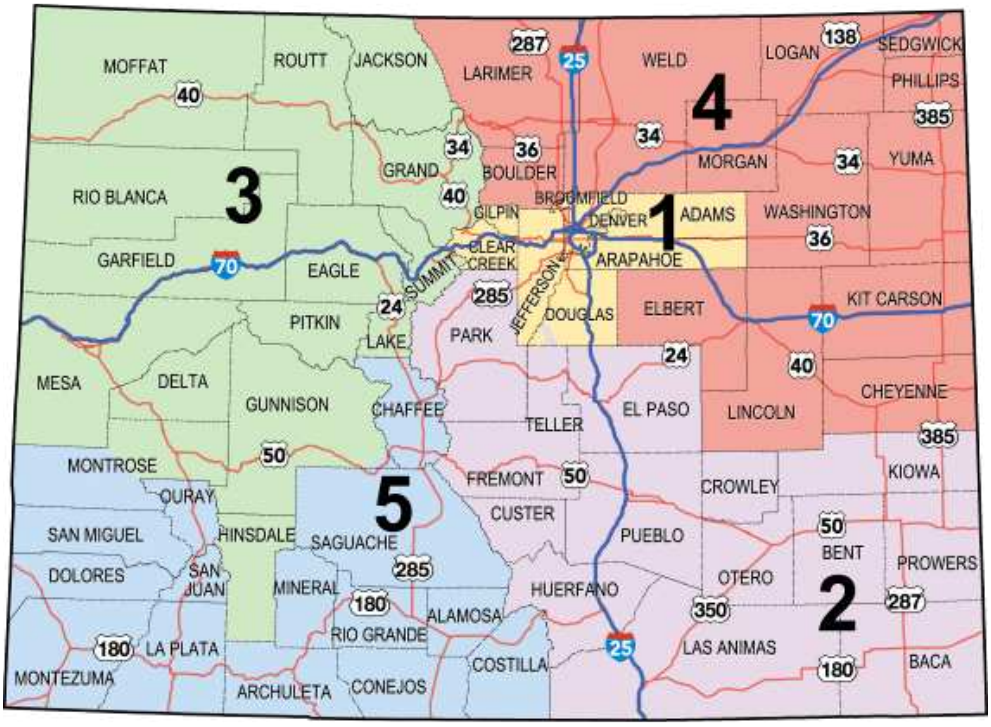

Figure 3-8. CDOT Regions (https://www.codot.gov/about/regions.html)

In total, ten concrete bridges and eight steel bridges were selected for the scratch gauge instrumentation. Of the ten concrete bridges selected, six of the bridges were oriented north to south and four were oriented east to west. Of the eight steel bridges selected, four were oriented east to west and four were oriented north to south. The different orientations are of interest because they receive different amount of radiation from the sun. Table 3.1 shows the orientation and girder material for each bridge selected. The reason for selecting bridges with different orientations is to assess the influence that that parameter has on thermal loading and deck joint behavior.

Table 3-1. Bridges Selected for Scratch Gauge Instrumentation

REGION	Bridge Name	Girder Material	Orientation
REGION 1	F-16-DX	Steel	North-South
	E-16-EM	Steel	East-West
	F-16-JX	Concrete	East-West
	F-18-T	Steel	East-West
REGION 2	L-26-H	Steel	North-South
	L-26-BW	Concrete	North-South
	L-28-AQ	Concrete	East-West
	L-24-D	Concrete	North-South
	L-24-A	Steel	North-South
REGION 3	F-08-BH	Concrete	North-South
	F-08-AU	Concrete	North-South
REGION 4	C-20-AS	Concrete	North-South
	B-24-O	Concrete	East-West
	B-24-P	Concrete	East-West
	B-16-FM	Steel	East-West
	C-17-AT	Concrete	North-South
REGION 5	J-12-AK	Steel	North-South
	I-12-T	Steel	East-West

The maintenance crews from each region performed the installation of the scratch gauges following instructions prepared by the research team. The instructions provided can be found in Appendix B. The ambient air temperature near the bridge at the time of installation was recorded and sent to the research team. Additionally, every three months, the maintenance crews that

installed the scratch gauge will take photos of the scratch gauges and send them to the research team. The scratch gauges will be left on the bridges for an amount of time that is yet to be determined by the Colorado Department of Transportation. The two bridges that are finely instrumented have scratch gauges that were installed by the research team at Colorado State University research team.

Scratch gauges, shown in Figure 3-9, were used to monitor relative displacement between two girders at a joint. The scratch gauges were constructed at the Colorado State University Structural Engineering Laboratory based on a prototype provided to the research team by CDOT. The black scratch surface is attached to one side of the deck joint and the aluminum scratch piece is attached to the other. The sharp point on the scratch piece will draw a line on the painted black surface of the scratch surface. These scratch gauges will be applied to many bridges across the region to assess overall movement of many bridges in different regions of Colorado.

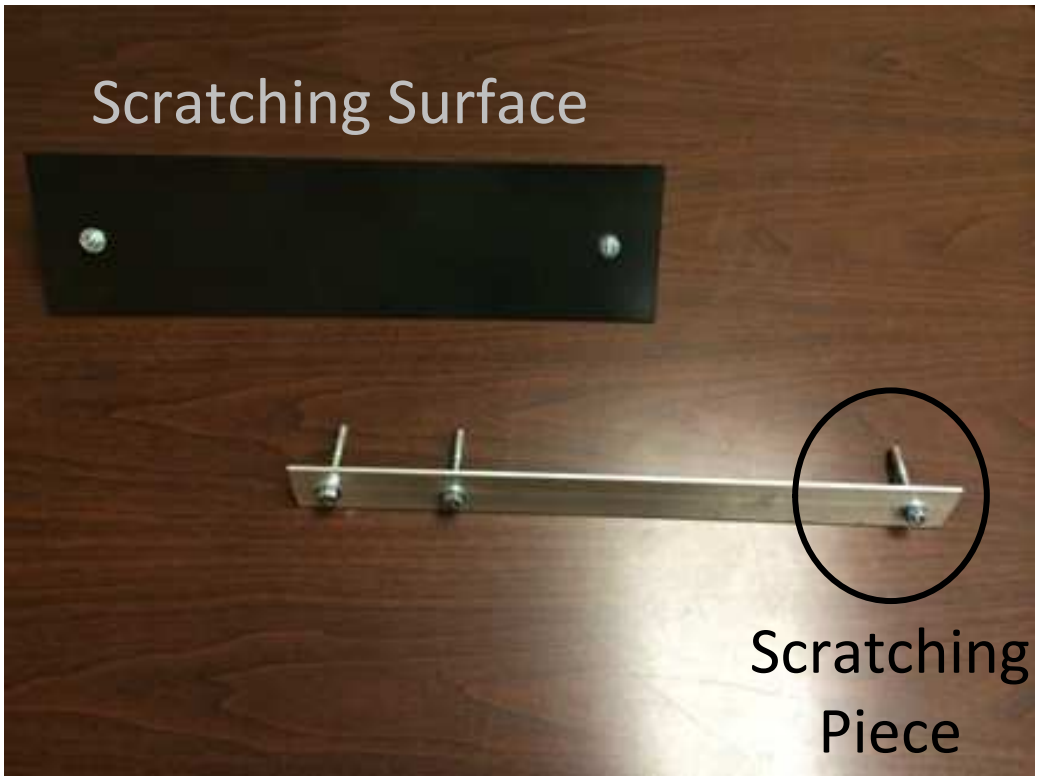

Figure 3-9. Scratch Gauge (gauge idea proposed by CDOT)

3.5 Field Instrumentation

Evaluation of current deck joint performance and validation of the finite element model was completed using field data collected through monitoring of in-service bridges in Colorado. The same instrumentation plan concept was used for both the concrete and steel bridge, although only the steel bridge is evaluated in this thesis as previously indicated. Different sensor models were used where appropriate to accommodate different bridge materials and span lengths. Sensors were installed on an existing deck joint for each bridge. The remainder of this section focuses on the selected steel bridge, B-16-FM. On the steel bridge, the instrumentation was installed on the centermost pier, Pier 3, that separated two simply supported steel spans. A

detailed description of the location of the strain gauges, thermocouples, and linear potentiometers can be found in Appendix C.

3.5.1 Access to Expansion Joint

To access the expansion joint on B-16-FM, an Aspen Aerial A-40 Inspection Unit was used. This unit was operated by CDOT employees. The truck has a platform for workers and/or inspectors to occupy. The arm of the snooper truck allows the platform to access tight areas. Figure 3-9 shows the truck reaching its position near the expansion joint on site. Figure 3-10 shows the position the platform was in for the majority of the instrumentation. One strain gauge was placed at mid-span and required a lane closure. The same snooper truck was used to achieve this installation.

Figure 3-9. Aspen Aerial A-40 Snooper Truck on B-16-FM

Figure 3-10. Snooper Truck in Position for Instrumentation

3.5.2 Displacement Sensors

Linear potentiometers were mounted on the bridge to evaluate the opening and closing of the joint. The sensors, manufactured by Celesco (model CLP 50), have a displacement range of 2 inches with a precision of 0.004 inches. An example of this displacement sensor is shown in Figure 3-11. The sensors were wired as a half bridge voltage signal.

Figure 3-11. Fully extended CLP 50 linear potentiometer in the Laboratory

In total, four linear potentiometers were installed on B-16-FM at the deck joint. The surface that the sensors were mounted to was ground and cleaned with acetone prior to installation. Three were installed on the plate girders (one near the bottom flange, one near mid-depth of the web, and one near the top flange). This distribution will allow future researchers to assess the potential uneven opening and closing of the joint along the depth of the plate girder. The initial opening of the joint at the plate girder was recorded upon instrumentation. Figure 3-12 shows the linear potentiometers on the plate girder.

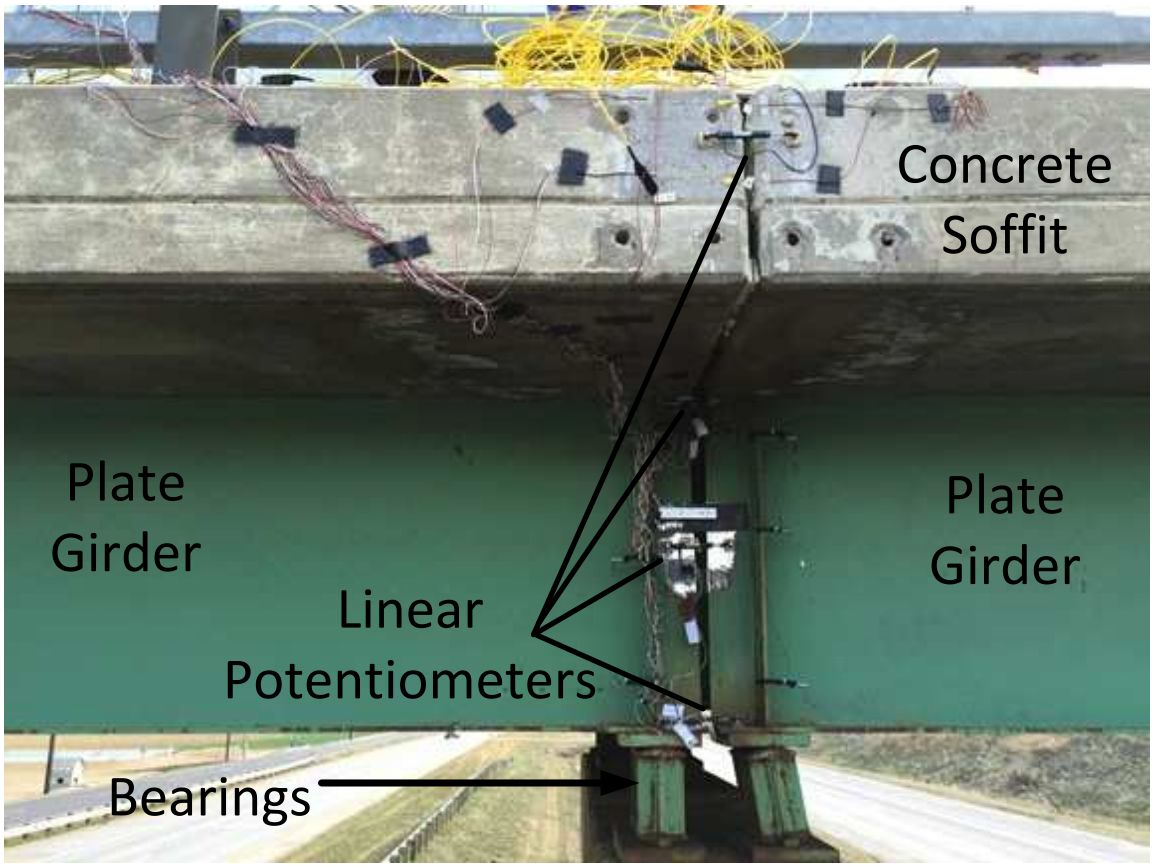

Figure 3-12. Linear Potentiometers on Plate Girder

The fourth linear potentiometer was placed at mid-depth of the side of the concrete deck to assess the opening and closing of the joint near the deck surface. Figure 3-13 shows the linear potentiometer on the concrete soffit.

Figure 3-13. Linear Potentiometer Installed to Measure Relative Displacement at Deck Level

In order to mount the linear potentiometers onto the bridge, small mounts were constructed at the Colorado State University Structural Engineering Laboratory. They were made of 5/8” thick acrylic squares with an embedded threaded bar. Each end of the linear potentiometer was secured to the threaded bar with appropriately sized nuts. The mount was

attached to the bridge surface using epoxy and Gorilla Glue. The mounts are shown in Figure 3-13 above. Then, the linear potentiometers were covered with a half of a PVC pipe to protect the sensor from the weather and outdoor elements. The PVC pipe covering was only attached to one side of the joint such that it does not inhibit joint movement. Figure 3-14 shows the linear potentiometers after covered by the PVC pipe.

Figure 3-14. Linear Potentiometer covered by PVC pipe

3.5.3 Temperature Sensors

Thermocouples were used to assess the temperature variations throughout the bridge depth. The thermocouples installed were produced by Omega Engineering, Inc. The sensors, type K, model SA2F-K-120 with 3 m lead wires, have a temperature range of -50 to 200°C (-58°F to 392°F). Figure 3-15 shows the sensor in the laboratory.

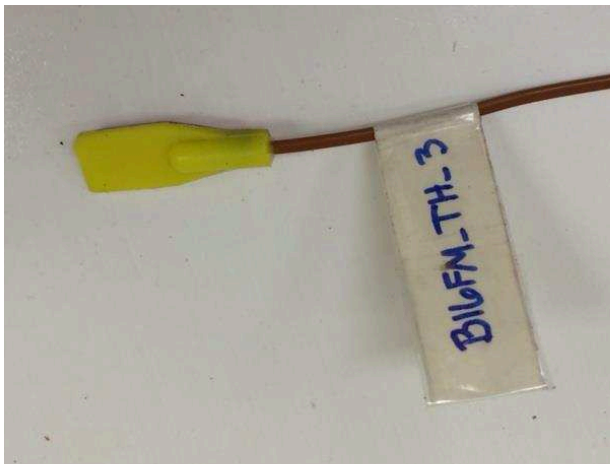

Figure 3-15. Thermocouple Sensor

Type K thermocouple extension wire was used to connect the sensors to the data acquisition system. Type K thermocouple connectors were used to connect the sensor to the extension wires as shown in Figure 3-16.

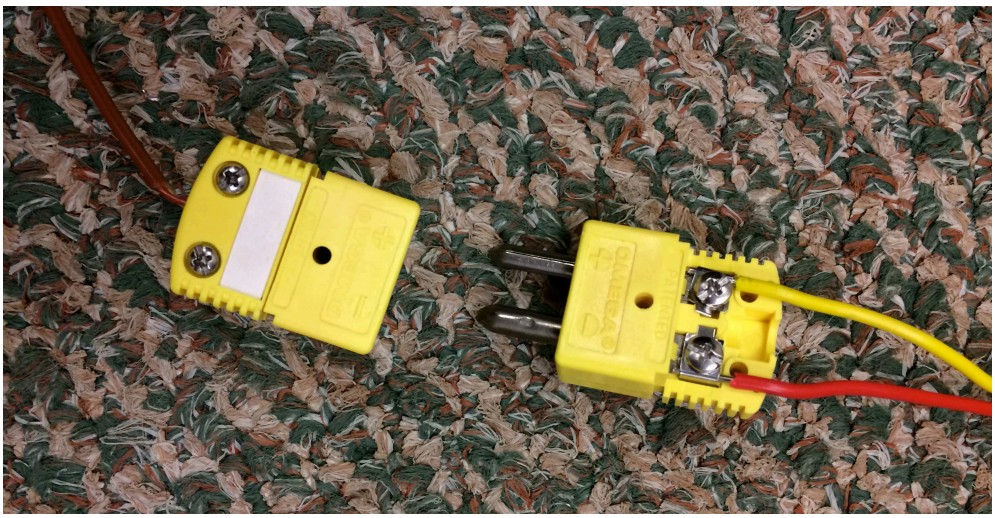

Figure 3-16. Type K Thermocouple Couple Connector

To install the thermocouples, the surface was ground and cleaned with acetone. The sensor was then attached with epoxy and secured such that no tension in the wires was allowed at the sensor. Figure 3-17 shows an installed thermocouple on the plate girder.

Figure 3-17. Installed thermocouple on B-16-FM to Measure Relative Displacement between Girder Ends

In total, five thermocouples were installed. Three were installed throughout the depth of the plate girder and two were installed on the soffit of the concrete deck. On the plate girder, one was installed on the bottom flange, one at mid-depth, and one on the top flange. On the concrete soffit, one was placed near the deck surface and the other was placed at mid-depth of the soffit. This is shown below in Figure 3-18.

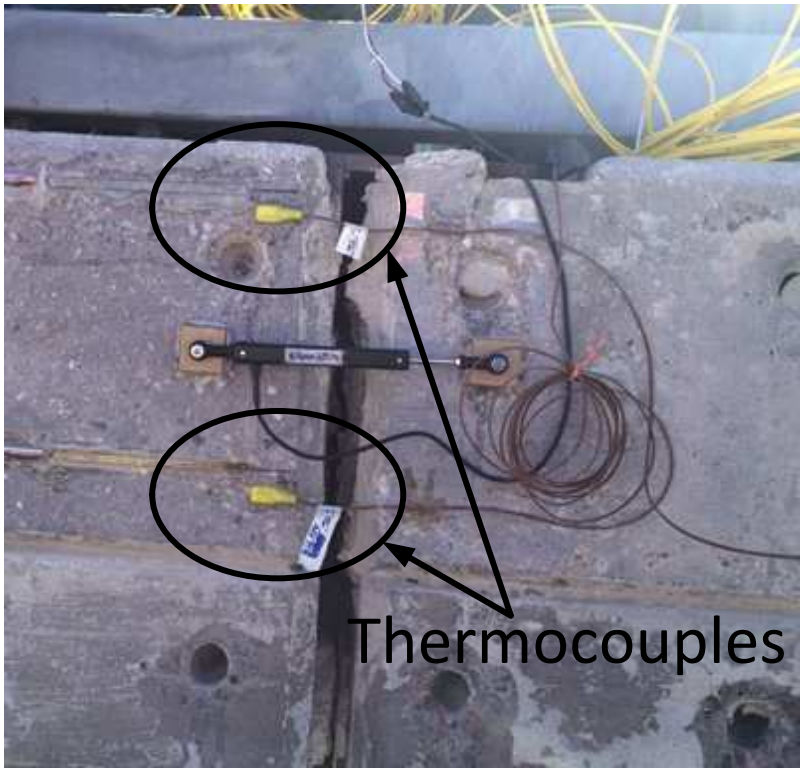

Figure 3-18. Thermocouples Installed on Concrete Soffit

3.5.4 Strain Gauges

A strain gauge manufactured by Omega Engineering, Inc. was used at the steel locations. The model was SGD-5/350-LY11 which has a 5 mm grid and a resistance of 350 ohms. This strain gauge was used at all steel locations. These gauges for the steel locations were soldered in the lab prior to going to the site of B-16-FM.

A longer strain gauge, also manufactured by Omega Engineering Inc., was used for the two concrete gauge locations. The model used was SGD-150/240-LY40 which has a length of 150 mm and a resistance of 240 ohms. The longer gauge was necessary because concrete is a nonhomogeneous material. If a shorter gauge was used, it would capture the strain on one or only a few of the aggregates, not of the structural element's overall performance. These strain gauges were soldered in the field. Figure 3-19 shows this concrete gauge being soldered in the field.

Figure 3-19. Soldering Quarter Bridge wires to Concrete Strain Gauge

Strain gauges were installed at the deck joint throughout the depth of the plate girder and the concrete soffit. At the top and the bottom flange, two strain gauges were installed in approximately the same location to create redundancy in the data acquisition set up. An additional strain gauge was installed at mid-depth of the plate girder's web. In total, five strain gauges were installed on the plate girder. Figure 3-20 shows the two gauges as they were initially placed on the bottom flange at the joint.

Figure 3-20. Initial Installation of Strain Gauges on Bottom Flange on B-16-FM

After the strain gauges were installed, they were covered with a butyl rubber covering from Vishay Measurements, Inc. (Barrier E Butyl Rubber Vinyl, Part number MMF022872 EAR99). Then the cover connected to the girder surface with caulk and epoxy. A covered strain gauge is shown below in Figure 3-21.

Figure 3-21. Covered Strain Gauge using Butyl Rubber Vinyl Barrier E

An additional strain gauge was installed at mid-span of the simply supported girder following the same procedures. Data from this gauge was collected during a control load test. This data was then used to further validate the finite element model.

3.5.5 Data Acquisition System

A Campbell Scientific CR9000X Data Logger was used for the collection of the data. The logger is a high-speed, multi-channel, 16-bit system configured with digital and analog filters to assure noise-free signals. Real-time data were viewed while on site by connecting the logger directly to a laptop computer. This was done in order to assure that all sensors were functioning properly and to review the response of the bridge during testing when data collection was started and stopped manually using the laptop.

The CR9000X data logger was enclosed in a weather-tight job box at the instrumented deck joint, as seen in Figure 3-22. Figure 3-23 contains a photograph of the inside of the box. The job box was placed under the east abutment of the bridge and locked to the bearing.

Figure 3-22. Weather Tight Job Box Containing CR9000X Data Logger

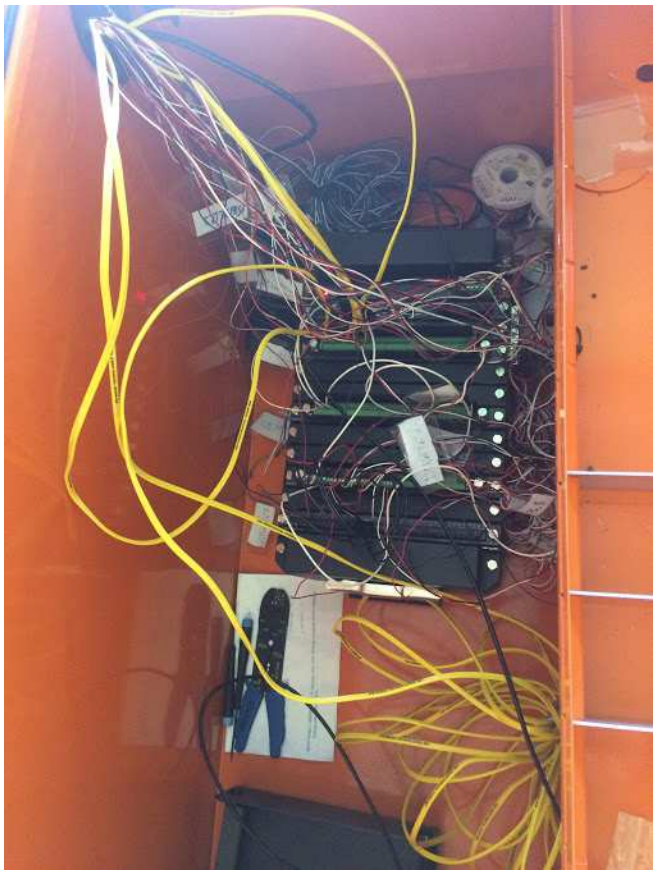

Figure 3-23. Inside of Weather Tight Job Box Containing CR9000X Data Logger

The wires were run from the joint, under the guardrails, and then down to the job box that contained the CR9000X data logger. The wires under the guard rail were placed in halved PVC pipes and the PVC pipes were zip tied to the guard rails as shown in Figure 3-24. An AC power outlet supplied by CDOT was placed at the abutment such that power is always supplied to the data logger.

Figure 3-24. Wires Placed in PVC pipe and Secured to the Guard Rail

To retrieve the data, two methods are available to researchers. The CR9000X contains a 250 MB memory card that stores data. The card will not be full for over 3 years. Additionally, a wireless data collection was established to allow researchers to view real-time data from the laboratory. A Campbell Scientific RAVENXTV modem was used in congruence with Version Wireless to send the data wirelessly back to the laboratory.

3.6 Initial Thermal Data

Though the sensors will remain on the bridge for several seasons, one month of data is available as of the completion of this thesis. Figure 3-25 below shows the initial temperature data measured by the thermocouples placed throughout the depth of the expansion joint.

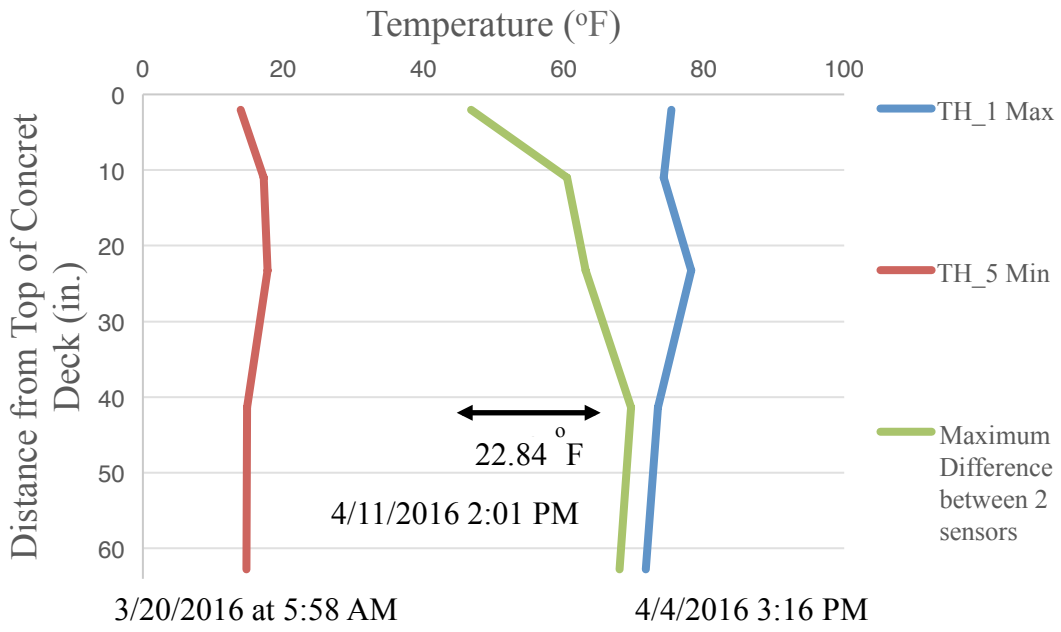

Figure 3-25. Initial temperature data - One month of data collection

The blue line in Figure 3-25 shows the temperature distribution when the first thermocouple (TH_1) is at its highest values for the month of data being examined. The first thermocouple (TH_1) is located 2 inches below the deck surface on the concrete soffit. This highest value for TH_1 occurred on April 4, 2016 at 3:16 PM. The thermal distribution for this point in time is relatively uniform, as expected, because the bridge has had the entire afternoon to be heated. This maximum temperature is 75.32°F.

The red line in Figure 3-25 shows the temperature distribution when the fifth thermalcouple (TH_5) is at its lowest value for the month of data being examined. The fifth thermocouple (TH_5) is located at the bottom of the web at the joint. This lowest value for TH_5 occurred on March 20, 2016 at 5:58 AM. This thermal distribution is relatively uniform, as expected, because the bridge has had the entire night to cool. This minimum temperature of the fifth thermocouple is 13.97°F.

The green line in Figure 3-25 shows the temperature distribution when the difference between any two thermocouples was the greatest. This occurred on April 11, 2016 at 2:01 PM and there is a difference of 22.84^{o}F between the sensor nearest the deck surface and the sensor at mid-depth of the web. The maximum considered difference between temperatures in the depth of the section, as described by AASHTO for a bridge in Colorado, is 40^{o}F. The overall temperature range for this month is also illustrated by Figure 3-25. The bridge experienced a tempearture change of 60^{o}F from March 11, 2016 to April 7, 2016.

3.7 Conclusion

Two bridges, one with concrete girders and one with steel girders, were selected for the in-service assessment of the joint behavior. The steel bridge was instrumented to assess thermal loading. The concrete bridge will be instrumented in the following summer season. The majority of the sensors were placed at the deck joint and one strain gauge was placed near mid-span to validate the finite element model during control load testing. In addition, 16 other bridges will be instrumented with scratch gauges at various locations in Colorado to assess movements in bridges. Further information about the finite element model and the control load testing can be found in Chapter 4 and Chapter 5, respectively.

CHAPTER 4

FINITE ELEMENT MODEL AND PREDICTIONS OF FIELD BEHAVIOR

4.1 Introduction

One of the primary objectives of this study was to establish a finite element model to assess thermal movements, thermal stresses, and joint removal retrofit options. The developed design and assessment procedures were developed with the intent to be used in industry for eliminating bridge joints. Therefore, choosing a finite element software that is widely used by practicing engineers is vital to correct implementation of the developed procedure. CSi Bridge software (same developers as SAP2000) was chosen by CDOT due to its prevalence of use in private practice. This chapter focuses on the model for the steel bridge; B-16-FM. Theoretical calculations were performed using composite beam theory in order to verify the finite element model.

Multiple loading scenarios were considered. Dead loads due to self-weight, uniform loads, and point loads were considered first during the verification process. Then, live loads due to AASHTO HS20-44 loading and a CDOT A-40 snooper truck were examined. Agreement between the CSi Bridge model, the theoretical calculation, and field measurements was found to be very good. The strong validation of the finite element models solidified confidence in the results of the parametric study discussed in Chapter 6.

4.2 B-16-FM: Steel Plate Girder Bridge with Concrete Slab

Geometric and structural properties specific to B-16-FM, and the modeling techniques, are discussed in this section. The structural information and dimensions were obtained from the construction documents provided by CDOT. The bridge is described in Section 3.2 with photos from the site. Steel plate girders support three spans with a length of 75 ft each and one shorter approach span (44 ft) at the end of the bridge is supported by concrete girders. The steel span's superstructure consists of three plate girders that are spaced at 10 ft on center in the transverse direction.

The top and bottom flange thickness of the plate girders varies along the length. The flanges nearest to the vertical supports are 5/8" thick. The thickness of the flanges increases to 1 1/4" after a distance of 11 ft from the supports is reached. Finally, for the central 32 ft of the girders, the flanges are 1 ¾" thick. Figure 4-1 shows the layout of flange variance in one girder that is typical for all three steel spans.

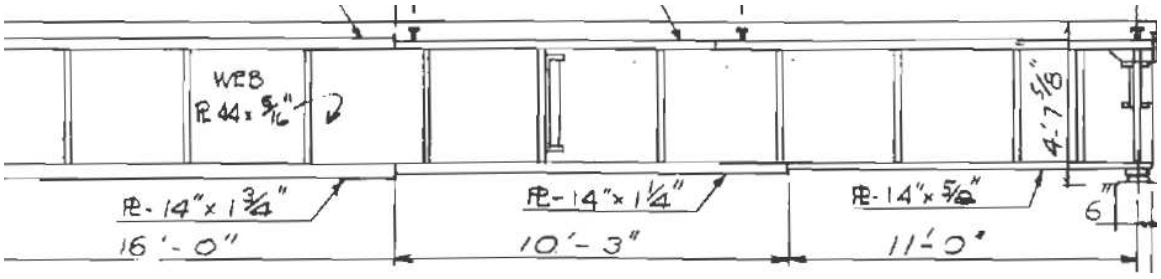

Figure 4-1. Plate Girders in Construction Documents for Bridge B-16-FM (Courtesy CDOT)

Intermediate stiffeners are located along the length of the plate girders and bearing stiffeners are located near the supports. The web is 5/16" inches thick and 44" in height. The diaphragms between girders were excluded from the model. The main function of the

diaphragms is to tie the girders together during construction so their absence in the finite element model is trivial. In the case of bridge skewedness or curvature, then torsional stresses could develop, which would require that the diaphragms are kept in place. Since this bridge does not possess any skew, curvature (no torsion-induced loading), the diaphragms are excluded from the finite element model. Figure 4-2 shows the extruded view of the plate girders with the intermediate and bearing stiffeners. The slab is excluded from this view to better show the girders.

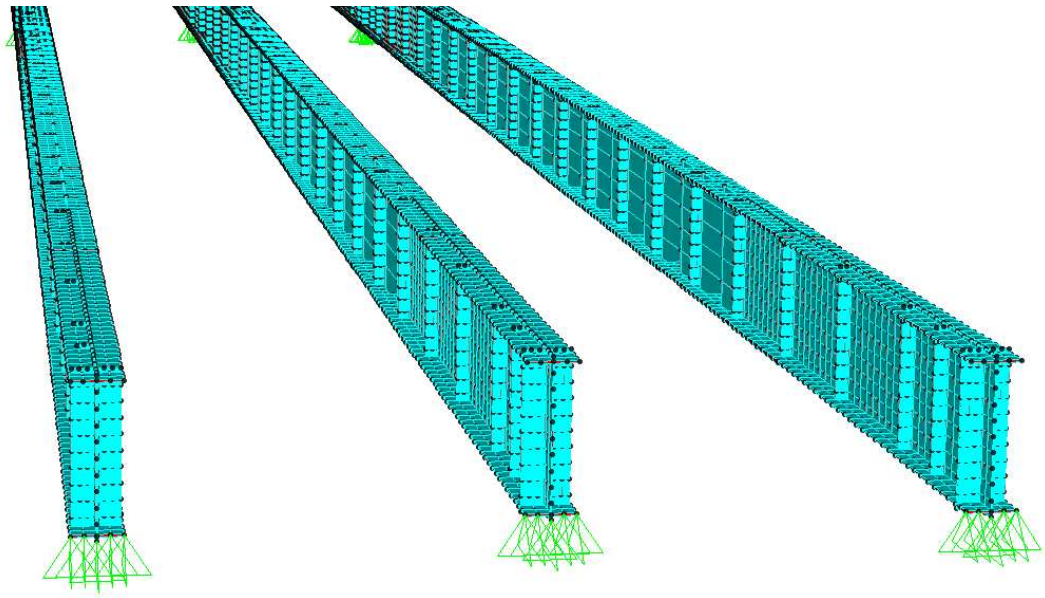

Figure 4-2. Plate Girders for Bridge B-16-FM

The slab was modeled considering the super-elevation described on the construction documents. The high point of the slab is along the centerline of the roadway and a slope of 0.015 ft/ft downwards exists on each side until the centerline of the outside girders. Then the slab ceases to change elevation. This results in an elevation at the edge of the deck that is 2.4 inches lower than at the centerline. Figure 4-3 shows the slab geometry in the construction documents and Figure 4-4 shows the slab geometry in the finite element model.

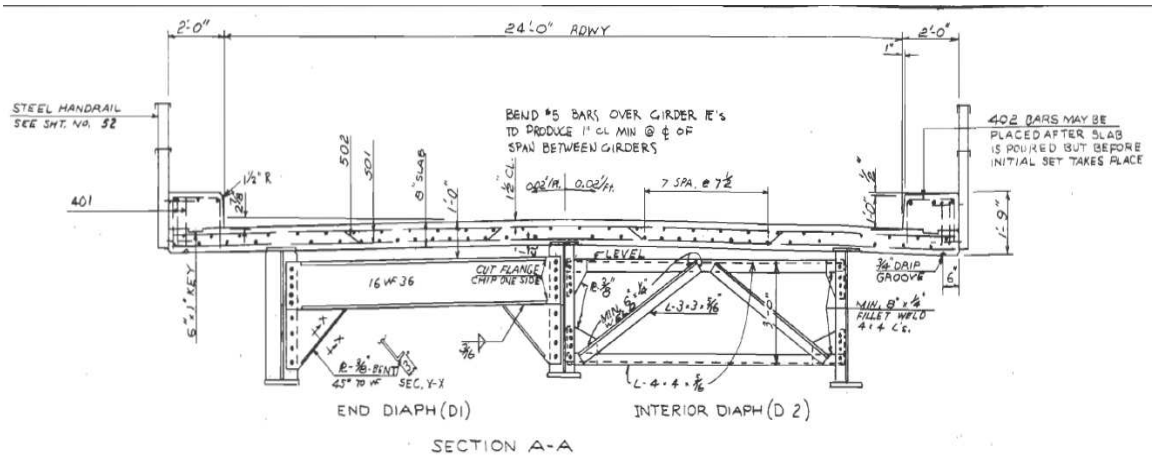

Figure 4-3. Slab Geometry described in the Construction Documents (Courtesy CDOT)

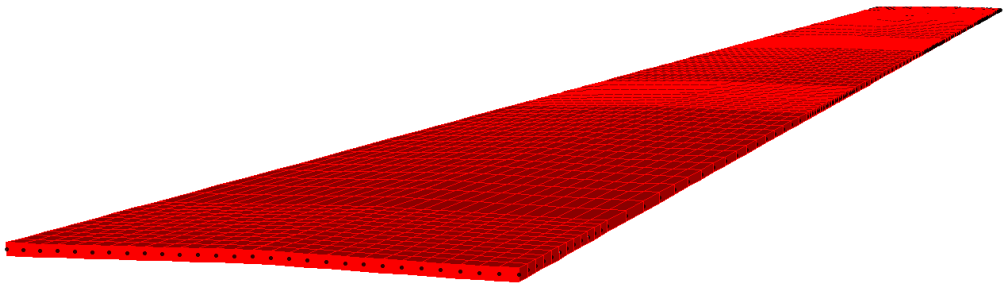

Figure 4-4. Finite Element Model Illustration of super-elevation described in the Construction Documents

The bridge's bearings transfer the superstructure load to the pier caps. The bearings for the steel bridge disallow translation and allow rotation at the end of each girder. Therefore, the supports are modeled as pin connections that prevent translation in all directions and allow rotation about all axes. The boundary conditions are further discussed in Section 4.3.5.

A few more views of the full-scale bridge model are shown in the following figures. The different materials are represented by different colors, cyan and red for the steel and concrete,

respectively. Figure 4-5 shows an extruded view of the superstructure. Figure 4-6 shows all spans in the superstructure.

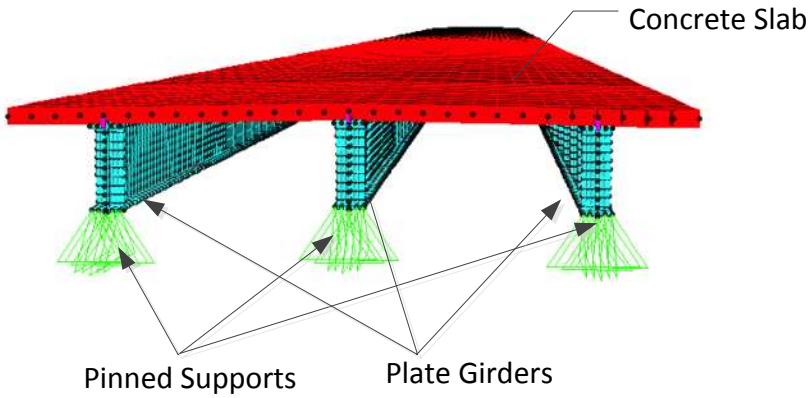

Figure 4-5. Extruded View of B-16-FM Superstructure

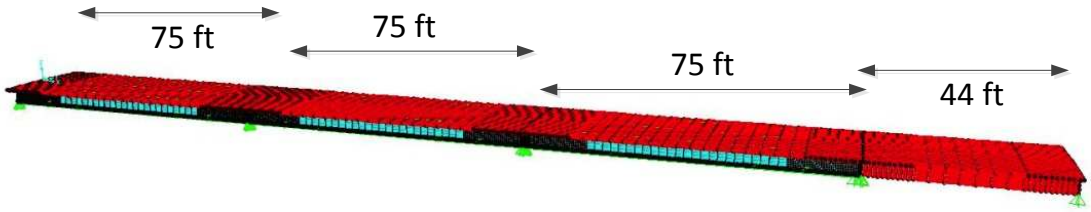

Figure 4-6. Alternative view of B-16-FM Bridge Model (unstressed, unloaded state)

4.3 CSi Bridge Model Methodology

A three-dimensional model was used to capture both the localized behavior at the joints and the global response to thermal loading with great accuracy. To build the three-dimensional model, shell and frame elements were used in CSi Bridge to represent various bridge elements. The model was used to examine the effects of gravity loading, dynamic loading, thermal loading (both uniform temperature changes and non-uniform gradients), deck joint performance, on the

behavior of the bridge. After validating the model's responses, the model was used to perform the parametric study discussed in Chapter 6.

4.3.1 Shell and Frame Elements

Shell elements were used for the majority of the structural elements in the bridge.. Flange, web, intermediate stiffeners, and bearing stiffeners were modeled individually with properties of Grade 50 steel and with the thickness as described in the construction documents. The built up plate girder was connected to the slab with shear studs composed of an appropriately sized, steel frame sections. Finer mesh sizes were utilized in areas of interest near the joints and for more detailed thermal gradients.

4.3.2 Composite Behavior

Short, frame elements were used to model shear studs between the top of the girders and the slab component of the bridge. The total cross-sectional area of the shear studs was the same as that provided by the shear connectors described in the construction documents. In both the actual bridge and the CSi Bridge model, the concentration of the shear stud elements was greater near the supports to accommodate greater shear transfer in regions of high shear demand. The spacing of the studs in the model differed slightly from those on the actual bridge due to node locations in the model that accommodated the changing of the flange thicknesses along the length of the span.

The frame elements used to model shear studs were connected from a node of the girder to a node of the slab that was directly above. The frame elements were given a modulus of elasticity of 29,000 ksi, typical of steel, and were assigned a yield strength of Grade 50 steel. However, the shear studs are not anticipated to yield in this study and all behavior is considered

linear-elastic. The top of the web section is connected to the centroid of the slab section with these frame elements. The frame elements were assessed for proper behavior and shear transfer. Figure 4-11 shows the shear load in the frame elements for one girder under self-weight. Shear lag behavior is evident directly above the supports. The maximum shear force is observed near the supports. The minimum shear force is observed at mid-span and the shear load switches direction at mid-span. This behavior is reasonable and expected.

4.3.3 Thermal Analysis

Shell and frame elements were assigned temperatures in degrees Fahrenheit to simulate thermal loading scenarios. Various temperature loads were assigned to flanges, web, and slab elements to simulate vertical temperature gradients and uniform temperature changes. The thermal gradients considered were put into the model by determining an equivalent piece-wise distribution such that individual shell elements could be assigned one temperature. Prior to using this method in the bridge model, validation analysis was conducted to ensure that this procedure yielded reasonable results. The number of shell elements in the depth of the plate girder varied between five and ten elements, depending on proximity to the joint. Further information on this validation is discussion in Section 4.4: Model Validation.

4.3.4 Boundary Conditions

A pinned boundary condition refers to a joint restraint at that allows free rotation with respect to the x-, y-, and z- axes, but does not allow translation in the x-, y-, or z- axes. A fixed boundary condition refers to a joint restraint that does not allow rotation or translation in any direction or axis. The bearings on the steel bridge display behavior that is very close to that of pinned joints. Therefore, the supports at the ends of the girders were modeled in this manner.

Due to the shell element configuration of the model, many nodes were available upon which the pinned boundary conditions can be imposed. The boundary conditions had to be applied to multiple nodes in the model to achieve pinned support behavior. Figure 4-7 below shows an end view of one of the girders. Each node with a triangle beneath it has had the translation restrained but not the rotation. Different configurations of joint restraints were considered without significant effects on the global performance of the bridge. However, the boundary configuration chosen, and indicated in the figure, was that which displayed the greatest similarity to the expected localized stress distributions at a pinned joint due to shear lag behavior. The local behavior at the joints was crucial to this study that this boundary condition was investigated in detail.

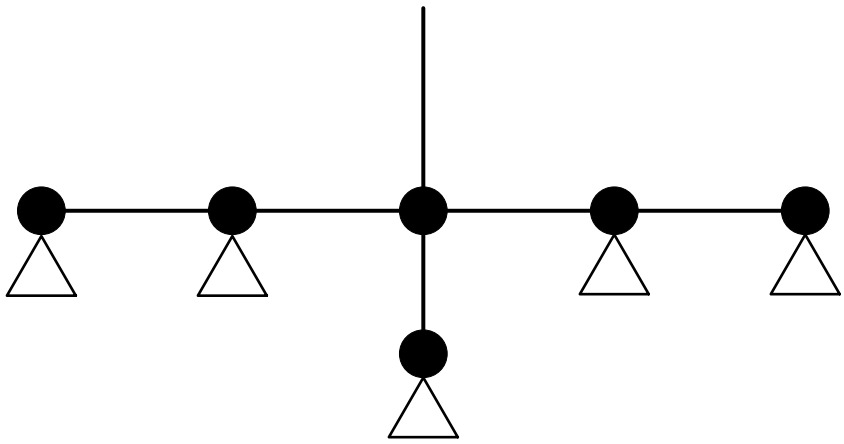

Figure 4-7. Nodes pinned to simulate pinned boundary condition at support

Figure 4-8 gives the stress distribution in the model for the boundary condition scenario shown in Figure 4-7. The shear lag behavior is clear.

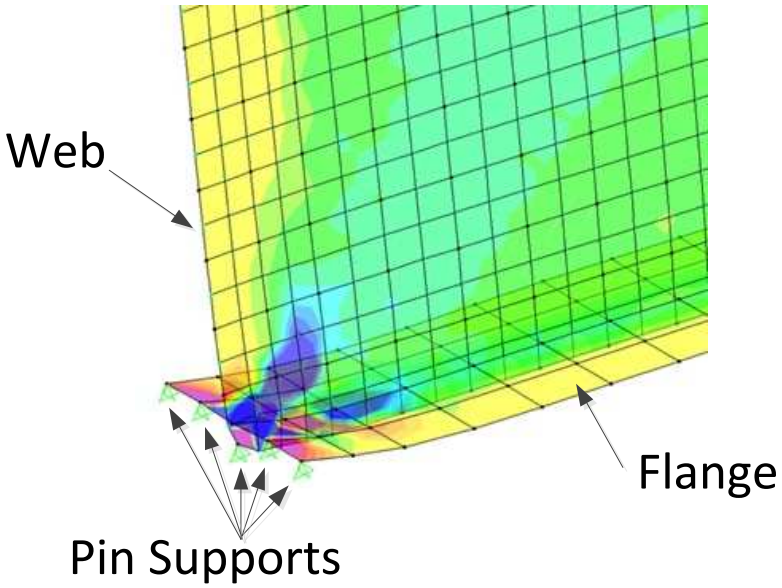

Figure 4-8. Girder Stress Distribution under Self-Weight Showing Shear Lag Behavior

4.4 Model Validation

Model validation was performed in two phases due to the size and complexity of the selected steel bridge. This was the most efficient method because troubleshooting and methodology adjustments initially took place on a small scale with models that required less computational time. Behavior under gravity loads, thermal behavior, and composite action were of vital importance.

First, each of these behaviors was modeled in CSi Bridge using shell elements with a textbook or tutorial example to ensure correct behavior. At first, one composite girder and slab section was built using shell elements and agreement with theoretical behavior was achieved. After the methodology of the model construction was confirmed to produce results aligning with the theoretical prediction for the behavior of interest, the same methodology was used to model the entire bridge. The second stage of model validation occurred after the entire bridge structure was modeled in CSi Bridge and instrumentation of the selected bridge occurred in the field. A

control load test was performed on site on bridge B-16-FM. A strain gauge was placed at mid-span of the centermost girder and a truck with known axle weight was parked on the bridge. The strain was compared to the stress results in the model when subjected to the same loading scenario. This validation is discussed further in Chapter 5.

Theoretical calculations were used to validate the model for thermal and gravity loads. In these calculations, the bridge was treated as a composite, transformed section. The effects of moving loads were also considered in the model validation process. The combination of theoretical calculations and control load testing in the field was used to validate modeling of this behavior in the CSi Bridge model. The fully validated model will be further calibrated after two years of temperature and strain gauge data is collected and processed.

4.4.1 Composite Behavior and Global Performance

Composite behavior was achieved through connecting the girder to the slab with small, steel frame elements. To validate the behavior, the frame elements that are acting as shear studs can be selected and the shear force they experience for a given load can be shown in the software.

A smaller scale example was first followed to validate this method of achieving composite behavior. Then, after validation, the method was utilized to build the entire bridge structure in CSi Bridge. A simply supported beam with a span of 18 ft is considered. A W18X35 rolled section supports a 5 ½" normal weight concrete slab. Small steel frame sections were used to achieve composite behavior in the model and the results obtained were compared to the theoretical behavior.

The example on composite beam behavior was also used to calculate the theoretical behavior of the full-scale bridge model. The total moment of inertia of the three girders was considered and perfect composite action was assumed in the theoretical calculations. The results

indicated outstanding agreement between the theoretical behavior and the model results. Figure 4-9 and Figure 4-10 below shows this agreement graphically.

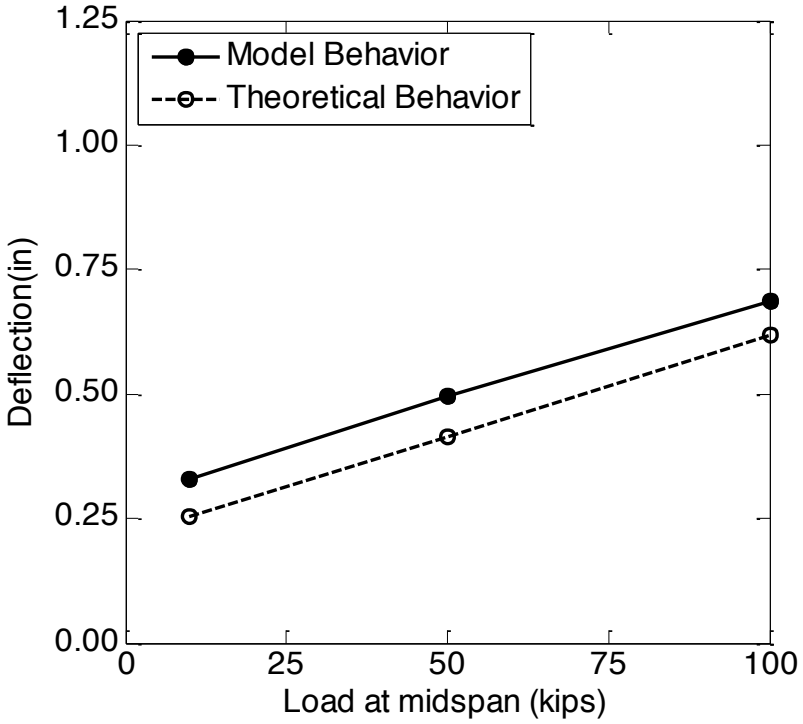

Figure 4-9. Model Validation of B-16-FM: Deflection at Mid-span

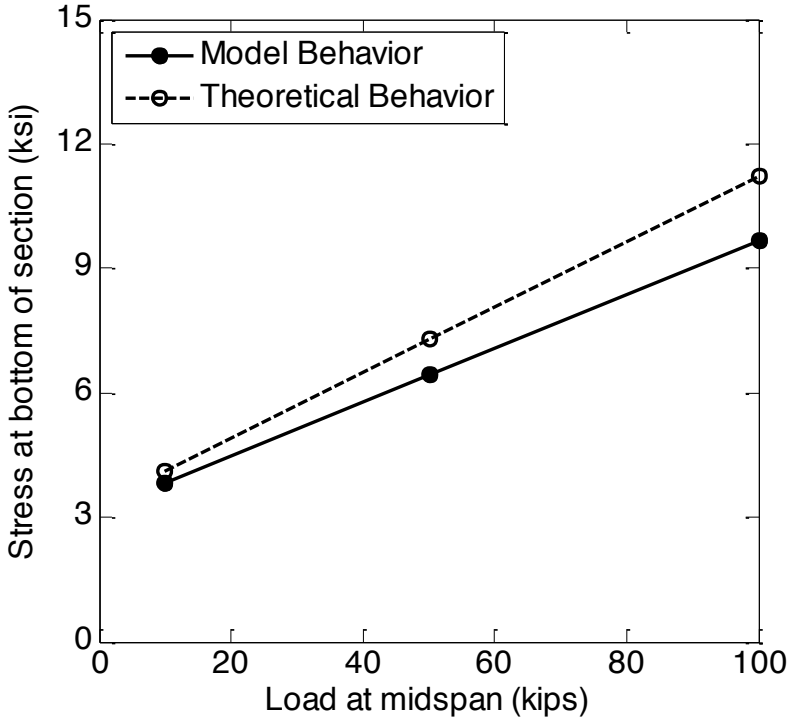

Figure 4-10. Model Validation of B-16-FM: Tensile Stress at bottom of centermost girder at Mid-span

The deflected shape under self-weight is shown in the Figure 4-11 below.

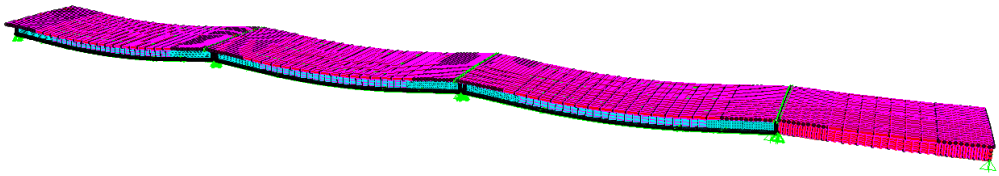

Figure 4-11. Deflected Shape (magnified 100X) of superstructure under self-weight

4.4.2 Thermal Loading

The finite element models developed should allow for analysis to be performed using both uniform and non-uniform thermal loading along the cross section with acceptable level of

accuracy. Since the girder is modeled using shell elements, a piece-wise equivalent thermal load was used to model thermal gradients.

Prior to applying this method in the large, full scale steel bridge model, the method was used with a textbook example to ensure similar results were obtained using a piece-wise thermal gradient. An example entitled *Temperature Changes and Fabrication Errors* from Matrix Analysis of Structures by Aslam Kassimali (2012) was used. Figure 4-12 shows the beam to be analyzed. It is three spans with three roller supports and a fixed connection at one end. It should be noted that this textbook did not include self-weight in the analysis and so it was also neglected in the CSi Bridge model.

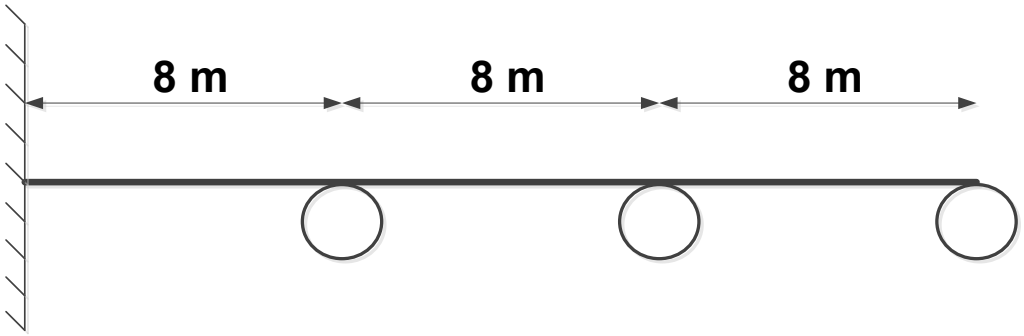

Figure 4-12. Textbook Thermal Gradient Beam Example

The material properties for this beam are provided in the example and are used in the finite element model. The modulus of elasticity, E, is specified as 70 GPa (approximately 100,000 ksi). The moment of inertia of the beam, I, is 102 x 10^6 mm^4 and the coefficient of thermal expansion is 2.36 x10^{-5} mm/^{o}C. The vertical thermal gradient described by the textbook is shown in Figure 4-13 below.

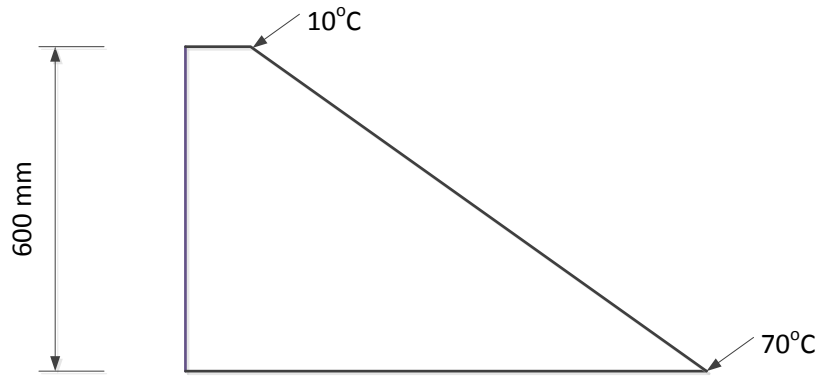

Figure 4-13. Textbook Thermal Gradient Beam Example: Exact Thermal Gradient Specified

The piece-wise approximation of this gradient is shown in Figure 4-14 below. The depth of the girder was divided into 12 elements. Each shell element was assigned a single temperature based on the equivalent piece-wise distribution.

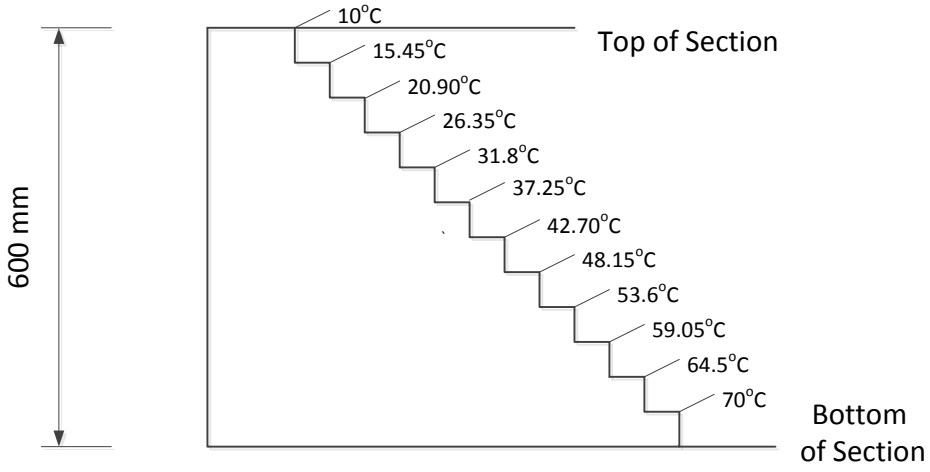

Figure 4-14. Textbook Thermal Gradient Beam Example: Piece-wise Thermal Gradient used in model

Figure 4-15 shows the beam modeled in CSi Bridge. Each node throughout the depth on the left end is fixed (no rotation or translational allowed). The three roller supports are also visible at 8 meter increments. The top shell element row was assigned temperature value of 10

^{o}C, the second row was assigned a value of 15.45 ^{o}C, and this pattern was continued in accordance with Figure 4-14.

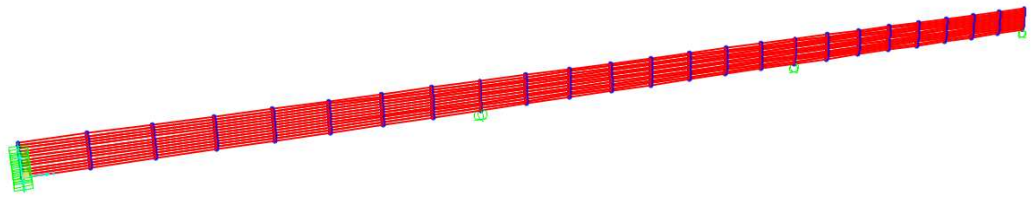

Figure 4-15. CSi Bridge Model of Textbook Thermal Gradient Example

The model was run and support reactions were compared to the theoretical results for accuracy. Figure 4-16 shows the resulting magnified deformed shape. The blue values show the joint reactions from the CSi Bridge Model and the grey values show the theoretical results from the textbook example using matrix analysis. The results are then further summarized in Table 4-1.

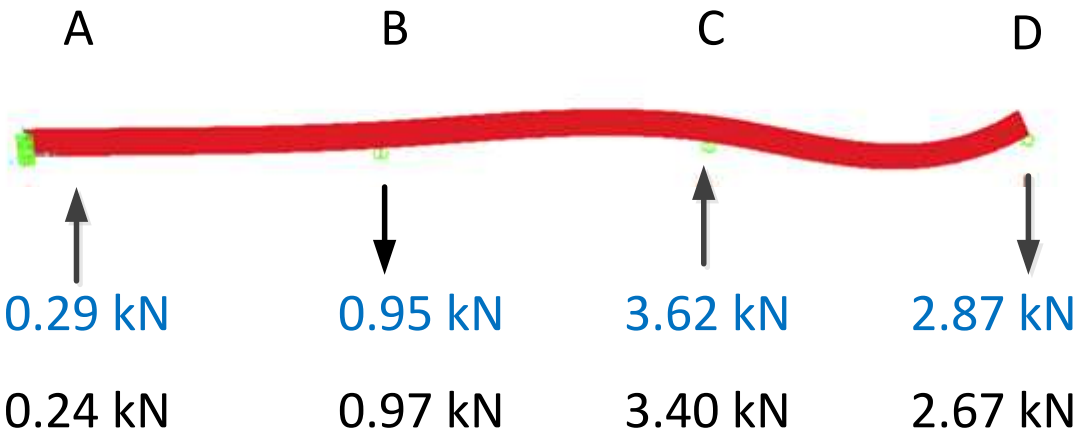

Figure 4-16. CSi Bridge Model of Textbook Thermal Gradient Example

Table 4-1. Comparison of theoretical behavior to piecewise gradient in model

Reaction	A (kN)	B (kN)	C (kN)	D (kN)
CSI Bridge	0.29	0.95	3.62	2.87
Textbook Results	0.243	0.972	3.4025	2.673
% Difference Between CSi Bridge and Textbook	19.34%	2.26%	6.39%	7.37%

Overall, reasonable agreement was achieved using the piecewise gradient method. The method was then used in the full-scale bridge model to model various thermal gradients described in regulatory codes.

4.5 Model Limitations

The models developed in CSi Bridge only consider the superstructure of the bridges selected. The abutment and soil conditions are not considered. If these elements were developed an even more complete picture of the bridge performance could be achieved. However, the research team was most interested in the behavior of the superstructure because it is most affected by thermal loading and deck joint elimination.

Additionally, neither geometric nor material non-linearity was considered in the model. The loads were all at or below design loads and no yielding or torsion was expected. If the bridge response under extreme loading scenarios or non-symmetric loading scenarios was desired, additional work would need to be performed to accommodate non-linear behavior.

CHAPTER 5

CONTROL LOAD TESTING AND FIELD VALIDATION

5.1 Introduction

To validate the finite element model, control load testing was performed on the bridge following the conclusion of field instrumentation. Specifically, a truck with known axle weights and dimensions was parked on the bridge and continuous data collected. Comparisons were made between measured response and the response obtained from the finite element model.

5.2 Vehicle Information

The vehicle utilized for the control load testing was provided and operated by CDOT. The vehicle used for the load test, an Aspen Aerials A-40 Bridge Inspection Unit Truck, was the same truck used to install the sensors. Figure 5-1 shows the axle weights and dimensions for the truck while the inspection arm is fully contracted. The axle weights shown are within +/- 2% of the exact axle weight, according to the manufacturer's drawings. This contracted position is how it was parked on the bridge during the load test.

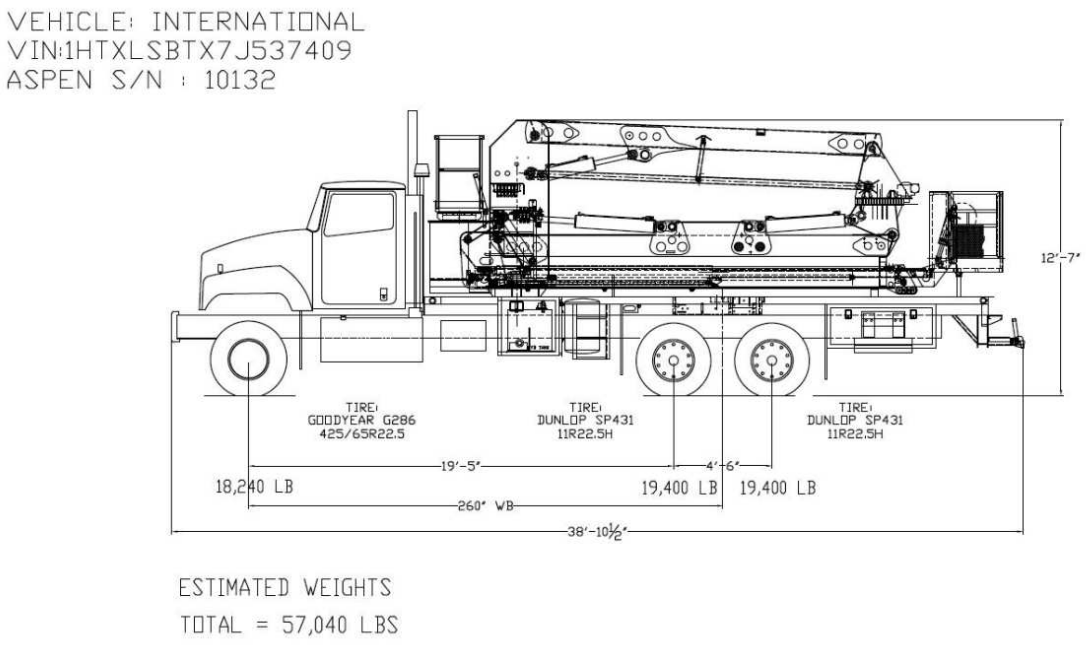

Figure 5-1. Aspen Aerials A-40 Bridge Inspection Truck Dimensions and Axle Weights

5.3 Model Input and Predictions

The effect of the truck described above was included in the finite element model discussed in Chapter 4through inputting the axle weights as point loads. Two scenarios were considered: 1) when the truck was parked with its front axle at the mid-span location and 2) when the truck was parked with its two back axles over the mid-span location.

For the sake of validating the numerical model, the strain gauge that was installed at the top of the bottom flange at mid-span of the bridge was monitored during the load test. The gauge was installed on the centermost girder and therefore strain values from the same girder were extracted from the numerical model. Since the strain gauge data were recorded in microstrain, the corresponding stress values were calculated using the modulus of elasticity of the steel, 200 GPa (approximately 29,000 ksi). The measured field stress was then compared to the stress obtained from the numerical model and the results are discussed.

In the model, when the front axle is located at the mid-span of the bridge, the stress on the top of the bottom flange at mid-span is 1.39 ksi. When the back axles are split across the mid-span, the model predicts the stress on the top of the bottom flange at mid-span to be 2.20 ksi.

5.4 Results and Comparison to Finite Element Model

Control load tests were performed with the front axle at mid-span and again with the rear axles at mid-span to match the scenarios that were modeled. During each test the data from the mid-span strain gauge was collected in the field at five second intervals for approximately one minute. Some noise in this data was expected due to the length of the wires being approximately 240 ft. Collecting several data points allowed a moving average to be applied to the data to determine the actual strain. Figure 5-2 shows the microstrain at mid-span when the truck was parked with its front axles at mid-span. Figure 5-3 shows the microstrain at mid-span when the truck was parked with its rear axles at mid-span.

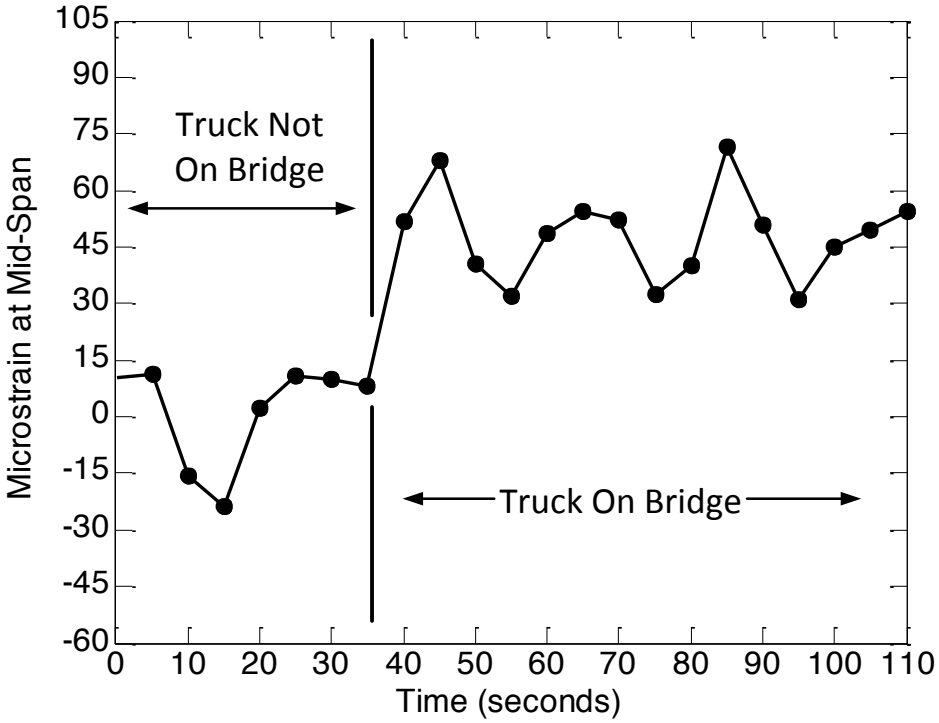

Figure 5-2. Field Control Load Test with Front Axle of A-40 Truck at Mid-Span

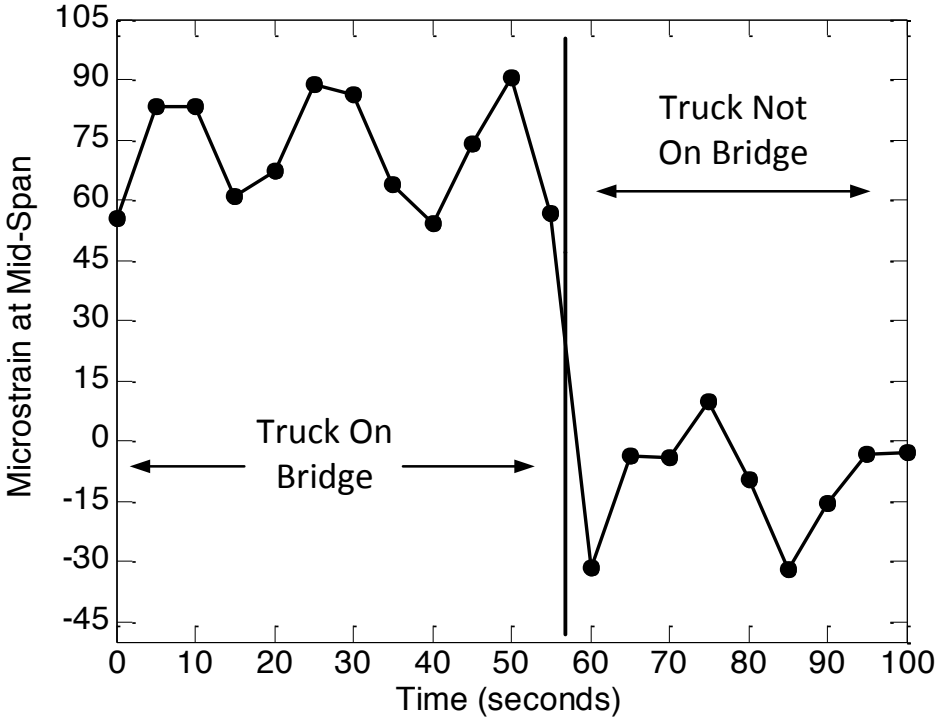

Figure 5-3. Field Control Load Test Microstrain with Back Axles at Mid-Span

A simple average of the data collected was used to determine the average microstrain for each scenario. The average microstrain when the front axle was located at mid-span was 47.36 while the average microstrain when the back axles were located at mid-span was 71.99. The microstrains were converted into stress using the modulus of elasticity. Table 5-1 shows the comparison of the model predictions to the measured field response. As shown in the table, excellent agreement was achieved.

Table 5-1. Comparison of Field Stress to Modeled Stress Predictions

	Front Axles at Mid-span	**Back Axles at Mid-span**
Predicted Stress (ksi)	1.39	2.20
Measured Stress (ksi)	1.37	2.09
Percent Difference (%)	-1.22%	-5.10%

5.5 Conclusion

The field measurements of strain at mid-span validated the finite element model's ability to predict global behavior of the selected bridge. The modeling techniques were verified through closely capturing the correct field behavior. The combination of the field validation and theoretical validation further solidifies the model's ability to predict the global behavior and supports the reliance on the model for performing the parametric study discussed in Chapter 6.

CHAPTER 6

PARAMETRIC STUDY

6.1 Introduction

This chapter describes a parametric study performed using CSi Bridge with the validated three-dimensional numerical model of the instrumented steel bridge. The objective of the study was to consider different scenarios of joint elimination for the purpose of providing guidance to DOT engineers on possible alternatives for joint removals. The effects of thermal loading and underperforming deck joints and the implications of deck joint removal were examined. Links between the spans were built in the model to represent a joint that was clogged with debris. Four joint-removing connection types, three thermal loading scenarios, and three link stiffness options (representing different types of joint clogging material) were examined.

6.2 Joint-Removing Connection Types Considered

While it is recognized that there are numerous alternatives for connecting two spans following the removal of a joint, this parametric study focus on previous alternatives that are considered common among transportation agencies. This is to allow for the results of this study to be related to typical field practices. Specifically, connection types used in the two-dimensional study performed by Tsaistas and Boardman (described in Chapter 2) were examined with the three-dimensional model developed for this project. This provided an opportunity to compare results and draw conclusions about how necessary a three-dimensional model is to assess joint removal and thermal loading. The four connection types chosen were 1) Deck Only, 2) Deck and

Top Flange, 3) Deck, Top Flange, and Bottom Flange, and 4) Full-Moment Splice. Localized stresses and alterations in bending behavior were assessed for each connection type.

To model the deck only connection, the slab was connected in the finite element model using the same types of shell elements. Flanges were connected similarly, by connecting the steel sections with the same shell elements. The full moment splice was achieved by connecting the slab, web, and both flanges with their respective shell elements. The bearing was retained as a pinned boundary condition (allowing rotation, but no translation).

6.3 Thermal Gradients Considered

To assess the effect of removing joints on the superstructure's response to different thermal loading scenarios in the modeled bridge, three vertical thermal distributions were utilized. Two of the distributions had a gradient while the third had a uniform thermal distribution. The first thermal gradient considered was adopted from the AASHTO LRFD Bridge Design Specifications and the second thermal gradient considered was based on the New Zealand bridge design code. This New Zealand code was selected because a previous study conducted by French et al. (2013) (see Chapter 2) showed reasonable agreement between this fifth order gradient curve and the field-measured thermal loading on the bridge. Lastly, a uniformly distributed temperature change of 50^{o}Fwas applied. Both the AASHTO and New Zealand distributions are described in details in Section 2.8.4. The uniform temperature distribution entailed an increase of 50^{o}F, which was applied to the entire cross-section along the length of the spans in order to determine how thermal stress and behavior from a uniform thermal gradient compares to varying vertical thermal gradients. An increase of 50^{o}F was chosen because all bridges in Colorado experience this temperature change over the course of one year.

6.4 Connection Link Stiffness Considered

Previous research described in Chapter 2 has identified that joints are commonly clogged with debris quickly after they are put into service. To model this in CSi Bridge, links were used and axial stiffness coefficients were assigned to the links to simulate a bridge joint clogged with debris. The axial stiffness coefficients were assigned based on the moduli of elasticity of soils that are known to clog these joints: sand and gravel. Typically, stiffness values (commonly assigned the variable 'k') are found as EA/L, where E represents the modulus of elasticity, A represents the cross-sectional area, and L represents the length of the element.

To calculate the axial stiffness of the links to reasonably represent the clogged joint, the structural element considered is the soil volume blocking the joint. Common moduli of elasticity for gravel and sand are 150 MPa (~22 ksi) and 50 MPa (~7 ksi), respectively (Briaud 2013). The length of the debris clog that is being modeled as an additional structural element is taken as the joint opening as described in the construction documents (L=0.625 in). The area is found by multiplying the transverse dimension of the bridge by the height of the debris that is causing the clog. The height of the clogged debris was assumed to be 3 inches. This depth was chosen because 3 inches is a common depth of compression seals that are used at the expansion joints. Using these assumptions a total stiffness of the debris clogging the joint is determined. Then, the stiffness is distributed evenly across the joint in the model with a link every foot in the transverse direction. This method assumed that the joint is evenly clogged, and thus there are no resulting torsional effects. Using this method, stiffness coefficients of 30 kip/in for a totally gravel filled joint and 10 kip/in for a totally sand filled joint were selected. Additionally, a stiffness of 20 kip/in was selected for a joint that is clogged with a mixture of sand and gravel. These stiffness values were implemented in the parametric study.

6.5 Parametric Study Matrix and Overview

In order to examine the effects of different combinations of connection types, clogged joints, and vertical thermal gradient, on local behavior and global performance, a parametric study matrix was developed and is shown in Figure 6-5 below. Two categories of joint alterations (connection types and clogged joints) are analyzed with each type of thermal gradient. All analysis took place in the finite element model described in Chapter 4 and Chapter 5. Results and conclusions drawn are discussed in Section 6.6.

		Stiffness of Deck Clogging Links Between Spans			Connection Types			
		10 kip/in	20 kip/in	30 kip/in	Deck Only	Deck and Top Flange	Deck, Top Flange, and Bottom Flange	Full Moment Connection
Temperature Gradient	AASHTO							
	New Zealand							
	Uniform (+50°F)							

Figure 6-1. Parametric Study Matrix

6.6 Results

The results of the parametric study are subdivided into two sections: results associated with clogged joints and results associated with various connection types. The numerical results from the analysis of different connection types are shown in bar charts because the connection types are discreet, qualitative variables. However, the stiffness assigned to the two-joint links are quantitative, continuous variables and the results from these analyses are presented in line graphs.

To analyze the effect that different connection types and clogged joints had upon the global performance and local behavior of the bridge, three different loading scenarios were

considered: 1) temperature gradient load only, 2) truck loading only, and 3) temperature gradient loading combined with truck loading. An AASHTO HS20-44 truck was used for the truck loading and is shown in Figure 6-2 below.

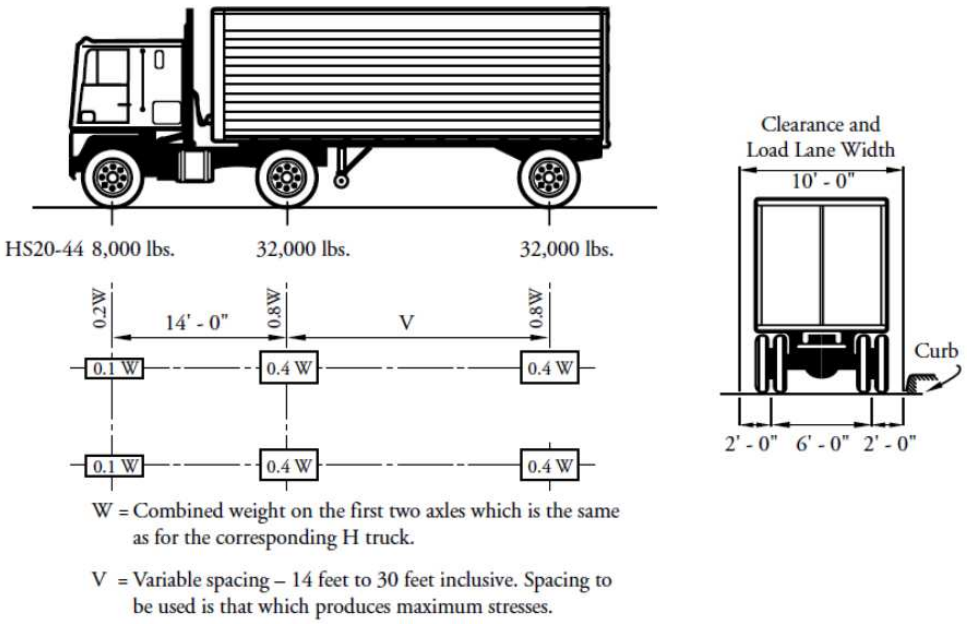

Figure 6-2. AASHTO HS20-44 Truck (Precast/Prestressed Concrete Institute, 2003)

An influence line analysis was conducted to determine the location of the truck that resulted in the maximum moment demand on the bridge spans. This location was determined to be when the font axel was at the over the bearing, near the beginning of the span and the last two axels were placed 14 feet from one another (when V = 14 feet in Figure 6-6 above). For the remainder of the chapter, *truck loading* refers to this AASHTO HS20-44 in this position on the superstructure.

6.6.1 Effect of Clogged Joints

Examination of the influence of clogged joints in the parametric study was conducted in a similar manner as the examination of the influence of connection type. The location of the truck

loading was not changed. However, since the value of stiffness of the links is a continuous variable, line graphs instead of bar charts are used to present the results of the study. Three values for link stiffness (k = 10 kip/in, 20 kip/in, and 30 kip/in) are examined with the thermal gradients described above. Local behavior and global performance were evaluated.

First, the compressive stress at the bottom of the girders near the bearings due to only temperature gradient was determined for each vertical gradient option for different 2-joint link stiffness options. Figure 6-3 below shows the results of this analysis. The model exhibited the maximum compressive stress, 60.29 ksi, when the uniform temperature increase of 50^{o}F is applied and a link stiffness of 30 kip/in is considered. Of the clogged joint stresses (k > 0), the minimum compressive stress, 26.91, was exhibited in the model when the AASTHO thermal gradient is applied with a link stiffness of 10 kip/in. Though the stresses shown in the figure exceed the yield stress, the analysis was conducted considering only the thermal loads and the dead load due to the self-weight of the superstructure is neglected. The self-weight will always be present on the bridge in the field and so the compressive stresses will be less than what is pictured in the figure that is only representing thermal loads.

The clogged joints (symbolized in the figure below by link stiffness values) do not have a significant effect on the global demand on the bridge superstructure as seen in Figure 6-3 below. The compressive stress range on the girders for the different stiffness of links are 0.80 ksi, 0.16 ksi, and 0.08 ksi for New Zealand Gradient, Uniform Temperature Increase, and AASHTO Gradient, respectively.

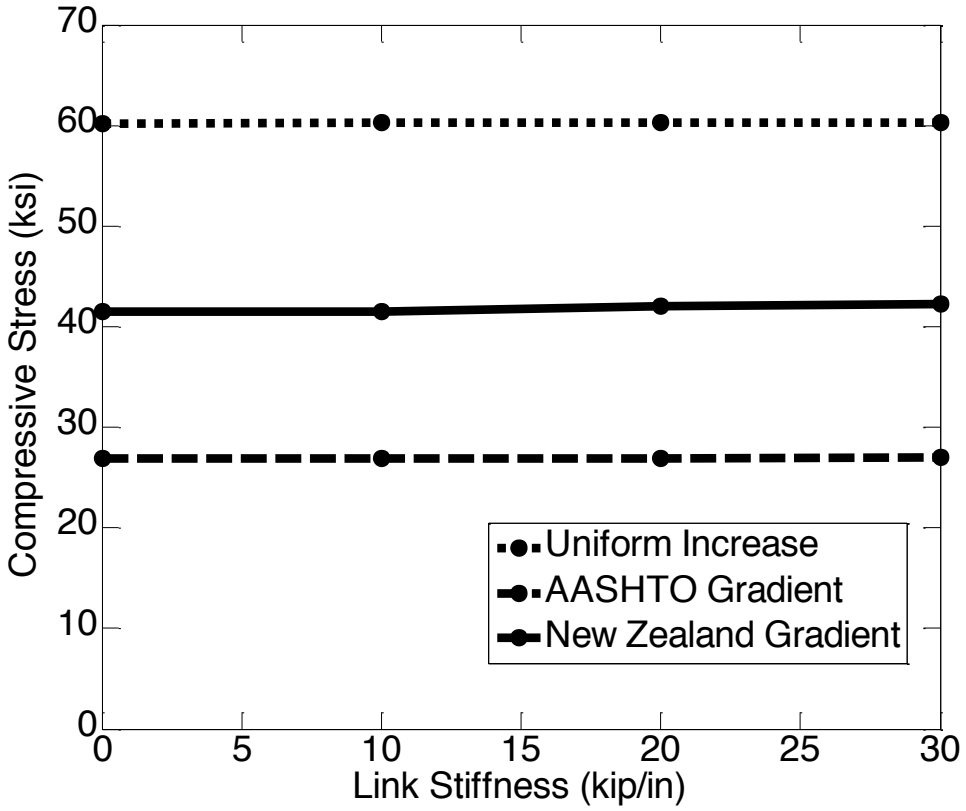

Figure 6-3. Compressive Stress at Bottom of Girder

Figure 6-4 shows the results of the analysis shown in Figure 6-3 normalized to the maximum value of compressive stress in the bottom of the girders for the Uniform Temperature Increase thermal gradient (60.29 ksi). The stress resulting from the gradient described by AASHTO is less than that of New Zealand by approximately 25%.

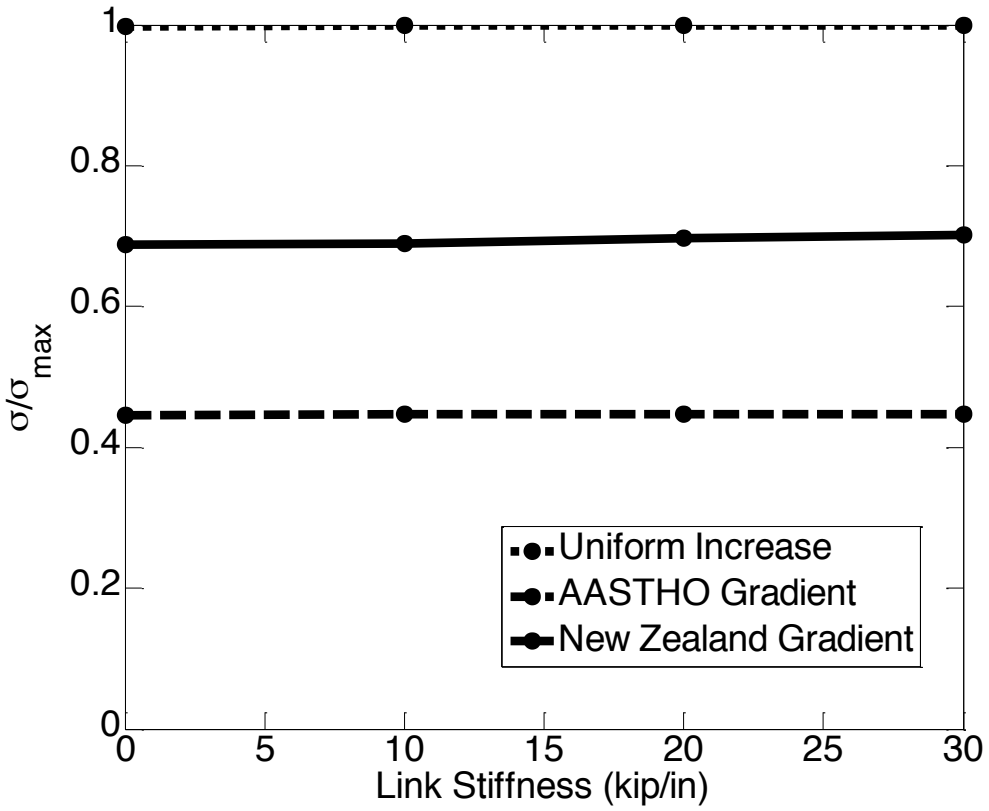

Figure 6-4. Compressive Stress at Bottom of Girder (Normalized)

Figure 6-5 below shows the local compressive stress in the concrete deck for the different thermal gradients and link stiffness options. The largest, middle, and smallest, localized compressive stress in the slab for each link stiffness type was exhibited by the New Zealand, Uniform, and AASHTO gradients, respectively. This result is in line with what was expected because the temperature values of the thermal gradient nearest to the top of the concrete deck for New Zealand, Uniform, and AASHTO distributions were 69.01^{o}F, 50^{o}F, 23.33^{o}F, respectively.

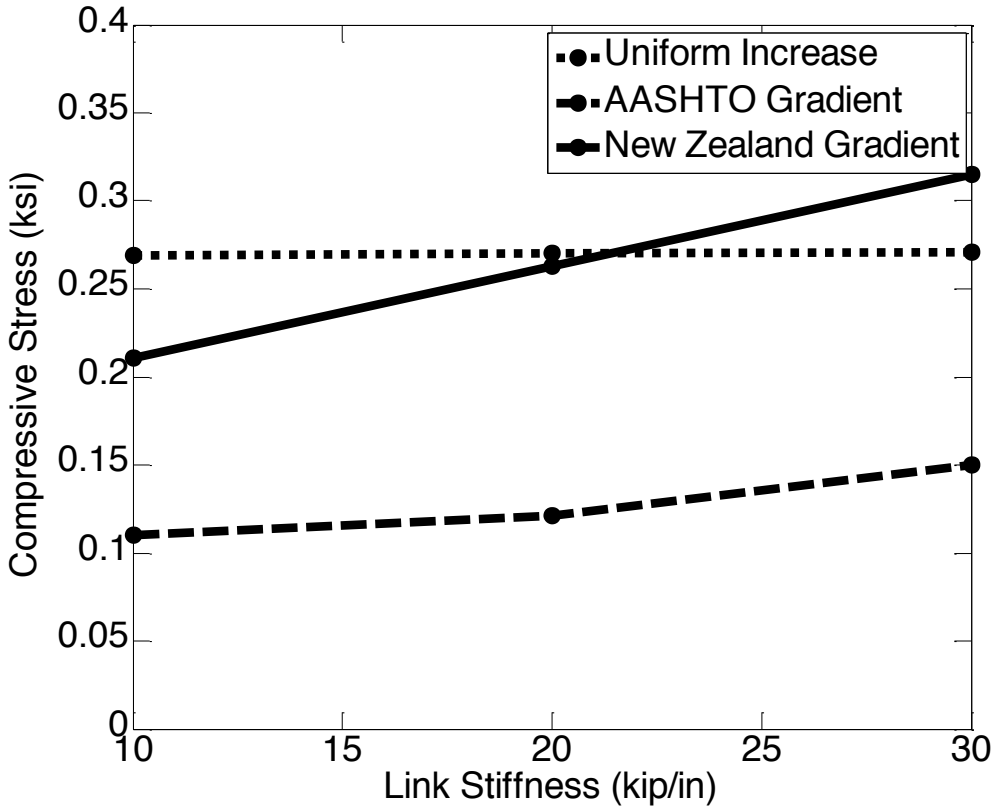

Figure 6-5. Local Compressive Stress in Deck due to Thermal Loading

Figure 6-6 shows the results of the analysis shown in Figure 6-5 normalized to the maximum value of 0.315 ksi. This figure shows that the AASTHO gradient results in localized compressive stress that is less than 40% of what results with a uniform temperature increase of 50^{o}F.

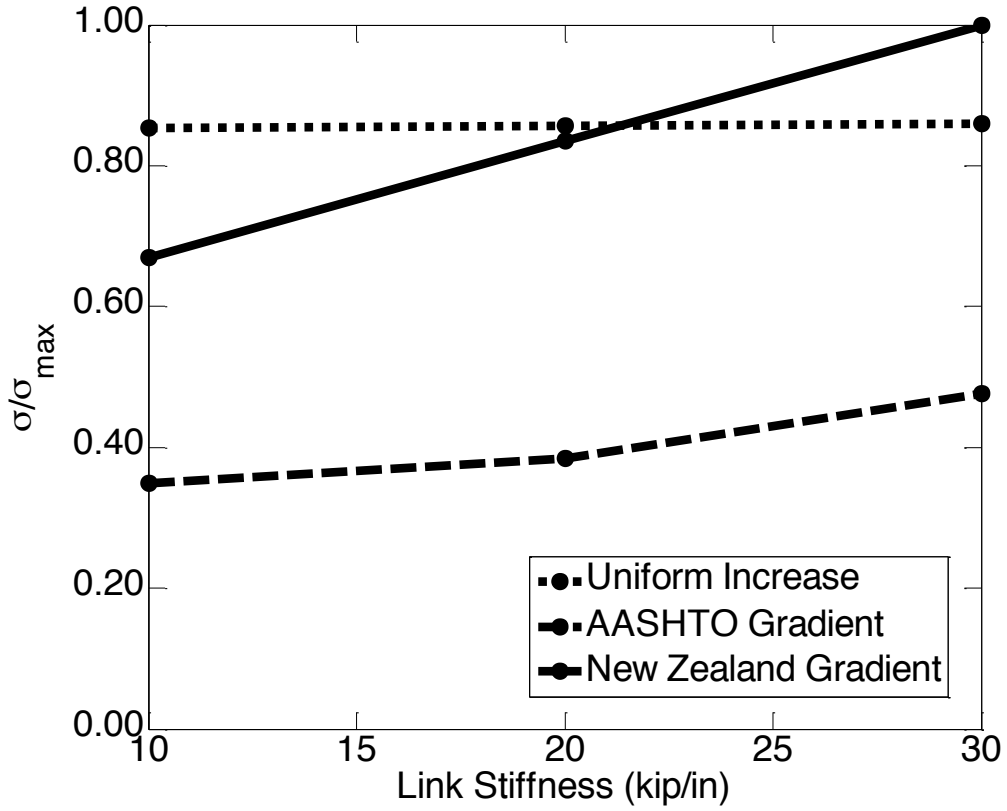

Figure 6-6. Local Compressive Stress in Deck due to Thermal Loading (Normalized)

Figure 6-7 shows the results of the model when only a truck load is considered. There is a slight decrease in moment demand on the bridge due to the clogged joints that are modeled by the links because they simulate a clogged joint holding the concrete deck together in a negative moment region. Unlike an unclogged joint then, some moment is transferred in the negative moment region and the moment demand in the positive moment region decreases slightly. However, this decrease of tensile stress demand under the truck load is less than 0.1 ksi (0.7%).

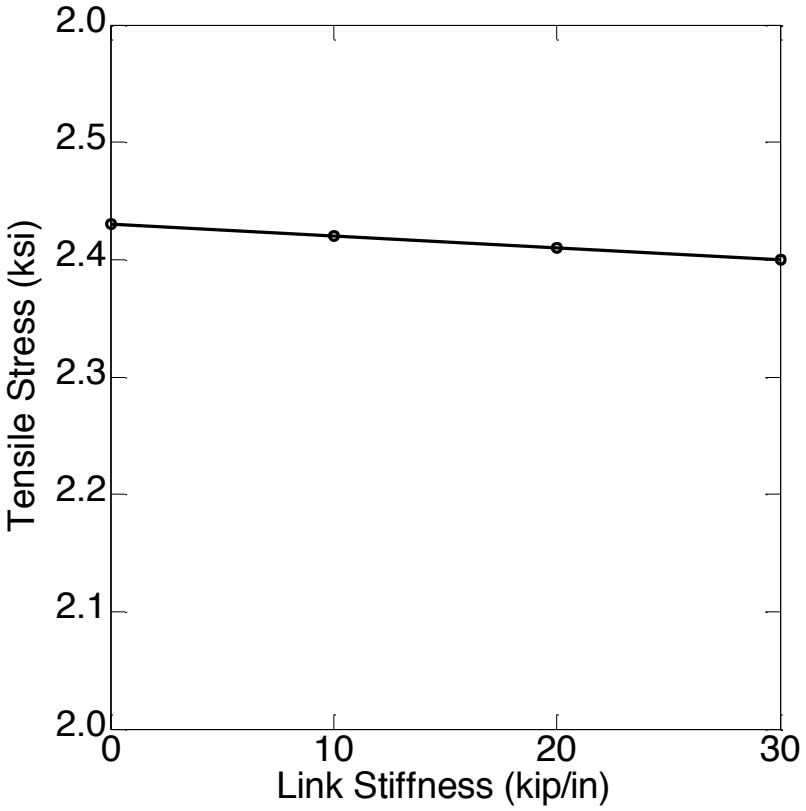

Figure 6-7. Tensile Stress at Bottom of Girder due to Only Truck Loading

After competition of analysis with separate thermal and truck loading, analysis was conducted with both loads applied and the results are shown in Figure 6-8 below. For each thermal gradient, the stresses remained compressive. Uniform Temperature Increase, New Zealand Gradient, and AASHTO Gradient exhibited the greatest, middle, and least compressive stresses, respectively.

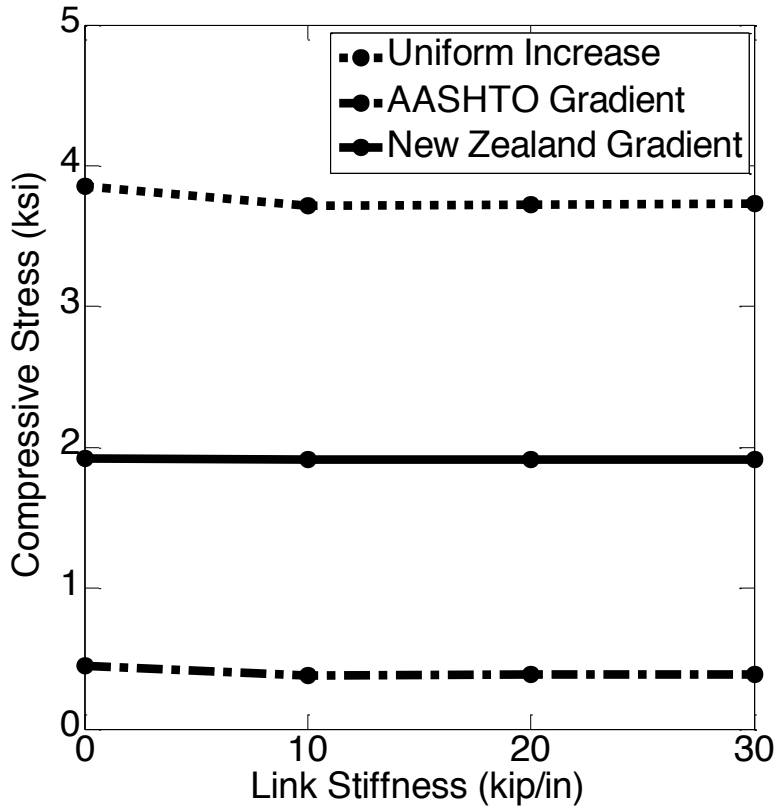

Figure 6-8. Stress at Bottom of Girder under the Truck Load due to Thermal and Truck Loading

Figure 6-9 shows the results of the analysis shown in Figure 6-8 normalized to the maximum compressive stress value of 3.855 ksi.

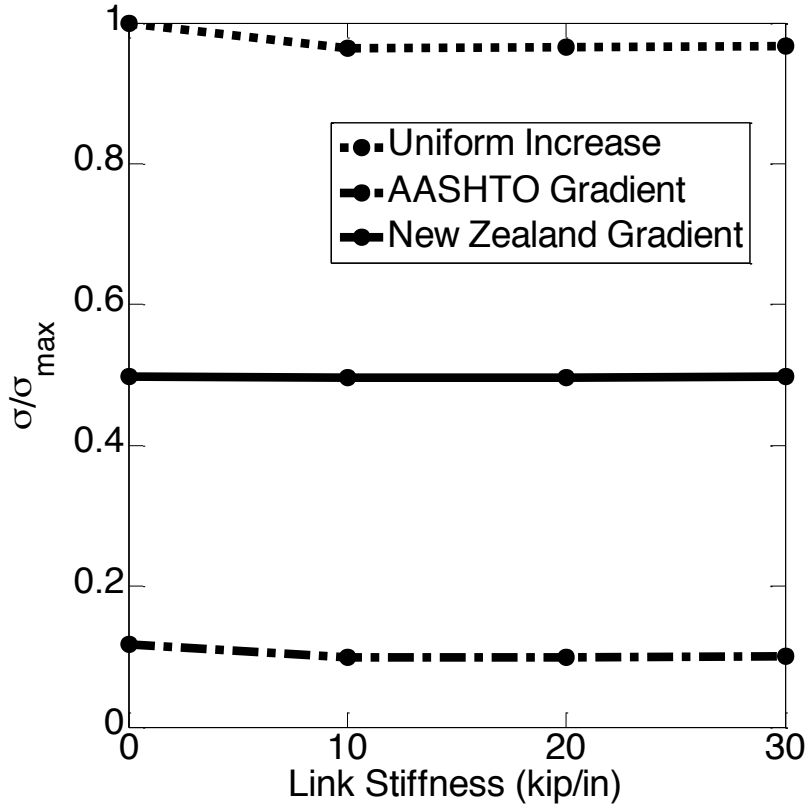

Figure 6-9. Stress at Bottom of Girder due to Thermal and Truck Loading (Normalized)

6.6.2 Effect of Connection Types

First, the compressive stress near the bearings in the bottom of the girders due to only temperature gradient was determined for each vertical gradient option and connection type. Figure 6-10 below shows the results of this analysis. The stresses induced by the AASHTO recommended thermal gradient are lower than those induced by the New Zealand gradient. Both of these gradients still result in lower stresses than the stresses that a uniform temperatures increase of 50^{o}F induces in the structure. The minimum compressive stress at the bottom of the girders, 7.1 ksi, is found when a Full-Moment Splice connection and the AASHTO defined vertical temperature gradient are considered. This is likely because the AASHTO thermal

gradient is the least intense of the thermal loading and the Full-Moment Splice transfers moment from one span to the other. The Full-Moment Splice induces a lower neutral axis (the *y* in the equation of stress, $\sigma = (M*y)/I$, is reduced). Therefore, less stress exists at the most extreme bottom fiber of a cross-section because the moment demand is lowered at the bottom of the cross-section. Similar to the clogged joint analysis, the stresses shown in this figure below (and exceed the yield point) are only depicting the effect of thermal loading and will be lower in the field when the self-weight of the superstructure is present.

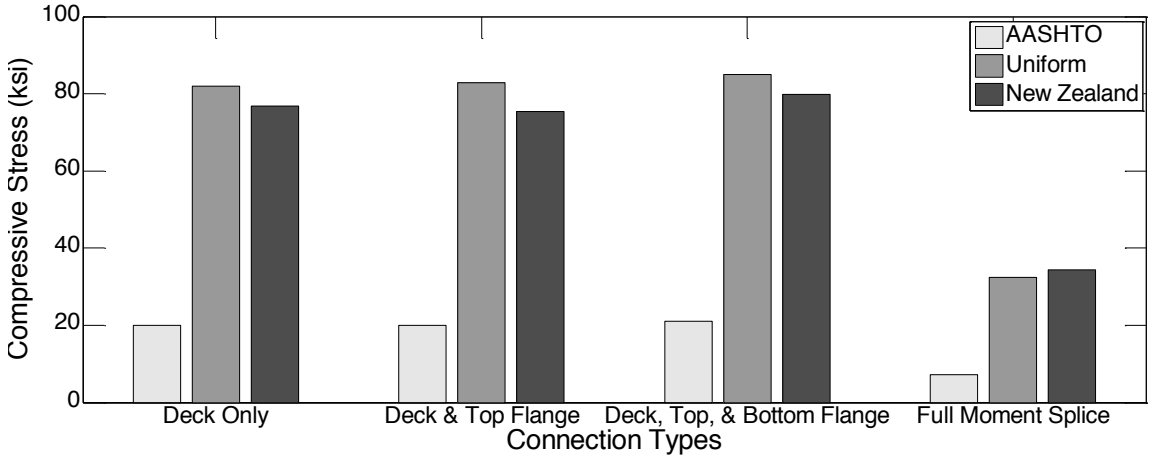

Figure 6-10. Compressive Stress at Bottom of Girder due to Only Thermal Loading

Figure 6-11 shows the results of the analysis conducted in Figure 6-10, but normalized to the maximum value. The maximum compressive value of stress was 85.0 ksi and was found when the compressive stress due to a uniform temperature increase of 50^{o}F and a Deck, Top, & Bottom Flange connection was considered.

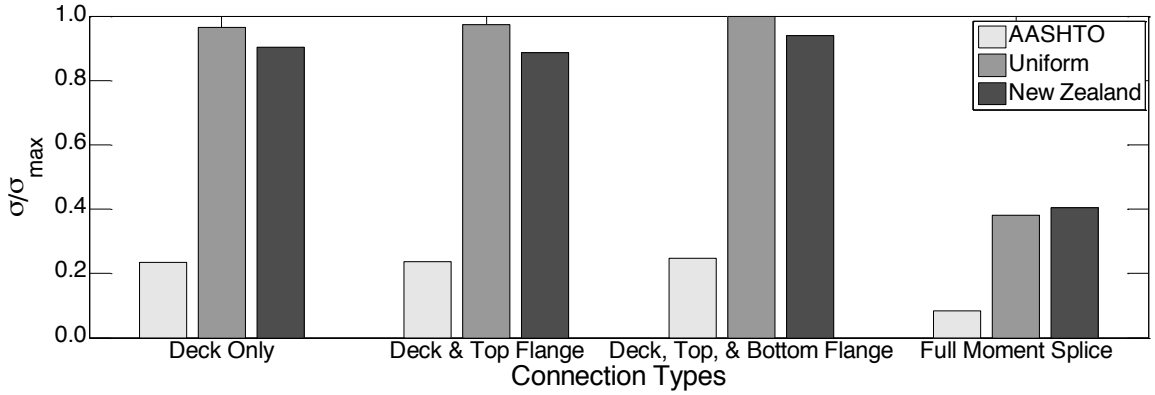

Figure 6-11. Compressive Stress at Bottom of Girder due to Only Thermal Loading (Normalized)

To examine the localized behavior at the joints that each thermal gradient and connection type induces into the structure, the compressive stress at the joint was retrieved from the model results (considering only thermal loading). Figure 6-12 shows the results of this analysis. The localized compressive stress induced was the greatest for each thermal gradient when considered with the Deck Only connection. The localized compressive stress did not significantly decrease, however, with increasing connectivity at the joint more than attaching one plate girder flange. In other words, the Deck and Top Flange, Deck, Top, and Bottom Flange, and Full Moment splice connections did not have progressively lower localized compressive stress.

The largest, middle, and smallest, localized compressive stress in the slab for each connection type was exhibited by the New Zealand, Uniform, and AASHTO gradients, respectively. This result is in line with what was expected because the temperature values of the thermal gradient nearest to the top of the concrete deck for the New Zealand, Uniform, and AASHTO distributions were 69.01^{o}F, 50^{o}F, 23.33^{o}F, respectively.

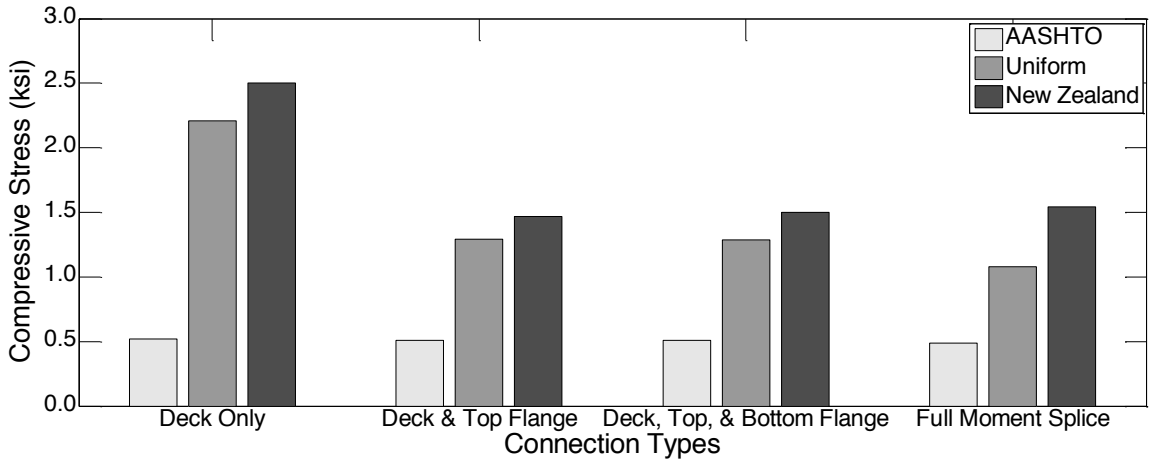

Figure 6-12. Local Compressive Stress in Concrete Deck due to Only Thermal Loading

Figure 6-13 shows the results of the analysis conducted in Figure 6-12, but normalized to the maximum value of local compressive stress. This value was found to be 2.5 ksi when the New Zealand vertical temperature gradient was placed on the structure with a Deck Only connection.

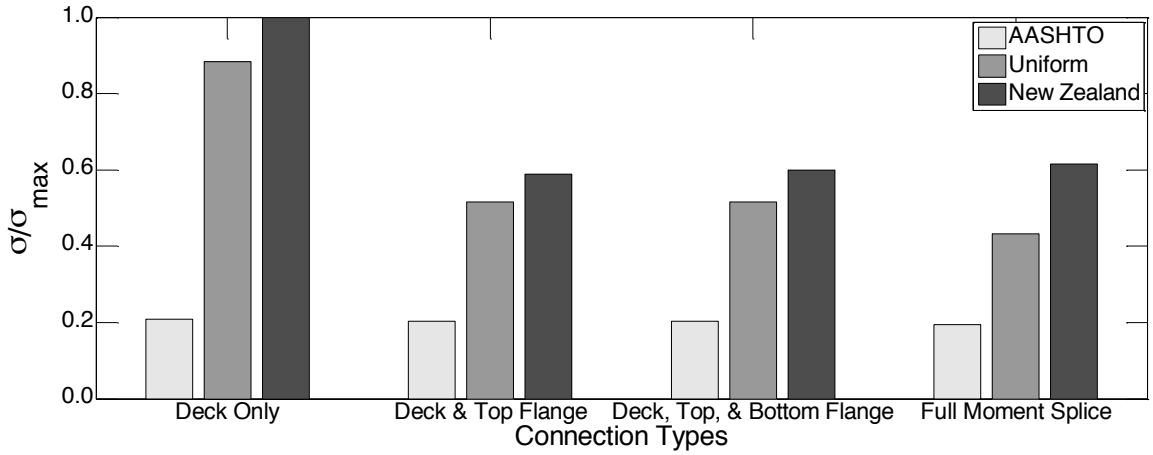

Figure 6-13. Local Compressive Stress in Concrete Deck due to Only Thermal Loading (Normalized)

To evaluate the potential increase in moment capacity of the span for the four connection types considered at the joint, analysis was conducted with only the truck loading and the connection types of interest. The maximum tensile stress in the bottom of the girder system was taken as a measure of the moment demand on the superstructure for a given connection type and the truck loading. The results of this analysis are shown in Figure 6-14 below. The moment demand on the structure did not decrease considerably until the Full-Moment Splice connection was utilized. The tensile stress for the Deck Only, Deck and Top Flange, and Deck, Top, and Bottom Flange was 3.22 ksi. However, when a Full-Moment Splice was analyzed, a reduction of the tensile stress to 2.51 ksi was observed in the span. This corresponds to a 22% decrease in the moment demand on the superstructure.

It is also important to note that connecting the flanges at the joint did not result in significant increase in moment capacity of the bridge. Therefore, the additional cost of increasing connectivity beyond the "Deck Only" connection may not be beneficial. This is because connecting the flanges only does not result in sufficient increase in the rotational stiffness of the connection; hence the moment transfer to the connection is limited.. Instead, if higher moment capacity increase is desired, a Full-Moment Splice connection should be utilized.

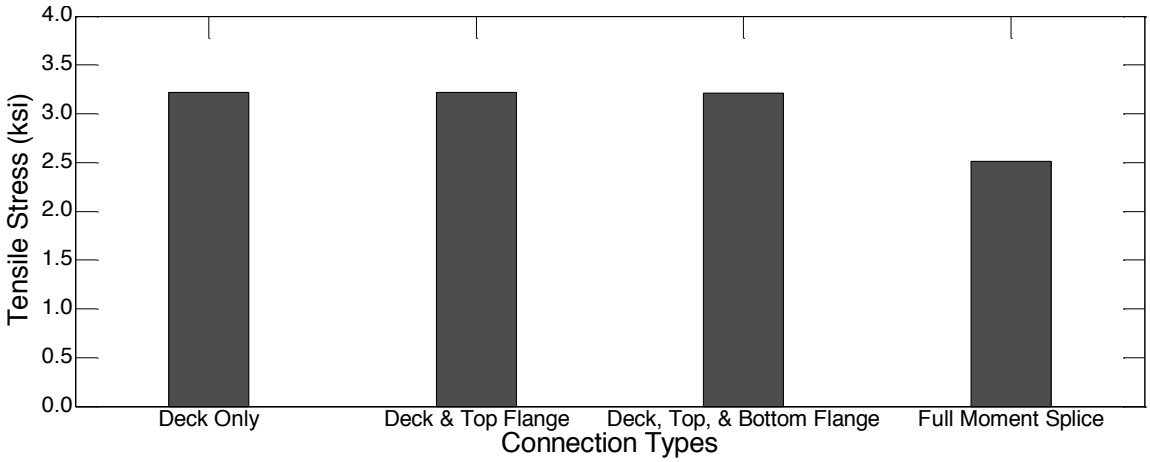

Figure 6-14. Tensile Stress at Bottom of Girder due to Only Truck Loading

Figure 6-15 shows the results of the analysis shown in Figure 6-14 normalized to the maximum value of tensile stress in the bottom of the girders. The maximum value is 3.22 ksi (found for the Deck Only, Deck and Top Flange, and Deck, Top, and Bottom Flange connection). The moment demand on the superstructure for the Full-Moment Splice connection is approximately 78% of the moment demand with the other connection types.

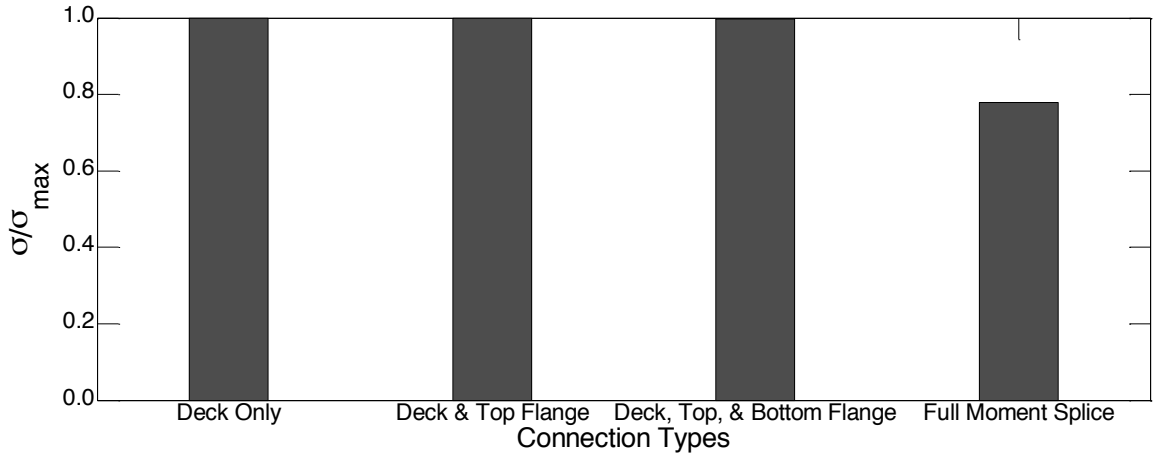

Figure 6-15. Tensile Stress at Bottom of Girder due to Only Truck Loading (Normalized)

After competition of analysis with separate thermal and truck loading, analysis was conducted with both loads applied and the results are shown in Figure 6-16 below. Due to the lesser amount of compression resulting from the AASHTO thermal gradient (when only thermal loading is considered), the stress at the bottom of the girders under combined AASHTO thermal gradient and truck loading resulted in a tensile stress at the bottom of the girders. However, the Uniform and New Zealand vertical thermal gradients induced enough compressive stress into the superstructure that the value of stresses in the bottom of the girders remained compressive while the truckload was applied.

The maximum compressive stress demand in the girders near the bearings due to thermal and truck loading was found when the Deck Only connection type was considered. The

maximum compressive stress demand in the girders when considering thermal gradients increased when the connectivity of joint increased and the maximum values were found with a Full-Moment Splice Connection. These results reiterate that the connection type at the joint influences the global performance and moment demand on the bridge.

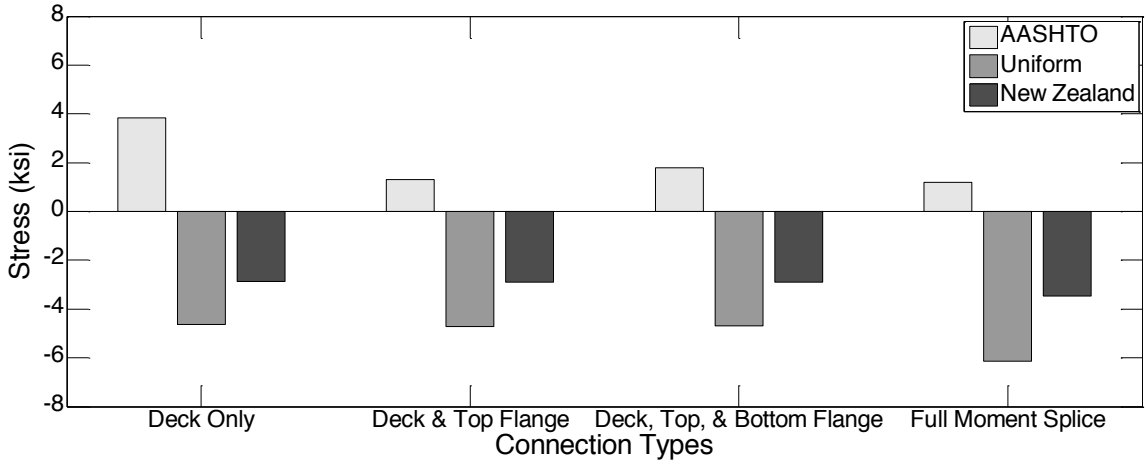

Figure 6-16. Stress at Bottom of Girder due to Thermal and Truck Loading

Figure 6-17 shows the results of the analysis shown in Figure 6-16 normalized to the maximum value of tensile stress in the bottom of the girders for the AASHTO thermal gradient (3.84 ksi). The compressive values from the Uniform and New Zealand thermal gradients are normalized to the maximum value of compressive stress in the bottom of the girders (-6.15 ksi).

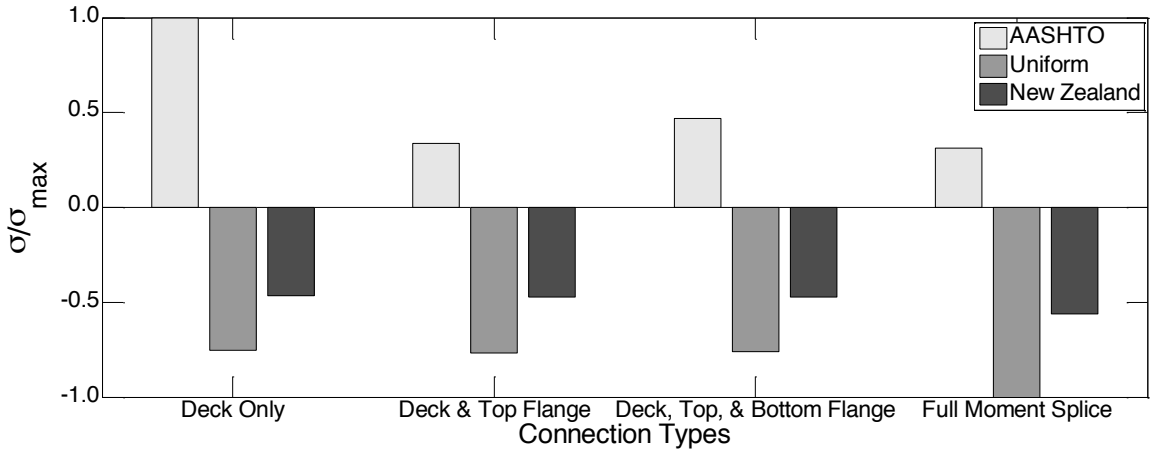

Figure 6-17. Stress at Bottom of Girder due to Thermal and Truck Loading (Normalized)

6.7 Conclusion

The parametric study results highlighted differences between the thermal gradients considered. The AASHTO described thermal gradient consistently resulted in lower stress demand on the structure compared to the New Zealand thermal gradient. The results from the field data will aid in further examination of the AASHTO described thermal gradient for bridges in Colorado.

The results also highlighted the extent of the effect that joint-removing connection types have compared to clogged joints. The effect of the clogged joints was primarily localized at deck surface behavior. However, the joint eliminating connection types influenced the global performance of the bridge as well. No significant decrease in moment demand on the superstructure was observed until a Full-Moment Splice was utilized.

CHAPTER 7

SUMMARY AND SIGNIFICANCE

7.1 Summary

To gain further knowledge of thermal loading and its influence on expansion joint removal practices, several tasks were performed in the completion of this thesis. First, an extensive literature review was conducted to gain an understanding of the current research that has been completed in this field of study. Moreover, a steel plate girder bridge in Colorado with simply supported spans separated by expansion joints was selected for field instrumentation, load testing, and long-term monitoring. In addition, a three dimensional finite element model of this bridge was developed using shell elements in CSi Bridge.

The selected bridge was instrumented with thermocouples, linear potentiometers, strain gauges, and a scratch gauge. The sensors installed on the bridge provide thermal loading data throughout the depth of the girders. The strain gauges will provide information on bridge performance and local behavior at the joint. The linear potentiometers will provide information about how much the joint is moving throughout the seasons and the day. The strain gauge installed at the center girder at midspan of the bridge was used to validate the finite element model and an excellent match was achieved.

Following, field instrumentation, load testing, and validation of the numerical model, a parametric study was performed to examine the effects of different connection types at the joint, different thermal gradients, and the effect of clogged joints. The moment demand on the structure was not significantly reduced until a Full Moment Splice connection was implemented. The clogged joints did not affect the global behavior of the bridge significantly. The AASHTO

described thermal gradient resulted in smallest thermal stresses on the superstructure compared to the New Zealand thermal gradient. Future analysis, using measured thermal gradient information collected from the bridge, will be used to further calibrate the numerical model using a realistic thermal distribution.

7.2 Significance and Further Research

The results of this work hold significance in two arenas: long term field data of thermal loading of a bridge and a modeling technique to examine thermal loading, connection types, and localized behavior of bridges. First, the long-term data collection from the instrumented bridge will provide The Colorado Department of Transportation with data on the thermal loading to which Colorado's bridges are subjected. Comparisons can then be made to design codes. Second, the three dimensional modeling technique developed can be used to capture localized behavior and global performance of other bridges. This study reaches the same conclusion from a global performance perspective as the two dimensional model developed by Tsiatas and Boardman in 2002: that the moment demand on the structures is not significantly reduced (or, the moment capacity of the bridge is not increased) until a Full-Moment Splice connection is utilized. It was also found that clogged joints of a depth of 3" do not significantly impact the global performance of the superstructure. However, clogged joints may influence the abutments, bearings, and other structural elements. Therefore, further investigation should be performed before dismissing the effect of the clogged joints entirely.

WORKS CITED

AASHTO LRFD Bridge Design Specifications. (2012). .

Albhaisi, S., and Nassif, H. (2014). *Simple Approach to Calculate Displacement and Rotations in Integral Abutment Bridges*.

Burke Jr., M. P. (1990). "The Integrated Constuction and Conversion of Single and Multiple Span Bridges." *Bridge Management*, 677–693.

Burke Jr., M. P. (1993). "Integral Bridges: Attributes and Limitations." *Transportation Research Record*, (1393), 1–8.

Burroughs, D., and Price, K. (1999). "High Performance Steel Bridge Concepts." *Modern Steel Construction*, (14).

Briaud, L. (2013). *Geotechnical Engineering: Unsaturated and Saturated Soils.* Wiley, New YorkCDOT. (2012). *Bridge Design Manual*.

Chen, Q. (2008). "Effects of Thermal Loads on Texas Steel Bridges."

"Congress Approves the Federal-Aid Highway Act." (n.d.). United States Senate: Art & History, <https://www.senate.gov/artandhistory/history/minute/Federal_Highway_Act.htm> (Mar. 7, 2014).

Cross, H. (1930). "Analysis of Continuous Frames by Distributing Fixed-End Moments." *American Society of Civil Engineers*, 919–928.

Federal Highway Administration. (n.d.). "History of the Interstate Highway System." <http://www.fhwa.dot.gov/interstate/history.htm> (Oct. 7, 2014).

French et al. (2013). "Investigation of Thermal Gradient Effects in the I-35W St. Anthony Falls Bridge." *J. Bridge Engineering* 18(1), 890-900.

Hawk, H. (2003). *Bridge Life-Cycle Cost Analysis*. 1–97.

Husain, I., and Bagnariol, D. (2000). "Design and Performance of Joinless Bridges in Ontario." *Transportation Research Record*, (1696), 109–121.

Kassimali, A. (2012). Matrix Analysis of Structures, 2nd Ed., Cengage Learning, Independence, KY

Kim, W., and Laman, J. a. (2010). "Integral abutment bridge response under thermal loading." *Engineering Structures*, Elsevier Ltd, 32(6), 1495–1508.

Koo, K. Y., Brownjohn, J. M. W., List, D. I., and Cole, R. (2013). "Structural health monitoring of the Tamar suspension bridge." *Structural Control Health Monitoring*, 20(March 2012), 609–625.

Lam, C., Lai, D., Au, J., Lim, L., Young, W., and Tharmabala, B. (2008). "DEVELOPMENT OF CONCRETE LINK SLABS TO ELIMINATE BRIDGE EXPANSION JOINTS OVER PIERS." *Annual Conference of the Transportation Association of Canada*, Toronto, Ontario, 1–20.

Li, D., Maes, M. A., and Dilger, W. H. (2008). "Evaluation of Temperature Data of Confederation Bridge : Thermal Loading and Movement at Expansion Joint."

Liu, J. (2013). <https://engineering.purdue.edu/~jliu/courses/CE591/PDF/CE591defl_F13.pdf> (August 10, 2015).

Loveall, C. L. (1985). "Jointless Bridge Decks." *ASCE Journal of Civil Engineering*, ASCE Journal of Civil Engineering, 55(11), 64–67.

Milton, J. (2013). "Joint Maintenance and Best Practices in Deck Joint Replacement." *2013 Virginia Concrete Conference*, Virginia Department of Transportation.

Moorty, S., and Roeder, C. W. (1992). "Temperature-Dependent Bridge Movements." *Journal of Structural Engineering*, 118(4), 1090–1105.

Morcous, G. (2013). *Life-Cycle Assessment of Nebraska Bridges*. 1–67.

Ontario Ministry of Transportation. (2014). "Pulling the Teeth on Old Bridge Structures." *Road Talk*, <http://www.mto.gov.on.ca/english/transtek/roadtalk/rt17-1/#a8> (Apr. 9, 2014).

Precast/Prestressed Concrete Institute. (2003). Chapter 7: Loads & Load Distribution. In PCI Bridge Design Manual. Chicago.

Pugasap, K., Kim, W., and Laman, J. A. (2009). "Long-Term Response Prediction of Integral Abutment Bridges." *Journal of Bridge Engineering*, 14(April), 129–139.

Roeder, C. W. (2003). "Proposed Design Method for Thermal Bridge Movements." *Journal of Bridge Engineering*, 8(1), 12–19.

Rogers, C. E., and Schiefer, P. (2012). "Region Bridge Support Unit Bridge Field Services." (January).

Rogers, C. E., Schiefer, P., and Bouvy, A. (2012). *Alleviating the Effects of Pavement Growth on Strucutres*.

Savioz, P., Spuler, T., and Moor, G. (2014). "Life-cycle and total cost analysis of bridge expansion joints." *7th International Conference on Bridge Maintenance, Safety and Management (IABMAS)*, Shanghai, People's Republic of China, 2433–2440.

Shi, X., Fay, L., Yang, Z., Nguyen, T. A., and Liu, Y. (2009). “Corrosion of Deicers to metals in Transportation Infrastructure: Introduction and Recent Developemnts.” *Corrosion reviews*, 27(1-2), 23–52.

Tsiatas, G., and Boardman, W. G. (2002). *Expansion Joint Elimination For Steel Highway Bridges*. Kingston, RI, 1–129.

Vasseghi, A. (2013). “Effect of Pier Section Reinforcement on Inelastic Behavior of Steel I-Girder Bridges.” *Journal of Bridge Engineering*, 18(January), 31–41.

Wasserman, E. P. (1987). “Jointless Bridge Decks.” *American Institute of Steel Construction, Inc.*, 24(3), 93–100.

Zhu, Z., Davidson, M. T., Asce, A. M., Harik, I. E., Asce, M., Sun, L., and Sandefur, K. (2010). “Effect of Superstructure Temperature Changes on Intermediate Pier Foundation Stresses in Integral Abutment Bridges.” 1–11.

APPENDIX A

DECK JOINT REMOVAL SURVEY

The Colorado Department of Transportation and the research team were interested to understand the level of interest in deck joint removal on a nation scale. Therefore, a survey was developed and administered to all states' departments of transportation and all members on the AASHTO SCOBS list using a Google Form. Interest and the current state of deck joint removal were the main focus of the survey. The results of the survey indicated a strong interest in removing deck joints in existing bridges. Key results are highlighted in this Appendix and the survey is also presented. 62% of the Department of Transportation responded to the survey.

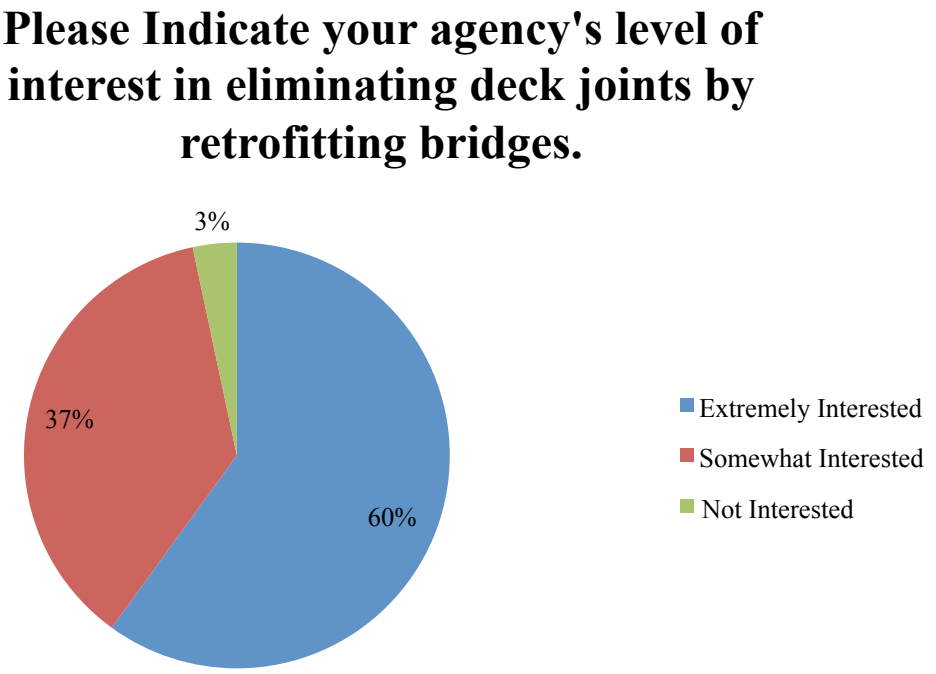

What is your agency's primary motivation for eliminating deck joints?

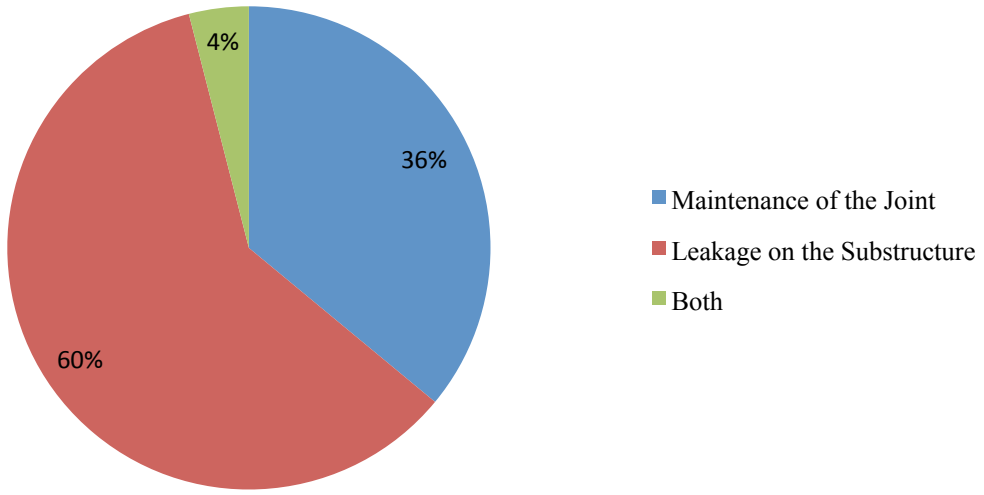

What is the longest length between back of face abutments of joint-less bridges in your agency's jurisdiction?

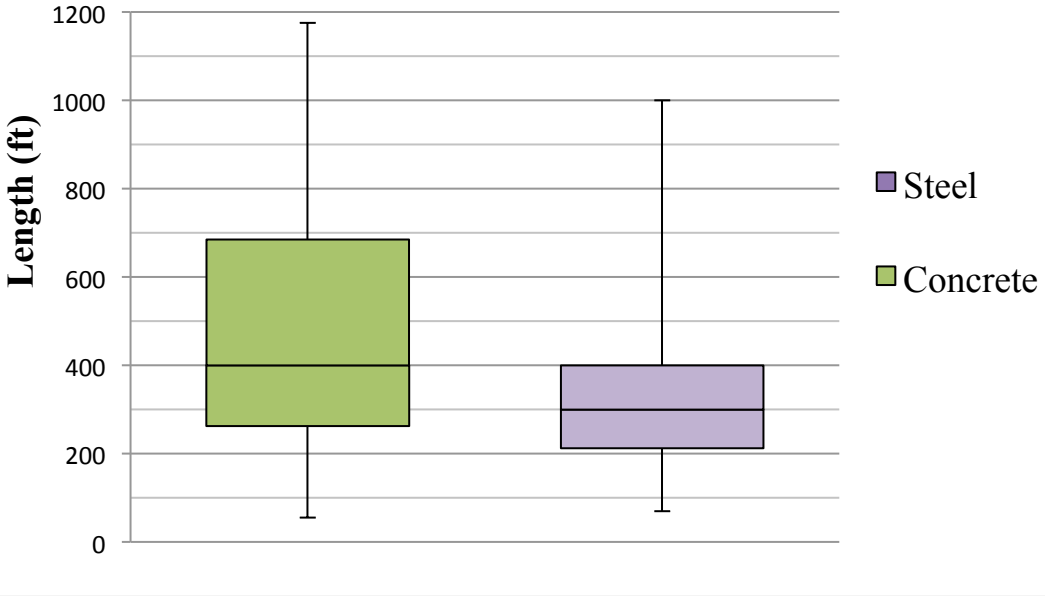

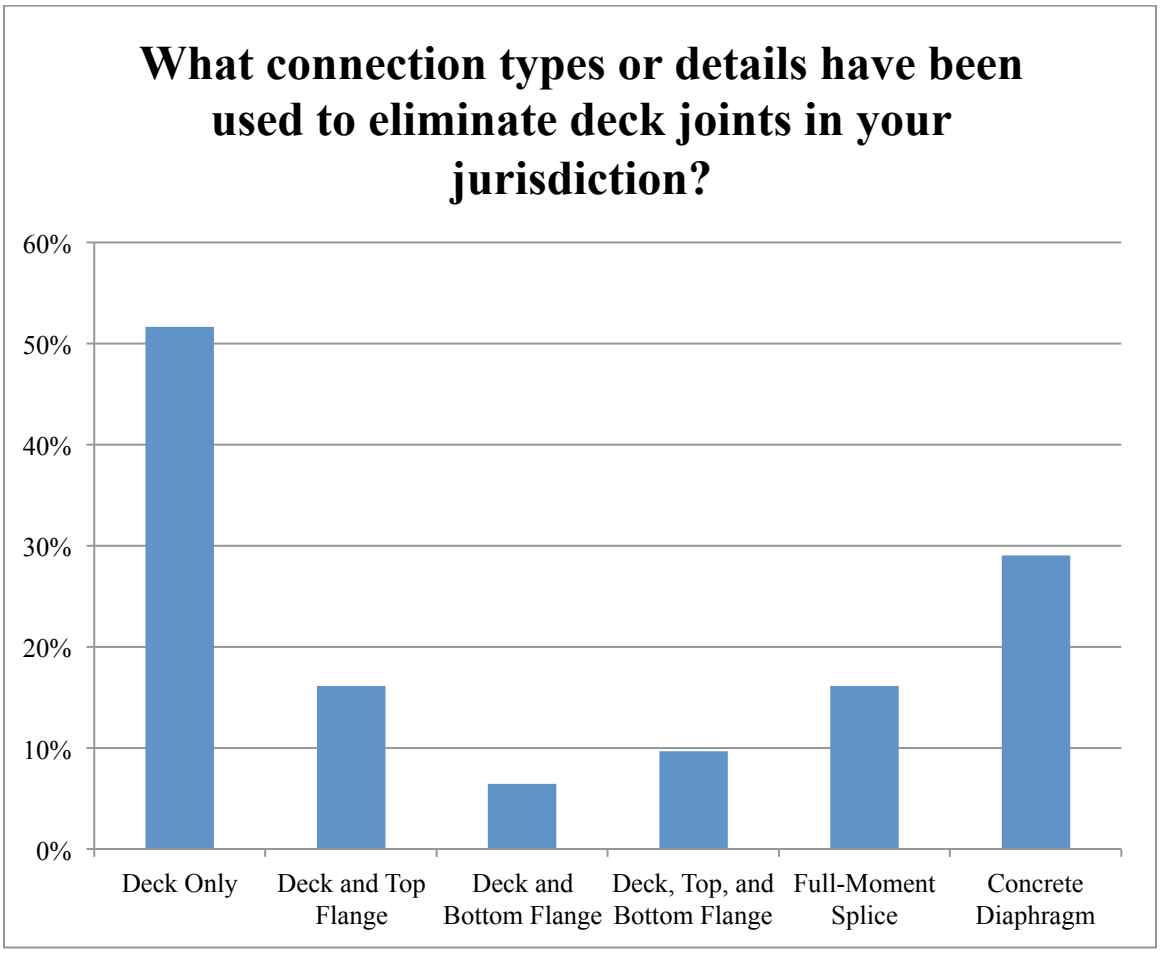
What connection types or details have been used to eliminate deck joints in your jurisdiction?
60%
50%
40%
30%
20%
10%
0%
Deck Only
Deck and Top Flange
Deck and Bottom Flange
Deck, Top, and Bottom Flange
Full-Moment Splice
Concrete Diaphragm

Have improvements in maintenance costs or other life cycle costs for retrofitted bridges been observed as a result of deck joint elimination?

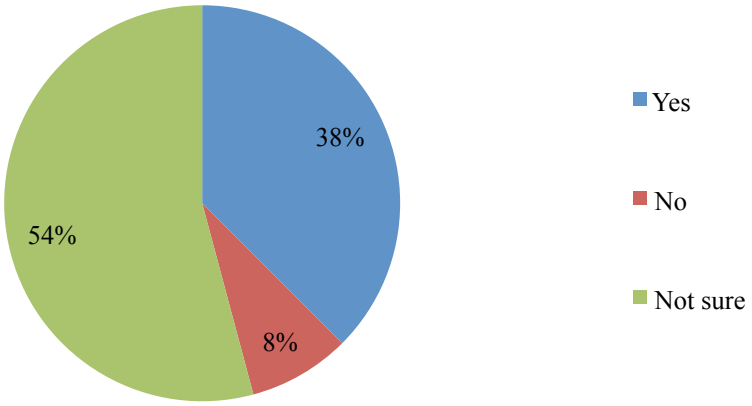

Does your agency promote newly constructed bridges to be designed and built without deck joints?

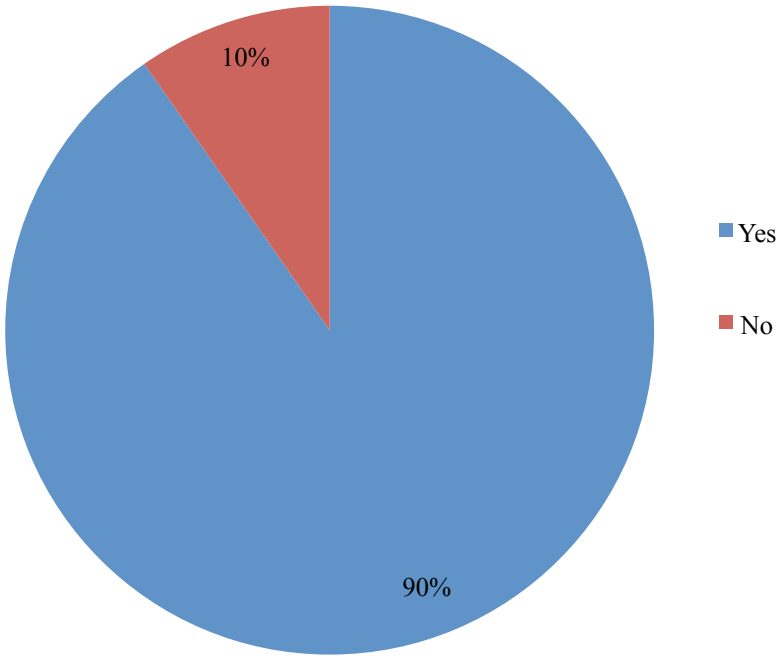

Deck Joint Removal Implications

Research funded by the Colorado Department of Transportation

* Required

Please indicate the agency you are representing.

Please indicate your agency's level of interest in eliminating deck joints by retrofitting bridges.

- Extremely Interested
- Somewhat Interested
- Not Interested

What is your agency's primary motivation for eliminating deck joints?

- Maintenance of the Joint
- Leakage on the Substructure
- Other:

In joint-less steel bridges in your jurisdication, what is the longest total length between back faces of abutments?

In joint-less concrete bridges in your jurisdication, what is the longest total length between back faces of abutments?

Has your agency already eliminated deck joints by retrofitting bridges? *

- Yes
- No

Does your agency provide a specific procedure (design guidelines and/or construction detail) for removing deck joints in bridges?

- Yes
- No

Continue »

Experience with Deck Joint Retrofits

What resources are available to guide the design of retrofits for deck joint elimination? Please check all that apply.

- [ ] Design Manuals
- [ ] Design Guidelines
- [ ] Design Examples
- [ ] Worksheets
- [ ] Other:

How many bridges have been retrofitted to eliminate deck joints in your jurisdiction? May provide answer numerically as an exact number, an approximation, or an approximate percentage. Please feel free to expand or explain your answer further as needed.

Have deck joints been eliminated in steel bridges, concrete bridges, or both?

- ( ) Steel
- ( ) Concrete
- ( ) Both

What connection type or detail was used to eliminate deck joints? Circle all that apply. *

- [ ] Deck Only
- [ ] Deck and Top Flange
- [ ] Deck and Bottom Flange
- [ ] Deck, Top, and Bottom Flange
- [ ] Full-Moment Splice
- [ ] Concrete Diaphragm
- [ ] Other:

Have improvements in maintenance costs or other life cycle costs for retrofitted bridges been observed as a result of deck joint elimination?

- ( ) Yes
- ( ) No
- ( ) Not Sure

Please use the space below to expand on any lessons learned from eliminating deck joints in your jurisdiction.

Deck Joints in New Bridge Construction

Does your agency promote newly constructed bridges to be designed and built without deck joints? *

- Yes
- No

« Back Continue »

Additional Comments

Would your agency be interested in the results of this survey and reading the final research report? If so, please provide an e-mail address of who to e-mail the report to.

If there are other comments, questions, concerns, or heightened interested in the implications of eliminating deck joints, please feel free to express them below.

Minimizing Deck Joints in New Bridge Construction

Do you promote elimination of deck joints in the following types of bridges? Please select one.

- ◯ Concrete
- ◯ Steel
- ◯ Both

What provisions or guidelines are used to implement this preference of minimizing deck joints in new bridge construction? Please check all that apply.

- ☐ Design Manuals
- ☐ Design Guidelines
- ☐ Design Examples
- ☐ Worksheets
- ☐ Other:

Consideration of Thermal Loading

Are the following thermal gradients considered in the design of the retrofit used to eliminate a deck joint? Please check all that apply.

- [ ] Vertical Gradient
- [ ] Transverse Gradient
- [ ] Longitudinal Gradient
- [ ] None of the above are considered
- [ ] Bridge Dependent
- [ ] Unsure

Is the consideration of a vertical thermal gradient considered when designing a new bridge or when eliminating a deck joint? *

- ( ) Yes
- ( ) No

« Back Continue »

Vertical Thermal Gradient

What design provisions are used for the consideration of a vertical thermal gradient?

- ( ) AASHTO LRFD Specifications (Section 3.12.3)
- ( ) Jurisdiction-Specific Procedure
- ( ) Both of the above
- ( ) Other:

How confident are you in designing for the thermal vertical thermal gradient demands given the procedure selected above?

- ( ) Extremely Confident
- ( ) Somewhat Confident
- ( ) Not Confident

Would a more clearly defined procedure in the AASHTO LRFD Bridge Design Specifications improve your agency's ability to consider vertical thermal gradients in new bridge design?

- ( ) Yes
- ( ) No
- ( ) Maybe

Information and Resources Needed

Would a more clearly defined procedure in the AASHTO LRFD Bridge Design Specifications improve your ability and confidence when choosing to retrofit bridges to eliminate deck joints?

- ◯ Yes
- ◯ No
- ◯ Maybe

What tools and information are still needed in order to help with the decision making process regarding deck joint elimination? Please check all that apply.

- ☐ Analytical Tools
- ☐ Design Procedures
- ☐ Field Data
- ☐ Life-Cycle Assessment
- ☐ Other:

« Back Continue »

Additional Comments

Would your agency be interested in the results of this survey and reading the final research report? If so, please provide an e-mail address of who to e-mail the report to.

If there are other comments, questions, concerns, or heightened interested in the implications of eliminating deck joints, please feel free to express them below.

APPENDIX B

SCRATCH GAUGE INSTALLATION INSTRUCTIONS

Deck Joint Removal Implications
Research Study 215.01
Scratch Gauge Installation and Maintenance Instructions

Introduction and Objectives of Study

The purpose of this research study is to assess implications of removing deck joints in Colorado's existing bridges. In order to do so, the performance and behavior of joints in existing bridges in Colorado must be assessed first. Structural and life cycle cost analysis will be conducted to evaluate the implications of removing joints. Two bridges will be finely instrumented near Colorado State University and eighteen (16) other bridges will be instrumented with scratch gauges across the five regions of the Colorado Department of Transportation jurisdiction. The two bridges (B-16-FM and C-17-AT) that will be finely instrumented with many sensors will also be instrumented with scratch gauges. The scratch gauges will serve to assess seasonal movement in multiple bridges with variations in geography, girder type, orientation, and joint type. This information will be used to assess implications of removing existing deck joints throughout Colorado.

Scratch Gauge Explanation

To gather data about the movements of existing deck joints, scratch gauges were developed by the Colorado Department of Transportation and manufactured at Colorado State University's Structural Engineering Laboratory. The main concept of the scratch gauges is that the paint on the Part 1, the black piece, will be scratched off when the deck joint opens and closes. The measurement of this scratch will describe how much the joint moved. Each piece will be attached to one of the spans that frame into the deck joint. Figure 1 and below shows an image of the two parts of the scratch gauge.

Figure 1. Scratch Surface of Scratch Gauge **(Part 1)**

Figure 2. Scratching Piece for Scratch Gauge **(Part 2)**

The Part 2 holds a beveled concrete wedge anchor against the black face of Part 1. Figure 3 shows an image of the piece of Part 2 that will scratch the paint off of Part 1.

Figure 3. Scratching Mechanism of Part 2

This pointed tip will scratch the black paint off when the joint opens and closes. The scratch is what will be measured and taken as the opening or closing displacement of the joint. The additional bolts on Part 2 (those that are not beveled into a point) will be used to connect the piece to one span that frames into the expansion joint. Both bolts on Part 1 are

not beveled and are used to hold Part 1 to the bridge girder. Figure 4 shows what scratches made by the silver piece on the black piece will look like.

Figure 4. Result of Scratch Gauge Movement

Installation Procedure

Both parts of the scratch gauge will be attached and flush to the side of a bridge girder. Ideally, the scratch gauge parts will be attached to the midpoint of the girder depth. The side that is to be against the girder (the face you will not be able to see after installation) is marked on Part 1 and Part 2. One piece will go on one side of the deck joint and one piece will go on the other. The wedge screws will be used to secure the scratch gauge to the girder. The beveled wedge anchor of Part 2 will be positioned in the centermost position in the black, painted side of Part 1**. A photo will be taken upon initial installation, the temperature of the ambient air will be recorded, and the girders number (3B and 2B, for example) between which the expansion joint is located will be recorded. This information will be sent to krager@rams.colostate.edu** upon installation. Note the girder numbers should be described based on the CDOT numbering system outline in Figure 5 below. All questions regarding the installation should be directed to Karly Rager at krager@rams.colostate.edu or (605)941-6478. Correct installation is vital, so please do not hesitate to contact Karly Rager with questions.

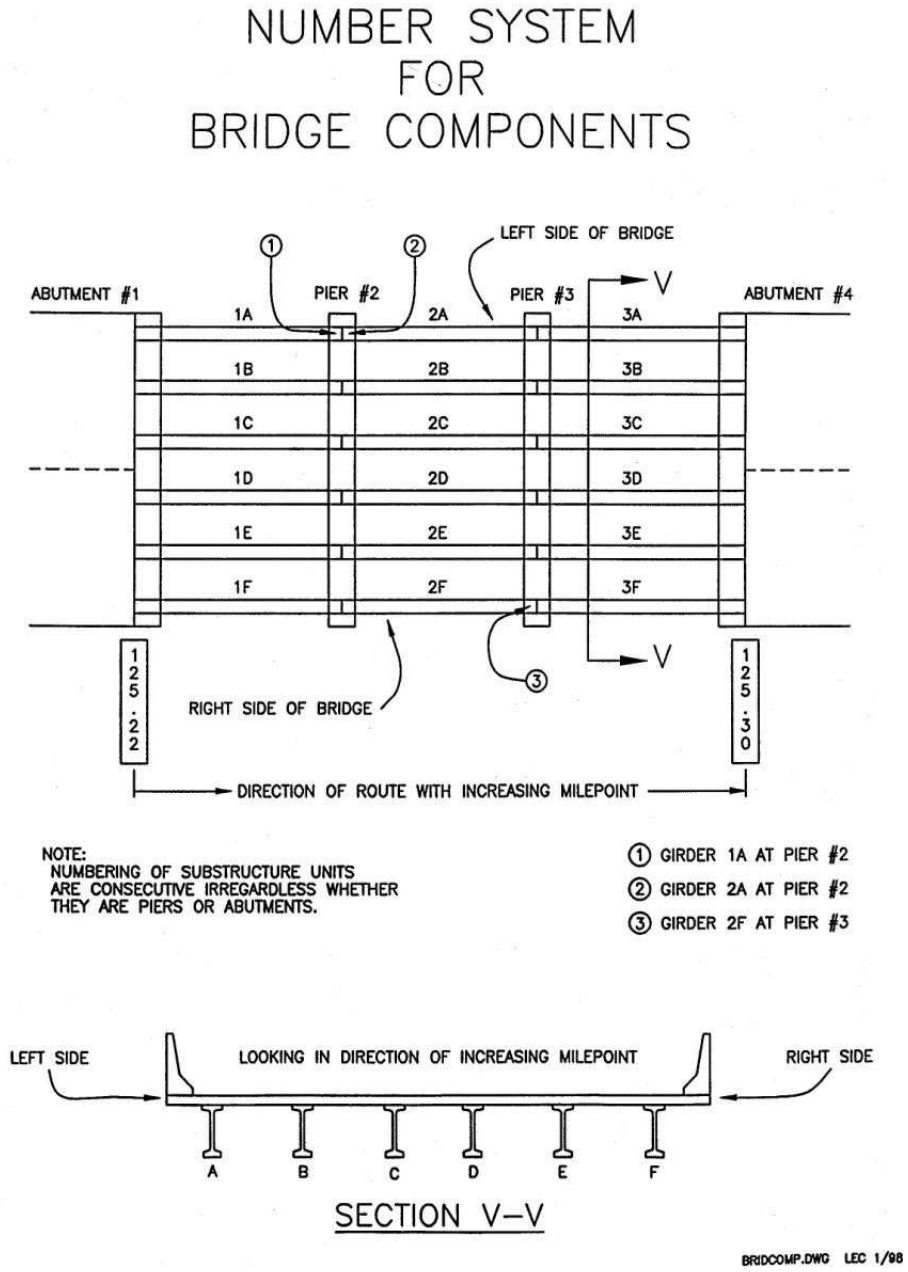

Figure 5. Numbering System for Bridge Components

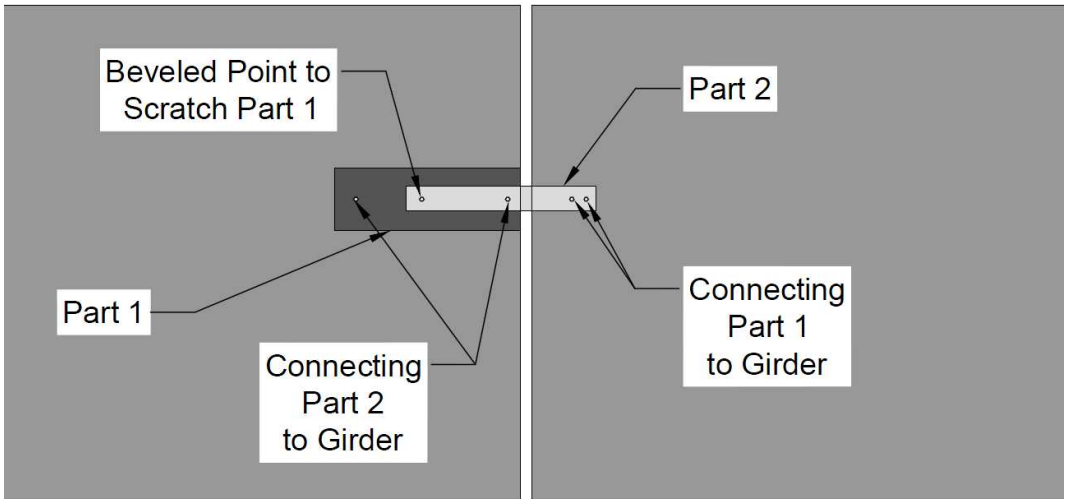

Figure 6. Sketch of Elevation View of Deck Joint after Installation

Bridge Selection

To select the bridges in which the scratch gauges would be installed, each region was contacted for initial suggestions. After all regions suggested the bridges of interest to them, the research team at Colorado State University condensed the list to include an approximately even variation of concrete and steel girders, joint types, orientation of the bridge, and distribution across the state of Colorado. Table 1 shows the variations of girder type, location, and orientation.

Table 1. Scratch Gauge Selections

REGION	Bridge Name	Girder Material	Orientation
1	F-16-DX	Steel	North-South
	E-16-EM	Steel	East-West
	F-16-JX	Concrete	East-West
	F-18-T	Steel	East-West
2	L-26-H	Steel	North-South
	L-26-BW	Concrete	North-South
	L-28-AQ	Concrete	East-West
	L-24-D	Concrete	North-South
	L-24-A	Steel	North-South
3	F-08-BH	Concrete	North-South
	F-08-AU	Concrete	North-South
4	C-20-AS	Concrete	North-South
	B-24-O	Concrete	East-West
	B-24-P	Concrete	East-West
	B-16-FM	Steel	East-West
	C-17-AT	Concrete	North-South
5	J-12-AK	Steel	North-South
	I-12-T	Steel	East-West

Data Collection and Maintenance

Photos of each scratch will be taken and sent to auralee26@gmail.com **once every three months.** Photo measurement technology will be used to determine the length of the scratch that is created by the scratch gauge. For example, if the installation occurs on January 1, 2016, photos would be collected and send on April 1, 2015, July 1, 2015, October 1, 2015, and January 1, 2017, etc. All questions regarding the data collection procedure should be directed to auralee26@gmail.com.

Thank you for your help and assistance in this research project!

APPDEDIX C

INSTRUMENATION DRAWINGS

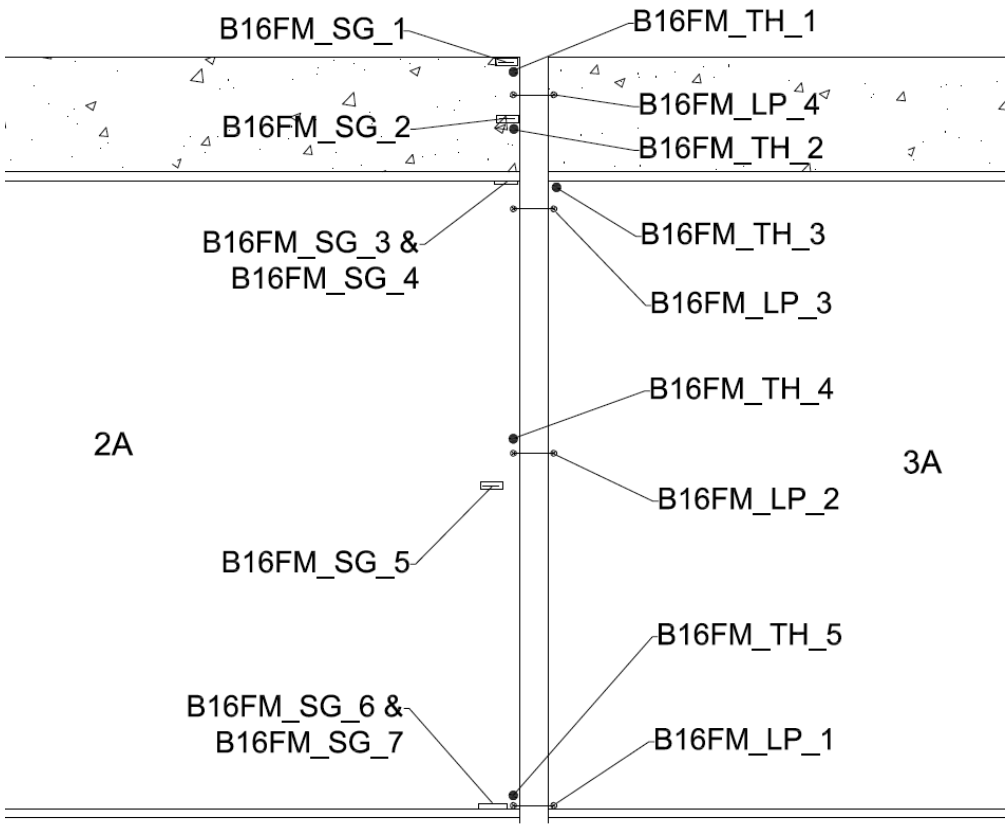

Legend

Thermocouple

Strain Gage

Linear Potentiometer

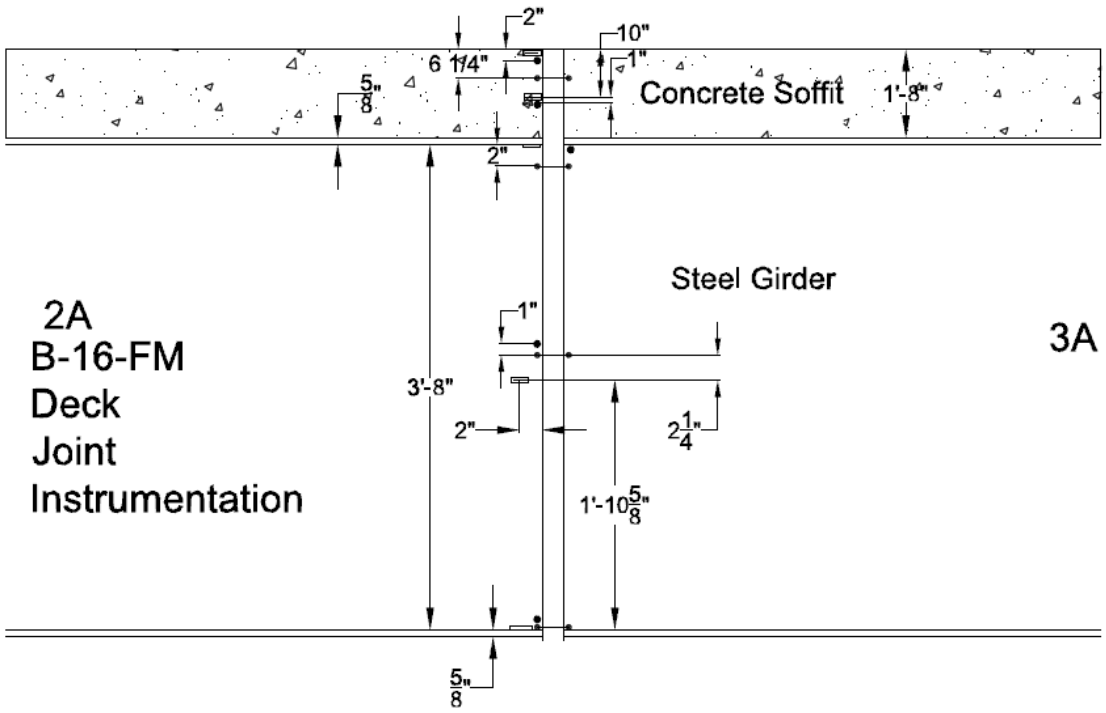
2"
10"
6 1/4"
1"
5/8"
Concrete Soffit
1'-8"
2"
Steel Girder
2A
B-16-FM
Deck
Joint
Instrumentation
1"
3A
3'-8"
2"
2 1/4"
1'-10 5/8"
5/8"